

Risk-Based Seismic Design Optimization of Steel Building Systems with Passive Damping Devices

Junshan Liu
Marquette University

Recommended Citation

Liu, Junshan, "Risk-Based Seismic Design Optimization of Steel Building Systems with Passive Damping Devices" (2010).
Dissertations (2009 -). Paper 74.
http://epublications.marquette.edu/dissertations_mu/74

RISK-BASED SEISMIC DESIGN OPTIMIZATION OF
STEEL BUILDING SYSTEMS WITH
PASSIVE DAMPING DEVICES

By

Junshan Liu, B.S., M.S.

A Dissertation submitted to the Faculty of the Graduate School,
Marquette University,
In Partial Fulfillment of the Requirements for
The Degree of Doctor of Philosophy

Milwaukee, Wisconsin

December 2010

ABSTRACT
RISK-BASED SEISMIC DESIGN OPTIMIZATION OF
STEEL BUILDING SYSTEMS WITH
PASSIVE DAMPING DEVICES

Junshan Liu, B.S., M.S.

Marquette University, 2010

Nonlinear time history analysis software and an optimization algorithm for automating design of steel frame buildings with and without supplemental passive damping systems using the risk- or performance-based seismic design philosophy are developed in this dissertation. The software package developed is suitable for conducting dynamic analysis of 2D steel framed structures modeled as shear buildings with linear/nonlinear viscous and viscoelastic dampers. Both single degree of freedom (SDOF) and multiple degree of freedom (multistory or MDOF) shear-building systems are considered to validate the nonlinear analysis engine developed. The response of both undamped and damped structures using the 1940 EI Centro (Imperial Valley) ground motion record and sinusoidal ground motion input are used in the validation. Comparison of response simulations is made with the OpenSEES software system and analytical models based upon established dynamic analysis theory.

A risk-based design optimization approach is described and formulation of unconstrained multiple objective design optimization problem statements suitable for this design philosophy are formulated. Solution to these optimization problems using a genetic algorithm are discussed and a prototypical three story, four bay shear-building structure is used to demonstrate applicability of the proposed risk-based design optimization approach for design of moderately sized steel frames with and without supplemental damping components. All programs are developed in MATLAB environment and run on Windows XP operating system.

A personal computer cluster with four computational nodes is set up to reduce the computing time and a description of implementation of the automated design algorithm in a cluster computing environment is provided. The prototype building structure is used to demonstrate the impact that the number of design variables has on the resulting designs and to demonstrate the impact that use of supplemental viscous and viscoelastic damping devices have on minimizing initial construction cost and minimizing expected annual loss due to seismic hazard.

ACKNOWLEDGMENTS

Junshan Liu, B.S., M.S.

I would like to gratefully and sincerely express my appreciation to Dr. Christopher M. Foley for his guidance, knowledgeable mentoring, and most importantly, his inspiration during my doctoral studies at Marquette University. I will never forget his consistent encouragement, his willingness of taking adventure with me in the research, and his patience in my numerous experiments.

I would like to take this opportunity to thank my doctoral committee members, Dr. Stephen M. Heinrich, Dr. Sriramulu Vinnakota, Dr. Baolin Wan and Dr. Jian Zhao. This dissertation holds not only the culmination of years of study at Marquette University, but also the relationships with these generous and inspiring people. I would never have been able to complete my dissertation without their guidance, helps and challenges.

For the assistance with computer clusters and continuous financial aids, I want to express my deepest thanks to the Department of Civil and Environmental Engineering.

Finally, I am very grateful to my parents for their love and encouragement. I would like to thank my wife, Peng Lin, for her continuous support, and for her standing by me through the good and hard times.

TABLE OF CONTENTS

ACKNOWLEDGMENTS	i
LIST OF TABLES	vi
LIST OF FIGURES	viii
CHAPTER 1 INTRODUCTION	1
1.1 Background and Literature Review	7
1.1.1 Automated Design with and without Supplemental Dampers	8
1.1.2 Probabilistic or Risk-Based Design	11
1.1.3 Genetic Algorithm (GA)	18
1.2 Objective and Scope	21
1.3 Thesis Overview	24
CHAPTER 2 TRANSIENT ANALYSIS OF SYSTEMS WITH VISCOUS AND VISCOELASTIC DAMPING	26
2.1 Introduction.....	26
2.2 Foundational Theory.....	27
2.3 Numerical Integration of the Equations of Motion	32
2.4 Response Simulation Algorithm Validation	37
2.4.1 Linear Viscous Damping	38
2.4.2 Linear Viscoelastic Damping	42
2.4.3 Nonlinear Viscous Damping	44
2.4.4 Nonlinear Viscoelastic Damping	47
2.4.5 Energy Dissipation	49
2.5 Case Study Comparisons with OpenSees	51
2.5.1 Case 1 - No Supplemental Damping Devices or Braces.....	53

2.5.2 Case 2 - Elastic Diagonal Braces and No Dampers	54
2.5.3 Case 3 and 4 - Supplemental Linear Viscous Dampers	55
2.5.4 Case 5 - Various Supplemental Devices	57
2.6 Additional Evaluation	62
2.7 Concluding Remarks	72
CHAPTER 3 RISK-BASED SEISMIC DESIGN OPTIMIZATION OF STEEL BUILDING SYSTEMS WITH SUPPLEMENTAL DAMPING DEVICES	73
3.1 Introduction	73
3.2 Structural Optimization Fundamentals	74
3.3 Fitness Function for initial Construction Cost	77
3.4 Fitness Function for Expected Annual Loss (EAL)	80
3.5 Genetic Algorithm Constraint Formulation	83
3.5.1 Strength	84
3.5.2 Local and Member Instability	86
3.5.3 Beam – Column Strength	87
3.5.4 Damper Stiffness	88
3.5.5 Designer Preference	89
3.6 Penalty Functions	90
3.7 GA Optimization Statement and Basic Flowchart.....	93
CHAPTER 4 APPLICATION OF THE GENETIC ALGORITHM TO OPTIMIZED DESIGN OF STEEL FRAMING SYSTEMS	97
4.1 Introduction	97
4.2 Introduction to Distributed Computing	98
4.3 Distributed Computing Implementation of GA Using MATLAB	102
4.4 Frame Design Case Studies	105
4.4.1 Genetic Algorithm Parameters	109
4.4.2 Fragility Curve Parameters and Repair Cost Ratios	110

4.4.3 Optimal Design Statements for Case Studies	111
4.5 Case Study Results and Discussion	116
4.5.1 Design Case 1	118
4.5.2 Design Cases 2, 3 and 4	122
4.5.3 Design Cases 5 and 6	135
4.6 Concluding Remarks	144
CHAPTER 5 SUMMARY, CONCLUSIONS AND FUTURE WORK	146
5.1 Summary	146
5.2 Conclusions	147
5.3 Recommendations for Future Work	150
REFERENCES	153
APPENDICES	159
Appendix 1	160
Appendix 2	161
Appendix 3	163
Appendix 4	164
Appendix 5	165
Appendix 6	167
Appendix 7.....	169
Appendix 8	171
Appendix 9	178
Appendix 10	183
Appendix 11	185
Appendix 12	186
Appendix 13	187
Appendix 14	189

Appendix 15 190

Appendix 16 191

Appendix 17 192

Appendix 18 193

Appendix 19 194

Appendix 20 197

Appendix 21 200

Appendix 22 203

LIST OF TABLES

1.1 Fragility Curve Parameters for Structural and Non-Structural Components in SIL Building and High-Code Design Level.....	17
1.2 Example of Crossover operator.....	20
2.1 Characteristics of the One-story Shear Building.....	39
2.2 Dynamic Properties of One – Story Shear Building (SDOF system)	50
2.3 3–Story Building Model Characteristics	52
2.4 System Parameters for the Three-Story Shear Buildings in Case 5.....	58
3.1 Supplemental Damper Device Costs.....	79
3.2 Fragility Curve Parameters for Structural and Non-Structural Components (S1L Building System and COM4 Occupancy Class).....	81
3.3 Repair Costs Expressed as Percentage of Building Replacement Cost (S1L Building System and COM4 Occupancy Class).....	81
3.4 Annual Probabilities for Earthquake Intensities Considered	84
4.1 Genetic Algorithm Parameters.....	110
4.2 Fragility Curve Parameters for Structural and Non-Structural Components in SIL building and High-Code Design Level	111
4.3 Repair cost Ratio in % of Building Replacement Cost for Structural and Non-Structural Components	111
4.4 Design Variables in the Last Generation, Case 1.....	120
4.5 The Distribution of Losses, Case 1	121
4.6 Design Variables in the Last Generation, Case 2	124
4.7 The Distribution of Losses, Case 2	125
4.8 Design Variables in the Last Generation, Case 3	129
4.9 Design Variables in the Last Generation, Case 4.....	131
4.10 The Designs with the Minimum Initial Cost from Cases 1 & 2	133
4.11 The Maximum Inter-story Drift and Acceleration for Minimum Initial Cost Designs in cases 1 & 2	133

4.12 Loss Distribution for Minimum Initial Cost Designs in Cases 1 & 2	134
4.13 Design Variables in the Last Generation, Case 5.....	137
4.14 Design Variables in the Last Generation, Case 6.....	142

LIST OF FIGURES

1.1 Longitudinal Cross Section of a Taylor Fluid Damper.....	4
1.2 Taylor Fluid viscous Damper	4
1.3 Buckling Restrained Brace	5
1.4 Typical Elevation of a BRB.....	5
1.5 Example Fragility Curves for Slight, Moderate, Extensive and Complete Damage.....	16
1.6 Example Probability for Structural Component in Damage State “Moderate”	16
1.7 Design Variables Mapped onto Binary Chromosome.....	19
2.1 Typical MDOF Shear-Building System with Inherent and Supplemental Damping.....	28
2.2 Nonlinear Spring Response Characteristics	29
2.3 Viscous Damping Behavior	30
2.4 Viscoelastic Damping Behavior	31
2.5 Flow Chart for Numerical Integration Algorithm.....	34
2.6 Single Degree of Freedom with Inherent Linear Viscous Damping and Equivalent Ground Acceleration.....	38
2.7 Hysteretic Response Comparison for SDOF System in Figure 2.6 with Linear Viscous Supplemental Damper	41
2.8 Hysteretic Response Comparison for SDOF System in Figure 2.6 with Linear Viscoelastic Damping.....	44
2.9 Displacement Comparison for SDOF System in Figure 2.6 with Nonlinear Viscous Damping, $\alpha = 0.5$	46

2.10 Hysteretic Response Comparison for SDOF System in Figure 2.6 with Nonlinear Viscous Damping, $\alpha = 0.5$	46
2.11 Displacement Time History Response Comparison for SDOF System in Figure 2.6 with Nonlinear Viscoelastic Damping, $\alpha = 0.5$	48
2.12 Hysteretic Response for SDOF System in Figure 2.6 with Nonlinear Viscoelastic Damping, $\alpha = 0.5$, $k_d = 50 \text{ k/in}$	48
2.13 Energy Dissipated by Dampers in One Cycle of Steady-State Vibration	50
2.14 The 3rd Floor (Roof Level) Displacement Time Histories	54
2.15 The 3 rd Floor (roof) Displacement Time Histories for Case 2	55
2.16 The 3 rd Floor Displacement Time Histories for Case 3	56
2.17 The 3 rd Floor Displacement Time Histories for Case 4.	57
2.18 The 3rd Floor Displacement Time Histories for Case 5 Systems	58
2.19 Force-Velocity Response for Nonlinear Viscoelastic Dampers in Three-Story Shear Building with Parameters in Table 2.4.....	60
2.20 Hysteresis Loops of Dampers at Story 1 in Three Story Frame	61
2.21 Hysteresis Loops of Dampers at Story 2 in Three Story Frame	61
2.22 Hysteresis Loops of Dampers at Story 3 in Three Story Frame	62
2.23 Five-Story Shear Building Frame	63
2.24 The 5 th Floor Displacement for the Five-Story Shear Building Described in Figure 2.23.....	64
2.25 Displacement Time History at Each Level Computed Using MDOF.....	65
2.26 Story Shear at Each Story Computed Using MDOF.....	66
2.27 Five Story Shear Building Frame with Nonlinear Viscous Dampers	67

2.28 Displacements at Each Story.....	68
2.29 Story Shear Forces vs. Inter-Story Drift at Each Story.....	69
2.30 Damper Forces vs. Inter-Story Drift at Each Story.....	70
2.31 Damper Forces vs. Relative Velocity at Each Story.....	71
3.1 Scaling Functions Used for Penalty Multipliers	92
3.2 Flowchart of Genetic Algorithm Implemented	95
4.1 Computer Cluster with 4 Workers	101
4.2 Serial Approach Vs. Parallel Approach	104
4.3 A MATLAB Administration System for Parallel and Distributed Computing	104
4.4 Basic Frame Topology Used for Design Studies	106
4.5 Ground Motion Record Suite Used for Frame Designs	108
4.6 Topology for Frame Design Case 1	112
4.7 Frame Design Case 2, 5 Design Variables, Linear Dampers.....	114
4.8 Frame Design Case 3, 5 Design Variables, Nonlinear Dampers, $\alpha = 0.5$	114
4.9 Frame Design Case 4, 5 Design Variables, Nonlinear Dampers, $\alpha = 1.5$	115
4.10 Frame Design Case 5, 9 Design Variables, Linear Dampers, $\alpha = 1.0$	117
4.11 Frame Design Case 6, 12 Design Variables.....	117
4.12 Pareto Front for Frame Design Case 1.....	119
4.13 Pareto Front for Frame Design Case 2.....	123

4.14 Pareto Front for Frame Design Case 3.....	128
4.15 Pareto Front for Frame Design, Case 4.....	130
4.16 The Comparison of Pareto Fronts for Design Cases 1 through 4.....	132
4.17 Pareto Front for Frame Design, Case 5.....	135
4.18 Pareto Front for Frame Design, Case 6.....	141
4.19 The Comparison of Pareto Fronts, Case 5 Vs. Case 6	144

Chapter 1 Introduction

In traditional seismic design, the lateral force resisting system in a structure is designed to be able to absorb and dissipate energy in a stable manner for a number of seismic shaking cycles. Earthquake energy in steel building systems is dissipated by ductile plastic hinge regions of beams and column bases, which are also a part of gravity load carrying system in a building structure. The structure is permitted to be damaged while it is subjected to lateral deformations associated with moderate or severe seismic events, but collapse is to be avoided.

Plastic hinges are regions of concentrated yielding within members that make up the building skeleton [1.1]. The development of plastic hinges relies on deformation capacity and inherent ductility of a structure. The more ductility demand a structure sustains during the ground motion event the more damage the structure will likely suffer. When a structure must remain functional after a major earthquake, as is the case of important structures (e.g. hospitals, fire stations), a traditional design approach that assumes significant damage will occur to the structural and nonstructural systems can be inappropriate. Current building code methods ensure that a structure is designed with sufficient strength within the elements of the framing system to prevent collapse. However, damage to nonstructural components may still occur and this damage can be significant.

To mitigate damage resulting from seismic hazard, an alternative design approach is to introduce seismic isolation systems or supplemental energy dissipation devices which can distribute energy dissipation within a structure when subjected to seismic

ground motions [1.1]. A variety of energy dissipation systems have been developed in the past two decades. Several will be discussed in this dissertation and a focus will be given to passive linear/nonlinear viscous and viscoelastic dampers available commercially.

Building system performance can be improved if a portion of the input energy can be absorbed by some type of supplemental devices, not by the structure itself. The energy relationship describing the components of energy input, absorption, and dissipation can be described in the following equation [1.2]:

$$E_e = E_k + E_s + E_h + E_d \quad (1.1)$$

E_e is the absolute earthquake energy input, E_k is the kinetic energy of the masses, E_s is the recoverable elastic strain energy, E_h is the irrecoverable hysteretic energy, and E_d is the energy dissipated by supplemental damping devices. The right hand side of the equation (1.1) is the energy dissipative and absorptive capacity of the structural system and the left hand side is the energy imparted by the ground motion to the structure.

The right hand side of equation (1.1) should be larger than the left hand side in a successful seismic design. In conventional seismic design, the energy capacity of a structure relies mostly on the hysteretic energy E_h to dissipate the ground motion input energy. This energy dissipation results from the inelastic deformations in the components of the structural system. The energy dissipation capacity of a structure, E_d , will be increased when supplemental dampers are added to the structure. A structure with supplemental dampers is normally designed for early engagement of dampers to dissipate the earthquake energy input prior to the development of yielding in localized regions in the primary structural system. A structure with added dampers has the potential to be

protected from earthquake damage and the building's performance can be improved during seismic ground motions.

Viscoelastic dampers have been utilized successfully in high-rise buildings for the reduction of earthquake-induced response within the United States for two decades [1.3]. A damper is an energy dissipater or absorber which is added to a structure to mitigate undesirable aspects of earthquake-induced structural response. Passive viscous dampers dissipate energy based upon the relative velocity between their two ends. They absorb the vibrations automatically without the need of an external electrical control system and the forces in the dampers are generated in reaction to the deformations induced during the seismic motion. This characterizes them as passive control systems. Passive control systems are generally low in cost and effective. Active control systems use computer-controlled actuators design to actively impart forces to the structural system in reaction to deformations generated by earthquake motions. Active mass dampers, active mass drivers, active tendon systems, pulse thrusters, and active variable stiffness systems are all active control systems and these are very effective in controlling oscillations in high winds and severe earthquakes. A combination of active and passive control systems can be used in a building structure to protect it from seismic damage. This type of control system is known as hybrid active-passive system. This research will focus on linear/non-linear viscous and viscoelastic dampers used as the foundation for a passive control system.

Passive energy dissipative devices generally fall into one of two categories: hysteretic where material yielding is relied upon to dissipate energy; and viscous where a viscous fluid is used to inhibit movement of a "plunger" within it and the resulting

damping force is proportional (or in some cases, non-proportional) to the velocity of the plunger moving through the fluid. Figure 1.1 shows a typical longitudinal cross section of a viscous fluid damper. It consists of a stainless steel piston with orifices and piston head and it is filled with silicone fluid. The difference in the pressure between inside and outside of the piston results in the damper resistive force to be generated. Fluid viscous dampers, which are the focus of this research effort, are made by Taylor Devices, Inc. [1.4]. Examples of fluid-viscous dampers and their size compared to a person are shown in Figure 1.2.

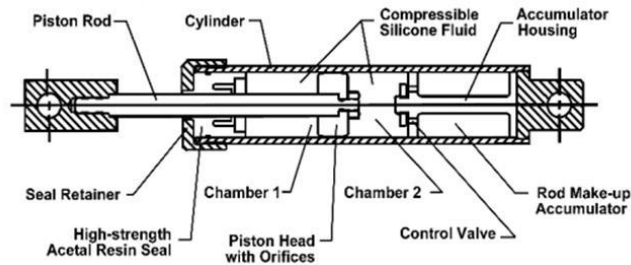


Figure 1.1 Longitudinal Cross Section of a Taylor Fluid Damper [1.4].



Figure 1.2 Taylor Fluid Viscous Damper [1.4].

Hysteretic energy-based devices rely on controlled yielding of material. The energy dissipation arises from this yielding. Common examples of hysteretic devices are buckling-restrained-braces (BRB's). A typical buckling-restrained brace has stable hysteretic yielding characteristics. Common BRB configurations are shown in Figure 1.3.

The most common BRB consists of a core steel plate jacketed by confining concrete encased in a steel tube to restrain buckling. Coating materials are used between the concrete and the core plate to prevent the transmission of axial forces between the two dissimilar materials. Figure 1.4 shows a typical elevation and components of a BRB made by Star Seismic LLC [1.5].



Figure 1.3 Buckling Restraint Brace [1.5].

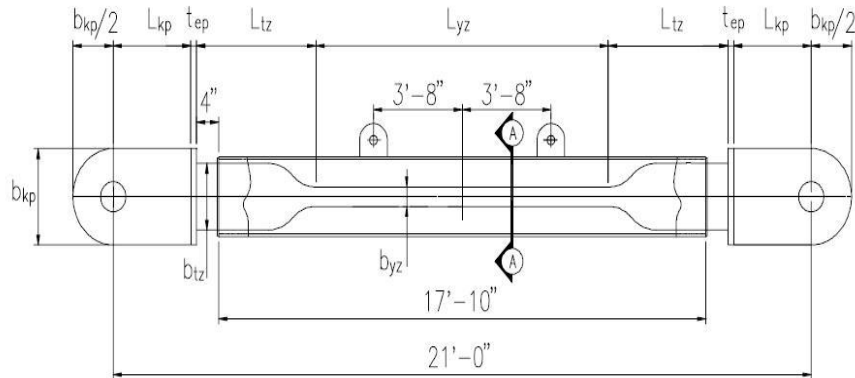


Figure 1.4 Typical Elevation of a BRB [1.5].

Analytical and experimental studies have shown that significant reduction in a structure's response to earthquake excitation can be achieved by adding viscoelastic dampers to the structure [1.6]. To address design issues related to structural applications of viscoelastic dampers, the structural engineer must decide the number, size, location,

and the parameters defining the relationship between velocity and force for the dampers being used with a defined structure topology (or configuration) to achieve a desired or targeted structural response level [1.7]. When all these issues are integral components defining the structural system and are dependent upon decisions made by the structural engineer, design using passive damping systems and the desire to balance energy dissipation among all potential components with the goal being economical and safe designs becomes a significant structural engineering challenge.

Historically speaking, building codes and design specifications establish minimum requirements for life-safety (*i.e.* prevention of collapse) of a structural system through prescriptive criteria that regulate acceptable materials used in construction, specify required minimum levels of strength and stiffness, and suggest appropriate construction detailing. Although these prescriptive criteria are intended to result in buildings capable of providing acceptable performance with regard to life-safety, they provide little guidance to the structural engineer with regard to reducing the potential of damage to non-structural components and systems, or excessively expensive initial construction cost. In addition, the performance of buildings designed using these prescriptive criteria can have high levels of variability in their performance during seismic events. Some buildings will perform better than anticipated by the code, while the performance of others could be worse.

Performance-based seismic design methods intend to include estimation of how a building is likely to perform through consideration of:

- a range of potential seismic hazards,
- uncertainties inherent in the quantification of potential hazard,

- uncertainties in assessment of the actual building response.

These newly developing methods permit design of new buildings or upgrade of existing buildings with a better understanding of the risk of casualties, occupancy interruption, and economic loss that may occur as a result of future earthquakes [1.8].

In the developed world, it is well known that buildings perform fairly well with respect to life-safety performance (*i.e.* complete collapse of buildings is rare). However, recent seismic events have revealed that the uncertainties listed above result in significant variability with respect to damage to structural and nonstructural systems. Supplemental damping systems have potential to allow building systems to achieve life-safety performance (*i.e.* no collapse) after large (rare) ground motion events while making mitigation of possible damage to structural and nonstructural components after less severe (more frequent) ground motion events. It is now timely to address performance-based design and analysis issues related to the applications of passive supplemental damper systems within the context of state of the art performance-based (probabilistic) seismic design procedures.

1.1 Background and Literature Review

An extensive body of knowledge related to evolutionary algorithms and their application in the performance-based probabilistic seismic design of a structure without supplemental dampers has evolved in the last decade. This section will include a review of previous passive damper design research efforts and the development of optimization methods applied in the field of seismic structural engineering and those that include use of supplemental damping systems in the optimization design problem statements.

In general, optimization algorithms can be classified as gradient-based or stochastic search. The major obstacle for a gradient-based optimization procedure is that continuous functions are required to represent design variables and objectives. Stochastic search techniques are not restricted by this requirement and the Genetic Algorithm (GA) is one of the most commonly applied stochastic search techniques. GA's do not require evaluation of gradients of objective and constraint functions. A GA is used to solve the optimization problems formulated in this research effort and its fundamental theory will be reviewed in this section. An overview of the current formulations for performance-based probabilistic seismic design will also be provided.

1.1.1 Automated Design with and without Supplemental Dampers

Previous studies related to the use of supplemental dampers within building structures involve a variety of methods. Algorithms designed to locate and size supplemental dampers in multistory 1:5 scale steel building have been undertaken [1.9]. Optimal control theory using a linear quadratic regulator (LQR) has been adapted to design linear passive viscous or viscoelastic devices. The design was aimed at minimizing a performance cost function, but provides the most suitable minimal configuration of devices while maximizing their effect to control the earthquake response by optimizing damper location and their coefficient factors. The term "linear-quadratic" refers to the linear structural analysis and the quadratic cost function. Newmark's numerical method was used for the linear dynamic analysis. The design algorithm was evaluated using three ground motions (1) El Centro N-S 1940 accelogram with peak ground acceleration

(PGA) of 0.34g; (2) Mexico City SCT 1985 accelogram (PGA 0.20g); and (3) Hachinohe 1968 accelogram (PGA 0.20g).

A sequential search algorithm has also been proposed as a method to allow the automatic selection of damper capacity for the design of optimal configurations of supplemental dampers [1.10, 1.11, 1.12]. Sequential search is known as a linear search algorithm, which is suitable for searching a list of data for a particular value. Every element in the list is checked one at a time until a match is found. The simplicity of sequential search means that less work needs to be done if just a few elements are to be searched. However, in many realistic problems, preparation of the list being searched, such as sorting the list, is required. Furthermore, direct search also can require more complex data structures. Simplified sequential search algorithms have been proposed [1.12]. The simplified sequential search algorithm can be easily integrated into conventional design procedures by structural engineers dealing with damper-added structures. Linear viscous dampers were added to a 6-story frame structure. It was found that the efficiency of damper configurations given by the simplified sequential search algorithm is comparable to the efficiency of damper configurations determined in previous efforts [1.10, 1.11].

Genetic algorithms have also been used to design passive dampers for linearly behaving building structures [1.13]. In this study, viscoelastic dampers and fluid viscoelastic dampers are employed in two building structures. The first building structure is a 24-story shear-building model. The second building is a six-story torsion system. The objective is to minimize the structural response such as the floor accelerations, shears, and inter-story drifts, etc. The design variables are the total number of dampers to be

placed in the structure which is constrained to a reasonable pre-defined number. The capacity of dampers is defined, the total required number of dampers is determined, and their location in the building were designed to achieve the maximum seismic response reduction. The response reduction was defined in terms of base shear, overturning moment or floor acceleration. Numerical examples for a shear building model and torsion building model were presented to show the distribution of three different types of dampers to achieve a desired seismic response reduction.

A genetic algorithm with integer representation was used to optimize passive fluid damper location to control the seismic response of a 20 – story nonlinear steel frame building [1.14]. In this research, a linear system transfer function, which measures the frequency response of a system, was utilized to define the objective function. A Genetic Algorithm (GA) was used to minimize the response in the second mode of vibration instead of the dominant first mode. The supplemental damper characteristics were predefined and the damper location at any story level was the only design variable. The constraints defined in this study were the number of dampers and the requirement of dampers being located between floor levels. The results showed that the damper location may vary significantly with different objective function H_2 or H_∞ -norms. The H_2 and H_∞ -norms are measures of the frequency response of a system. For the damper distribution optimization process, both H_2 and H_∞ -norms of the transfer function were utilized as objective function to compute average and peak response of the structure respectively. In all scenarios considered, the algorithm developed indicated that dampers should be concentrated in the lowermost and uppermost stories.

An automated seismic design procedure considering only one building performance level, Life Safety, has been presented [1.15]. The performance-based design concept was utilized and a three-dimensional (3D) space steel frame with six – stories without supplemental dampers was studied. The 3D space steel frame underwent linear and nonlinear deformation when subjected to natural and artificial ground motions. A GA was adopted to minimize the weight of the structure under behavioral constraints on stress and displacements. The dimensions of the cross section areas of the structural members were chosen as design variables. Maximum inter-story drift ratio equal to 2% was used in the nonlinear analysis to eliminate the need to consider $P-\Delta$ effects. The results from this research shows that less material weight with good seismic performance could be obtained when nonlinear time-history analysis is performed.

1.1.2 Probabilistic or Risk - Based Design

Performance-based seismic design (PBD) is a process intended to result in the design of buildings with a realistic and reliable quantification of the risk of loss of life and economic loss that may occur as a result of future earthquakes [1.16]. The first generation of performance-based seismic design procedures developed in 1990's and it focused on the evaluation and upgrade of existing building structures. The Federal Emergency Management Agency (FEMA – now within the Department of Homeland Security) then extended the PBD approach and recommended programs for carrying out the development of performance-based seismic design guidelines for existing and new buildings.

In the next generation PBD guidelines, both direct economic loss and indirect economic loss, in addition to potential of casualties, will be measured as building performance indices. Economic loss related to the structural system and nonstructural components and systems will be considered. Direct economic loss relates to repair or replacement of damaged buildings, building content losses and building inventory losses. The time required for damage repair and the duration of lost building function as a result of earthquake-induced damage are defined as indirect economic losses. In this research, only direct economic loss due to repair and replacement of damaged building components are considered. It is important to recognize, however, that indirect losses can be included within the optimization framework formulated in this thesis.

The framework for performance-based engineering developed by the Pacific Earthquake Engineering Research (PEER) center is convenient for calculating losses given seismic hazard. The framework consists of four main analysis steps [1.17-1.22]: hazard analysis; structural analysis (ground motion response simulation); damage analysis; loss analysis. The mean annual frequency of a decision variable (DV) being exceeded can be represented as [1.17];

$$\lambda(DV) = \int \int \int G(DV | DM) dG(DM | EDP) dG(EDP | IM) d\lambda(IM) \quad (1.2)$$

where: $G(DV | DM)$ is the probability that the DV exceeds specified values given that a particular damage measure (DM) is reached; $G(DM | EDP)$ is the probability that a DM will be exceeded given a particular engineering demand parameter (EDP); $G(EDP | IM)$ is the probability that an EDP will be exceeded given that a particular intensity measure (IM) occurs; and $\lambda(IM)$ is the mean annual frequency (MAF) of an intensity measure (seismic hazard curve). If the most general form of the PEER framework [1.18, 1.19] is

to be implemented, probability density functions describing all random variables must be available.

Examples of decision variables are: casualties, direct economic loss, and indirect economic losses. These variables are the basis for goals of minimizing “deaths, dollars and downtime” resulting from the seismic hazard [1.18]. Damage measures depend upon the type of building component. Common measures for structural components are Immediate Occupancy (IO) and Collapse Prevention (CP) [1.23]. Damage to displacement-sensitive non-structural building components (NSD), acceleration-sensitive non-structural building components (NSA), and the structural system (SS) has also been characterized using four damage measures: slight, moderate, extensive and complete [1.24]. Typical engineering demand parameters associated with these damage measures include inter-story drift, floor acceleration, column compression force, and column splice force. Decision variables and damage measures can be represented as binary damage state indicator variables [1.17] and the probabilities, $G(DV | DM)$ and $G(DM | EDP)$, can then be established using fragility curves or fragility surfaces [1.24, 1.8].

Equation (1.2) describes a highly complex structural engineering problem because each parameter (IM , EDP , DM , and DV) remains a continuous random variable. Losses resulting from damage to non-structural and structural components within the building system are most-often triggered in a discrete manner [1.25]. As a result, some of the integrations contained in equation (1.2) are carried out with discrete summation for all pertinent components [1.25]. In next-generation PBE methodologies, the decision variables are likely to be conceptualized relatively simply as deaths, dollars and downtime [1.18].

A fragility function is a mathematical relationship that indicates the probability that a component or system will experience damage at or in excess of a specific level, given that the component or system experiences a specific level of demand, expressed herein as EDP. The probability that the component reaches or exceeds damage state ds , given a particular EDP value, and idealized by a lognormal distribution,

$$P[ds | EDP] = \Phi \left[\frac{1}{\beta_{ds}} \ln \frac{EDP}{\overline{EDP}_{ds}} \right] \quad (1.3)$$

where:

\overline{EDP}_{ds} is the median value of the lognormal distribution,

β_{ds} denotes the logarithmic standard deviation

Φ is the standard normal cumulative distribution function.

In general, the total variability of each damage state, β_{ds} , is modeled by the combination of following three contributors to damage variability:

- uncertainty in the damage state threshold,
- variability in the capacity (response) properties of the model building type of interest,
- uncertainty in response due to the spatial variability of ground motion demand.

Each of these three contributors to damage state variability is assumed to be lognormally distributed random variables.

The fragility function can be used to evaluate that a component is in damage state ds , given the $EDP = z$, by performing the following calculation with the lognormal cumulative distribution function,

$$\begin{aligned}
P[D = DS_i | EDP = z] &= 1 - F_{ds_i}(z) & i = 1 \\
&= F_{ds_i}(z) - F_{ds_{i+1}}(z) & 2 \leq ds \leq 4 \\
&= F_{ds_i}(z) & i = 5
\end{aligned} \tag{1.4}$$

Damage States are defined separately for structural and non-structural systems or components of a building. A total five damage states are defined for structural and non-structural systems in this thesis. These are none (ds_1) slight (ds_2), moderate (ds_3), extensive (ds_4) and complete (ds_5) .

Figure 1.5 provides example fragility curves for the four damage states (Slight, Moderate, Extensive, and Complete) used in this methodology for structural systems (SS), non-structural displacement-sensitive (NSD) components, and non-structural acceleration-sensitive (NSA) components. Each fragility curve is defined by a median value of the engineering demand parameter (e.g. spectral displacement, spectral acceleration, PGA or PGD) that corresponds to the threshold of the damage state and by the variability associated with that damage state. The parameters used to develop the fragility curves seen in Figure 1.5 are given in Table 1.1.

Figure 1.6 illustrates how the lognormal fragility curve is used to define probabilities of specific damage states given a known engineering demand parameter. The figure includes an example of the probability that structural components in a building structure is in damage state “Moderate” for given interstory drift angle (ISDA) of 0.01. The probability is computed using the equation (1.4).

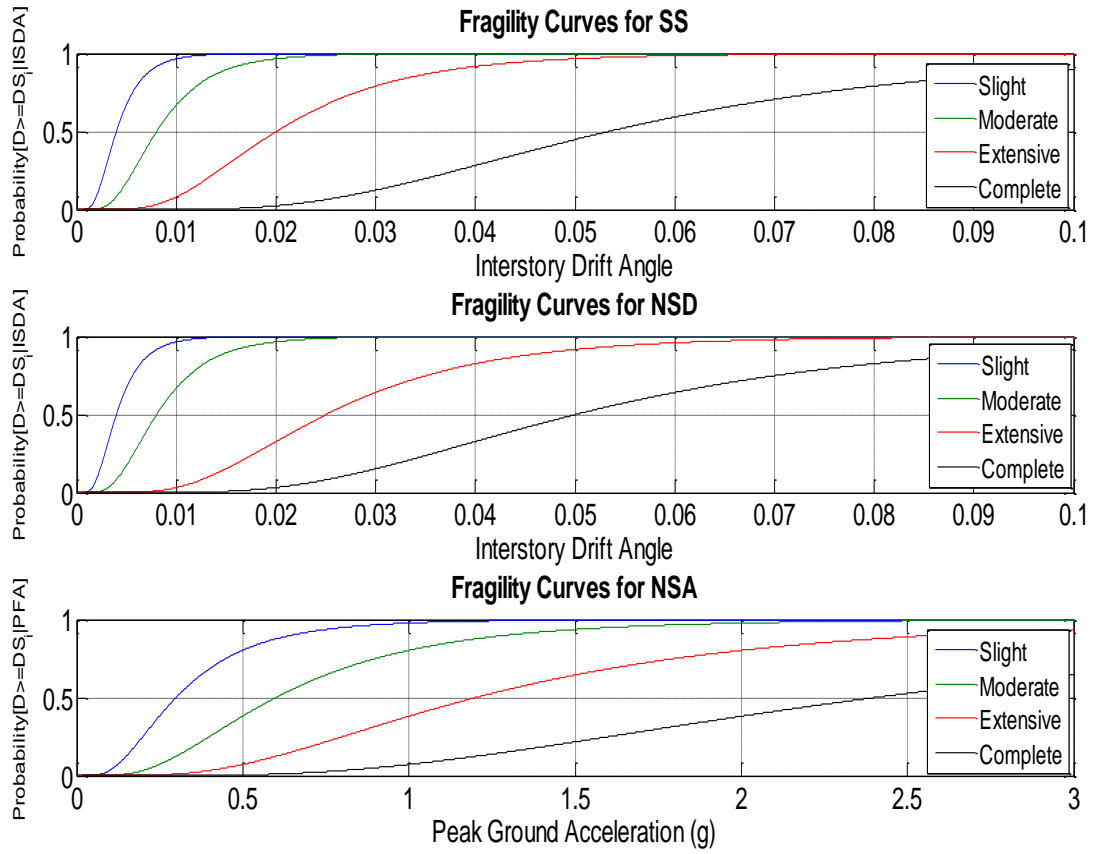


Figure 1.5 Example Fragility Curves for Slight, Moderate, Extensive and Complete Damage.

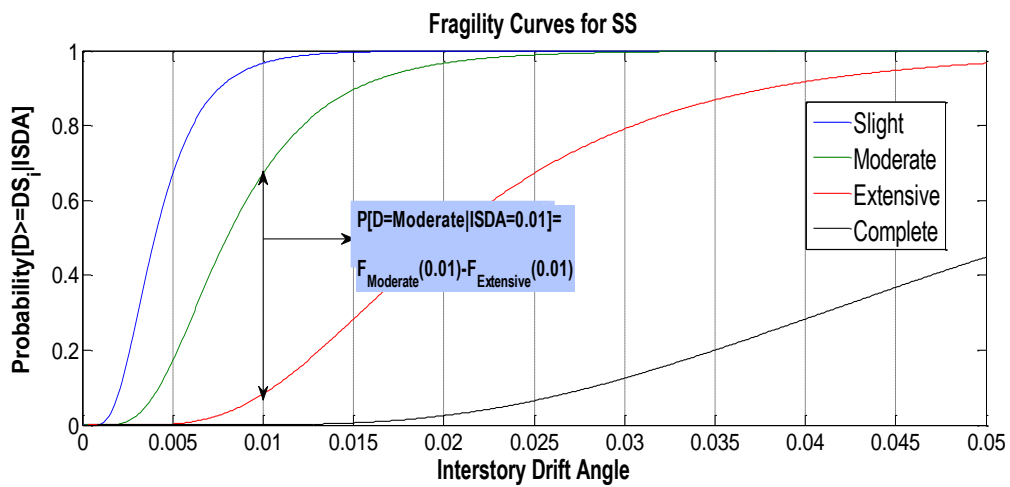


Figure 1.6 Example Probabilities for Structural Component in Damage State “Moderate”

Table 1.1: Fragility Curve Parameters for Structural and Non-Structural Components in SIL Building and High-Code Design Level [1.27].

Component	Fragility Curve Parameter	Damage State			
		Slight	Moderate	Extensive	Complete
SS	\overline{ISDA}_{ds}	0.004	0.008	0.020	0.0533
	β_{ds}	0.50	0.50	0.50	0.50
NSD	\overline{ISDA}_{ds}	0.004	0.008	0.025	0.050
	β_{ds}	0.50	0.50	0.50	0.50
NSA	$\overline{PFA}_{ds}(g)$	0.30	0.60	1.20	2.40
	β_{ds}	0.60	0.60	0.60	0.60

A probabilistic performance based design optimization problem can be formulated using the PEER center framework outlined in equation (1.2). The optimization problem statement that can be formulated potentially includes minimization of initial construction costs, minimization of damage (and resulting loss) to the structural system and minimization of damage (and resulting loss) to nonstructural systems and components. Formal optimization algorithms for this type of structural optimization problem have only recently been developed [1.28] and future application of performance based engineering procedures in structural engineering can benefit significantly from research activities in this area. Furthermore, algorithms suitable for tackling such optimization problems will likely be based upon evolutionary computation. Application of evolutionary computation to solve performance-based design optimization problems has occurred for structural systems without supplemental damping mechanisms, but

application of these algorithms in the design of systems with supplemental passive damping devices is a promising area of application that remains to be demonstrated and studied.

1.1.3 Genetic Algorithm (GA)

A genetic algorithm (GA) is used to solve the optimization problems formulated in this research. The GA is a stochastic global search method and optimization algorithm inspired by processes normally associated with natural biological evolution. GA's operate on a population of potential solutions applying the principle of survival of the fittest to produce better and better approximations to a solution [1.26]. At each generation, a new set of solutions (individuals) is created by the process of selecting individuals according to their level of fitness in the problem design space and exchanging characteristics of each (mating) using operators analogous to those found in natural genetics. "This process leads to the evolution of populations of individuals that are better suited to their environment than the individuals that they were created from, just as in natural adaptation" [1.26].

The GA simulates the rules of natural genetic evolution by systematically applying reproduction operations termed selection, crossover, and mutation. A population of individuals is generated and the genetic make-up of each individual is constructed by encoding its design variables into a single binary string, chromosome, composed over an alphabet. The genotypes (chromosome values) are uniquely mapped onto the decision variable (phenotypic) domain. The most commonly used representation in GAs is the binary alphabet $\{0, 1\}$, but other encodings are also possible (e.g. ternary, integer, real-

valued, objects [1.27, 1.30]). For example, a problem with two variables, x_1 , x_2 , may be mapped onto binary-string chromosome structure as shown in Figure 1.7. x_1 is encoded with 10 bits and x_2 with 15 bits, possibly reflecting the level of accuracy or range of the individual decision variables.

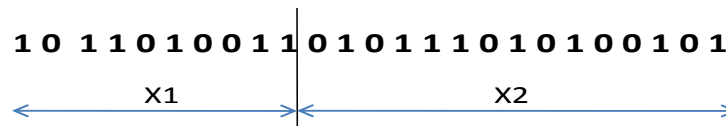


Figure 1.7 Design Variables Mapped onto Binary Chromosome.

A genetic algorithm initializes a population of solutions randomly, and then improves it through repetitive application of reproduction operations of mutation, crossover and selection. In each generation, the fitness of every individual in the population is evaluated. A fitness function, which is always problem dependent, is defined for each individual candidate solution. This fitness is used to evaluate the quality of the solutions in the population relative to one another. Multiple individuals are selected from the current population (based on their fitness) and modified (recombined and possibly randomly mutated) to form a new population. The new population is then used in the next generation of the algorithm. The GA is often terminated when termination criteria are satisfied (*e.g.* a certain number of generations).

The selection operator is used to produce the next generation of individuals. Common selection operators are fitness-proportionate and roulette wheel selection. With fitness-proportionate selection, the probability of being selected for reproduction is proportional to an individual's fitness. The value of individual's fitness is used in the selection to establish bias towards more fit individuals. Highly fit individuals, relative to

the entire population, have a higher probability of being selected for mating whereas less fit individuals have a correspondingly lower probability of being selected [1.29]. There are many other types of reproduction operators that have been proposed over the years, but they will not be reviewed here. The interested reader is referred to the seminal work by Goldberg [1.31] for additional selection mechanisms and discussion of their characteristics and implementation.

The simplest recombination operator is called single-point crossover. Single point crossover proceeds by cutting the pair of selected chromosomal strings at a random locus picked by selecting a random number between 1 and the chromosomal string length $L-1$ and swapping the tails to create two child strings. Considering the two parent binary strings in Table 1.2, if the crossover location is 4, the genetic information is exchanged between the individuals about this point, then two new offspring strings are produced. This crossover operation is not necessarily performed on all strings in the population. Instead, it is applied to chromosomal strings selected for breeding from the population with defined probability P_x . Crossover operations allow the search space to be explored in a wider or global manner.

Table 1.2 Example of Crossover Operator

Mating Individual	Parent Strings	Children Strings
1	1010 0010101	1010 1111111
2	1111 1111111	1111 0010101

Another genetic operator, mutation, is often applied to the new chromosomes with a small set probability P_m . Mutation causes the individual genetic representation to be changed slightly according to a defined probabilistic rule. The slight variation in the

individual chromosome that results from the mutation operations allows the search space to be explored in a local manner in the near vicinity of solutions. In the binary string representation, mutation will cause a single bit to change its state, $0 \rightarrow 1$ or $1 \rightarrow 0$.

Therefore, mutating the fourth bit of the following binary string: 1 0 1 (1) 1 1 1 0 leads to the new string 1 0 1 (0) 1 1 1 0. Mutation is generally considered to be a background operator that ensures the probability of searching a particular local subspace of the problem space [1.29]. This has the effect of inhibiting the possibility of converging to a local optimum, rather than the global optimum.

After recombination and mutation, the individual strings are then decoded, the objective function evaluated, a fitness value assigned to each individual and individuals selected from mating according to their fitness, and the process continues through subsequent generation. In this way, the average performance of individuals in a population is expected to increase, as good individuals are preserved and bred with one another and the less fit individuals die out.

1.2 Objectives and Scope

There are several objectives for this dissertation. The first is to develop an accurate time history analysis tool which is suitable for conducting nonlinear time-history analysis of 2D multiple degree of freedom steel frame structures with linear/nonlinear viscous and viscoelastic dampers and nonlinear material response. As will be discussed later in the dissertation, accurate modeling of nonlinear behavior that includes nonlinear viscoelastic damping components is difficult and accurate modeling algorithms and software do not exist at present. The simulation tool developed will be used to evaluate structural

response when a steel framing system is subjected to ground motion. The tool developed will then be used as the foundation for an automated and optimized design algorithm for steel framed structural systems with supplemental damping devices. While nonlinear analysis of steel systems with supplemental linear viscous damping systems is relatively well established, there is a need to develop accurate modeling tools for simulating structural response during ground motion with supplemental nonlinear viscous and viscoelastic damping elements and nonlinear material behavior.

The second objective is to develop, implement, and evaluate an optimization algorithm capable of automating the design of 2D frame structures modeled as shear buildings with linear/nonlinear viscoelastic dampers within the context of the risk- or performance-based engineering methodology. The design problems for which this algorithm will be targeted are limited to frames with known topology, loading, and material properties. The research will focus on the application of a genetic algorithm (GA) for identifying damper parameters (including viscous and viscoelastic properties), damper location; and wide-flange shape for column members from a database of available AISC wide flanged sections,

The optimization problem will include multiple competing objectives: (1) minimize the initial capital investment in the structural system including dampers; (2) minimize the expected direct economic losses due to the damage to structural and non-structural components. The structural model for the 2D frames considered used is the shear building model. As such, the beam members are considered rigid and are not assumed to be design variables. The area of multiple objective structural optimization is a

relatively new arena and automated design of steel framing systems with damping systems for multiple competing objectives has not been demonstrated and studied.

HAZUS [1.26] procedures are used to define and assess the damage to both Structural System components (SS), Non-structural Drift-sensitive components (NSD) and Non-structural Acceleration-sensitive components (NSA). Fragility curves [1.26] will be used to define the probability of SS, NSA, and NSD components residing in the pre-defined damage states of none, slight, moderate, extensive, and complete. The HAZUS [1.26] procedures will also be used to assign repair costs to these damage states. Transient analysis of the steel systems subjected to simulated and measured ground motions consistent with three recurrence probabilities is used as the basis for the damage assessment. While these procedures have been successfully implemented for steel framing systems without dampers [1.28], these risk-based design methodologies have not been explored within the context of the design of steel framing systems with supplemental damping systems.

The research will introduce the use of the distributed computing capability of MATLAB [1.32] and the distributed computing Toolbox™ [1.32] on a personal computer cluster with 4 computer nodes to speed up the optimization algorithm for automated design and handle larger data sets. Implementation of the algorithms developed will be done on this 4-node computational cluster. It is well known that distributed computing can speed up the application of a genetic algorithm, but applications within the realm of structural engineering have been sparse if not-existent. The proposed research will contribute to understanding the benefits of cluster computing

in this realm and will provide a concrete example of its implementation in the field of structural engineering optimization.

Finally, this study intends to illustrate the impact of supplemental damping systems and their characteristics for minimizing initial construction costs and minimizing expected annual loss due to a predefined seismic hazard. The dissertation also seeks to provide the reader with examples of how design variable number and arrangement changes the resulting frame designs. Finally, the design case studies provided in this dissertation intend to provide the reader with steel frame designs conducted within the context of multiple-objective risk-based optimization of steel framing systems to illustrate the trade-offs in initial construction cost and expected annual losses likely for systems that include supplemental damping components.

1.3 Thesis Overview

To accomplish the objectives mentioned above, an automated tool for risk- or performance-based seismic design optimization using an evolutionary algorithm for shear buildings with supplemental dampers is developed. Chapter 2 outlines the development and validation of an algorithmic approach for nonlinear time-history analysis of 2D steel frame structures with linear/nonlinear viscous/viscoelastic dampers. The validation is conducted via comparison to theoretical (analytically-based) solutions and comparison to solutions generated using research-grade software.

Chapter 3 provides an overview and discussion of the formulation of the risk- or performance-based seismic design methodology, the development of optimized design statements for the multiple objectives of minimizing total initial construction cost of the

structural system and expected annual loss. Detailed discussion of the constraints for the design problem considered and the use of penalty factors to transform the optimized design problem to one that is unconstrained is discussed. Detailed discussion of the genetic algorithm developed to tackle the multiple objective design problem formulated is also provided.

Chapter 4 of the dissertation includes illustration of the application of the automated-design algorithm to a single steel frame topology. Ten design cases are formulated and the algorithm developed is used to generate optimized designs that populate Pareto fronts in objective space. These cases are designed to explore the following: (a) variation in design variable number and configuration and its effect on the resulting Pareto fronts generated; (b) how damper characteristics affect designs and achieving the multiple objectives used as the basis for the optimization problem considered; and (c) how supplemental damping systems affect initial construction cost and expected annual losses for low-rise steel framing systems.

Chapter 5 includes a summary of the dissertation contents, provides conclusions and insights learned through completion of the dissertation, and provides the reader with recommendations on future research directions.

Chapter 2

Transient Analysis of Systems with Viscous and Viscoelastic Damping

2.1 Introduction

Simulating the response of damped structural systems to horizontal ground accelerations is the foundation for the research effort described in this dissertation. Therefore, the theory supporting this simulation is outlined in the present chapter and algorithms used to compute the response of viscous and viscoelastically damped single- and multiple-degree of freedom shear-building models are described. Newmark's method of numerical integration is used to solve the equations of motion of systems with added damping.

A single degree of freedom (SDOF) shear building model is used as the basis for discussion related to viscous and viscoelastic damping in governing the response of the system to a forcing function characterized by sinusoidal ground acceleration. The behavior of the SDOF system with viscous and viscoelastic damping (linear and nonlinear) is discussed. The impact of damping on the response of nonlinear (elastic-perfectly-plastic) systems is also discussed. Simulations using the algorithms developed are compared to analytical solutions developed using first principles (differential equations).

Six multistory MDOF shear-building models were used to develop and evaluate the algorithms formulated for computing response of systems that include supplemental passive damping to ground accelerations. Comparisons of response simulations made with recognized open- source research-grade software [2.1] are described. These

comparisons were made using the 1940 El Centro (Imperial Valley) ground motion record.

2.2 Foundational Theory

Passive fluid dampers have been studied and utilized for seismic protection of building structures for two decades. Characteristics of fluid dampers that are of particular importance to engineers include their reliability, their high-energy dissipation capacity and their ability to produce forces that are velocity-dependent [1.14]. Viscoelastic (VE) dampers installed in structures have been found to be effective for resisting lateral loads introduced by seismic and wind forces. The addition of VE dampers results in a significant increase in modal damping ratios and an accompanying increase in structure stiffness [2.2].

There are two fundamental modeling approaches for damping often used in simulating the response of structural systems with dampers: classical damping (often termed proportional or Rayleigh damping); and non-classical damping (sometimes called non-proportional damping). The discussion can begin by considering the 3-DOF system with inherent and supplemental damping as shown in Figure 2.1. Horizontal equilibrium of the mass at each level at any point in time gives the following coupled equations of equilibrium:

$$\sum F_x = 0$$

$$m_3 \ddot{u}_g(t) - f_3^S - f_3^D - m_3 \ddot{U}_3 = 0 \quad (2.1)$$

$$m_2 \ddot{u}_g(t) + f_3^S + f_3^D - f_2^S - f_2^D - m_2 \ddot{U}_2 = 0 \quad (2.2)$$

$$m_1 \ddot{u}_g(t) + f_2^S + f_2^D - f_1^S - f_1^D - m_1 \ddot{U}_1 = 0 \quad (2.3)$$

In general, the spring force, f_i^S and damping forces, f_i^D in equations (2.1) through (2.3) can be nonlinear functions of relative displacement and relative velocity. The spring and damping forces included in these equations need to be examined in significant detail to completely illustrate how modeling nonlinear spring behavior and linear/nonlinear damping occurs in this research effort.

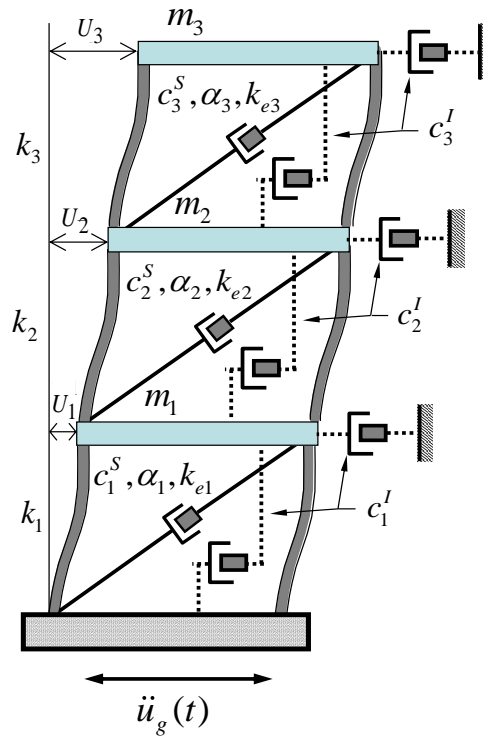


Figure 2.1 Typical MDOF Shear-Building System with Inherent and Supplemental Damping.

The discussion can begin with the spring forces. In general, the spring forces can be nonlinear functions of relative displacement. Therefore, the spring force at any level i can be written as,

$$f_i^S = f(k_i, u_i) \quad (2.4)$$

where k_i represents the linear spring stiffness at level i and u_i is the relative (interstory) displacement at level i . The spring stiffness response characteristics used in the present dissertation are assumed to be elastic perfectly plastic as shown in Figure 2.2.

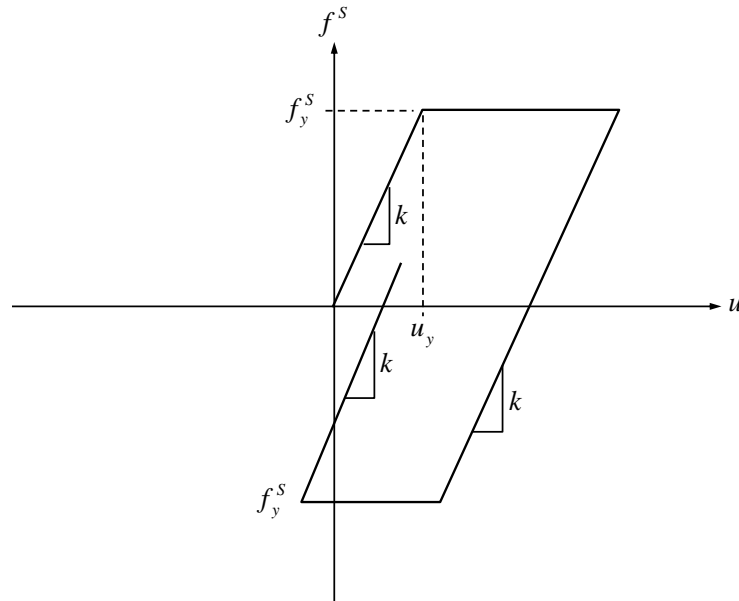


Figure 2.2 Nonlinear Spring Response Characteristics.

Damping forces are most often modeled using viscous damping characteristics. The general damping force versus relative velocity response characteristics at any level i is shown schematically in Figure 2.3. A viscous damping force model has the following general form,

$$f^D = f(c_i, \alpha_i, \dot{u}_i) \quad (2.5)$$

where \dot{u}_i represents the interstory (relative) velocity. Linear viscous damping response is modeled using $\alpha = 1$ and the slope of the response in force-velocity space is given by the damping coefficient c . It should be noted that Figure 2.1 illustrates two damping coefficients: (a) inherent damping $-c_i^I$ and (b) supplemental damping $-c_i^S$. The

inherent damping coefficient is formulated using summation of damping that is proportional to stiffness and proportional to mass (*i.e.* Rayleigh or classical damping).

Figure 2.3 illustrates supplemental viscous damper response in force-displacement space (hysteresis) and force velocity space. The area enclosed by the damping response in the hysteresis is called the hysteretic energy dissipated by the viscous damping. Hysteretic energy dissipation through yielding will also occur when the nonlinear springs with behavior described in Figure 2.2 are utilized.

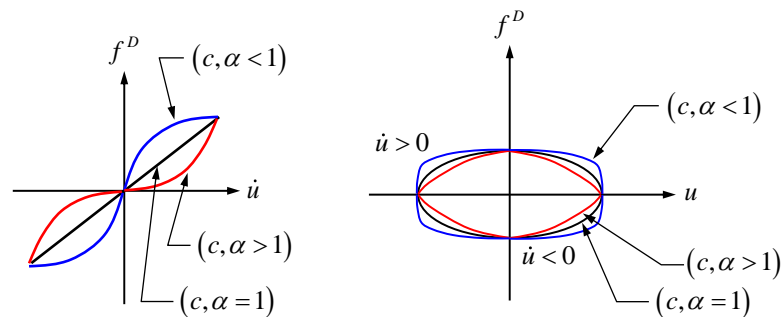


Figure 2.3 Viscous Damping Behavior.

A viscoelastic supplemental damping model is more general and viscous damping is a special case. The typical response characteristics of viscoelastic supplemental damper in force-velocity space are shown in Figure 2.4. The general expression for the viscoelastic damping force is given below,

$$f^D = f(c_i, \alpha_i, \dot{u}_i, k_{ei}^D) \quad (2.6)$$

where k_{ei}^D is the elastic stiffness corresponding to the viscoelastic damper (termed viscoelastic stiffness in the present research). Other than the tilt in the hysteresis, there is very little difference between viscous and viscoelastic damping when observing their

respective force-relative-displacement plots. There is very little difference in the force-relative-velocity behavior.

The damper hysteresis shown in Figure 2.4 illustrates the effects of the elastic stiffness component on the damper hysteretic behavior at any level i . It should be noted that the viscoelastic damping characteristics considered in this dissertation work are those arising from supplemental fluid viscoelastic damper devices.

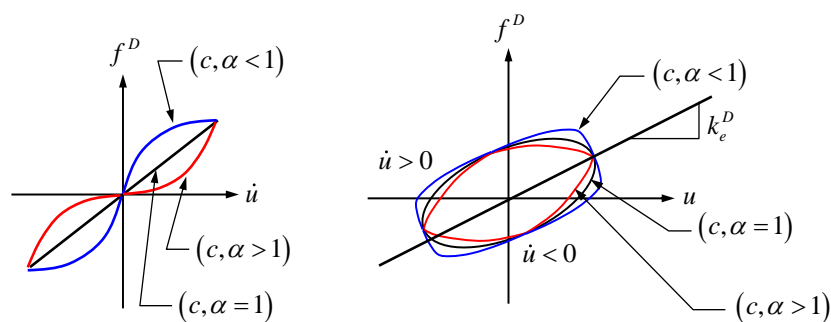


Figure 2.4 Viscoelastic Damping Behavior.

Inclusion of nonlinear response characteristics in the shear building model poses a unique challenge in the structural analysis. The equation of motion for the shear-building model shown in Figure 2.1 follows from equations (2.1) through (2.3) written in matrix form with consideration of equations (2.4) through (2.6) as follows,

$$[M]\{\ddot{U}\} + [C^I + C^D]\{\dot{U}\} + [K^S + K^{DE}]\{U\} = -[M]\{\ddot{u}_g\} \quad (2.7)$$

The terms in equation (2.7) are defined in the following. $[M]$ is the mass matrix. $[C^I]$ is the inherent damping matrix modeled using classical (Rayleigh) damping,

$$[C^I] = a[M] + b[K] \quad (2.8)$$

$[C^D]$ is the supplemental damping matrix where terms are functions of the damping coefficient, the nonlinearity parameter, and relative (interstory) velocity: $f(c_i^S, \alpha_i, \dot{u}_i)$.

The stiffness matrix is separated into the inherent spring stiffness, $[K^S]$, and the viscoelastic damper stiffness, $[K^{DE}]$. The spring stiffness $[K^S]$ is considered to have nonlinear characteristics and the viscoelastic damper stiffness contribution is assumed to be linear.

Stiffness and damping terms in equation (2.7) are functions of interstory (drift) displacement and interstory (relative) velocity, respectively. These equations are nonlinear coupled equations of motion and analysis in the time domain [2.3] is utilized in the present thesis to solve the equations of motion.

2.3 Numerical Integration of the Equations of Motion

A general approach for the solution of the dynamic response of structural systems governed by equation (2.7) is the direct integration of the dynamic equilibrium equations. In 1959, Newmark presented a family of single-step integration methods for the solution of structural dynamic problems for both blast and seismic loading [2.3]. During the past 50 years, Newmark's method has been applied to the dynamic analysis of many practical engineering structures. However, it was felt that outlining the procedure in this section of the chapter would provide the reader with a complete picture of the dissertation work.

Consider a set of coupled equilibrium equations at any instant in time as given below,

$$M \cdot \ddot{U} + C \cdot \dot{U} + K \cdot U = F \quad (2.9)$$

Where M , C , K are the mass, damping, and stiffness matrices respectively; \ddot{U} , \dot{U} , and U are the acceleration, velocity, and displacement; and F is the external force vector. It should be noted that the damping and stiffness matrices can be nonlinear. The well-known algorithm for the numerical integration of equation (2.9) is defined by [2.3],

$$U_t = U_{t-\Delta t} + \Delta t \dot{U}_{t-\Delta t} + \left(\frac{1}{2} - \beta\right) \Delta t^2 \ddot{U}_{t-\Delta t} + \beta \Delta t^2 \ddot{U}_t \quad (2.10)$$

$$\dot{U}_t = \dot{U}_{t-\Delta t} + (1 - \gamma) \Delta t \ddot{U}_{t-\Delta t} + \gamma \Delta t \ddot{U}_t \quad (2.11)$$

Two forms of integration have been used. The first is called the average acceleration method and the second is called the linear acceleration method. These two methods are all good for small solution time intervals. The average acceleration method is selected for the present dissertation. The parameter settings for these two methods are given below:

$$(1) \quad \gamma = \frac{1}{2} \text{ and } \beta = \frac{1}{4}, \text{ average acceleration method;}$$

$$(2) \quad \gamma = \frac{1}{2} \text{ and } \beta = \frac{1}{6}, \text{ linear acceleration method.}$$

Equations (2.9), (2.10), and (2.11) are used iteratively for each time step. The term \ddot{U}_t was obtained from Equation (2.9) by dividing the equation by the mass associated with the DOF. A flowchart of the algorithm is given in Figure 2.5.

A computer algorithm for nonlinear transient analysis of multiple degree of freedom (MDOF) systems with supplemental viscous or viscoelastic damping was developed based on Newmark's average acceleration method for use in this dissertation research. The Matlab m-file is called `inelasticMDOF.m` and it includes several additional functions that it utilizes. The source code for this m-file is included in

Appendix 9 of the dissertation. Each m-file utilized by `inelasticMDOF.m` is described in the following paragraphs. It should be noted that the discussion is framed within the context of an example MDOF system based upon the shear building model shown in Figure 2.1.

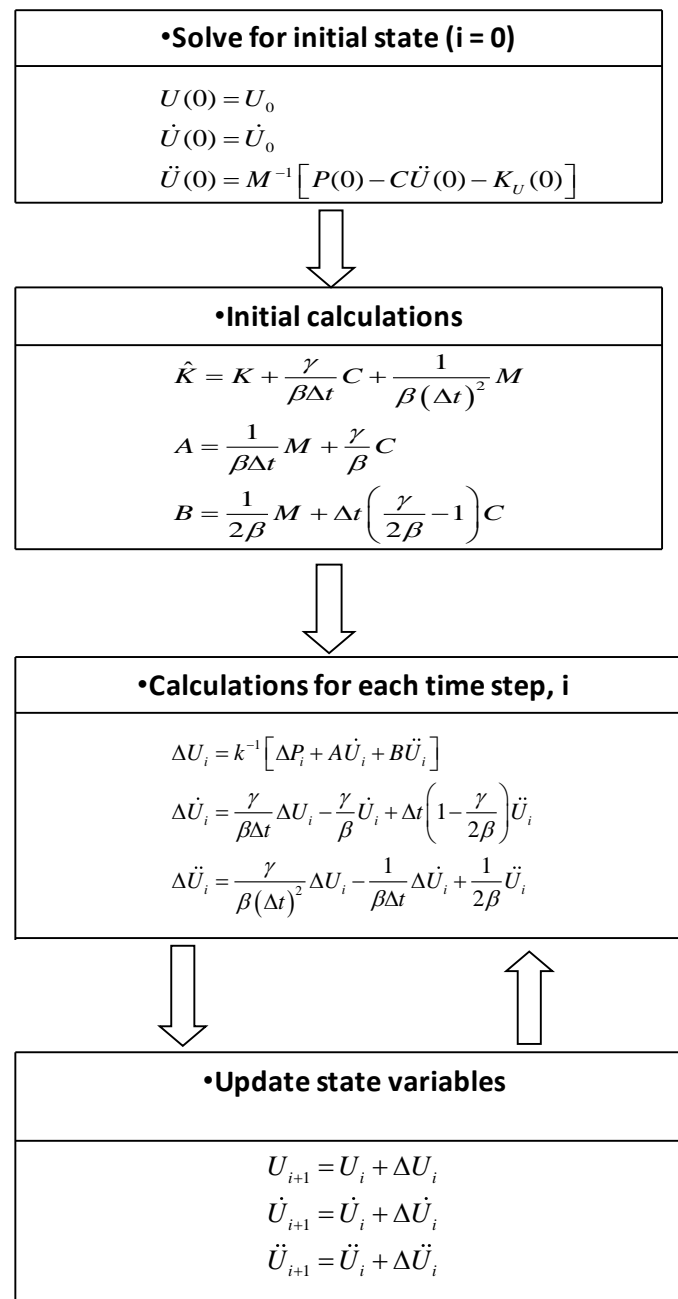


Figure 2.5 Flow Chart for Numerical Integration Algorithm [2.3].

The first m-file, `assembleK.m`, is used to generate the system linear stiffness matrix. For example, a 3-story shear building that includes story stiffness:

$k_1 = 150 \text{ kip/in}$, $k_2 = 100 \text{ kip/in}$ and $k_3 = 50 \text{ kip/in}$ would result in the initial stiffness matrix shown below,

$$K^S = \begin{bmatrix} 250 & -100 & 0 \\ -100 & 150 & -50 \\ 0 & -50 & 50 \end{bmatrix} \quad (2.12)$$

The second m-file is `kCurrent.m`. This m-file is used to calculate current story stiffness during instances in time during the ground motion simulation. If the story j considered is in the elastic stage, its stiffness is given by $k(j) = kElas(j)$. If the displacement of story j exceeds the yield displacement and no viscoelastic damper applied at story j , the stiffness for story j is $k(j) = 0$.

The m-file, `internalForce.m`, is used to calculate the shear forces in each story. It should be noted that the shear forces in the spring models in the story are limited by the yield force capacity of the story.

The m-file, `DamperSlope.m`, is used to calculate the slope of the damper response for the next increment of velocity;

$$F_{d-slope} = \alpha * C * |relVel|^{\alpha-1} \quad (2.13)$$

C is the damping constant in kip-sec/in, α is the velocity exponent and $relVel$ is the relative velocity between the two neighboring stories.

The m-file, `DamperForce.m`, is used to compute the damper force, which includes two parts. The first part is proportional to the relative displacement and is

defined by equation (2.14), and the second part is proportional to the relative velocity and calculated using equation (2.15);

$$F_{d-elas} = relDsp * kDamp \quad (2.14)$$

$$F_{d-visc} = C * relVel^\alpha \quad (2.15)$$

There are several parameters that are needed as input to the driving m-file, `inelasticMDOF.m`. These parameters are briefly defined below;

- `filename`, filename containing the ground acceleration record.
- `zeta`, the percentage of critical damping.
- `freq1`, the first modal frequency for Rayleigh damping computations.
- `freq2`, the second modal frequency for Rayleigh damping computations.
- `m`, the building mass at each floor level (vector).
- `kCol`, the building stiffness at each story (vector).
- `kDamp`, the damper stiffness matrix.
- `Coef`, the coefficient for the supplemental damper at each story (vector).
- `Alpha`, the velocity exponent for the supplemental dampers at each story (vector).
- `Vyld`, the story yield force (vector).
- `timeEnd`, the ending time for the response computation
- `nSol`, the number of solution substeps within ground motion time interval

Pseudo code for the algorithm used to conduct the nonlinear transient analysis of 2D MDOF systems with viscous/viscoelastic dampers is described in the following:

1. Read in the time-history acceleration data from `fileName` to matrix, $U_g_dd(numRec)$, where `numRec` is total number of Records.
2. Generate u_dd which is an array of time vs. ground acceleration at solution increment desired using linear interpolation method.
3. Initialize the stiffness matrix using function `assembleK.m`.
4. Generate the mass matrix for the shear building model.
5. Compute natural frequencies via, eigen value analysis.
6. Compute the classical damping matrix using Rayleigh damping method.
7. Execute the Newmark algorithm for numerical integration.

2.4 Response Simulation Algorithm Validation

The algorithm was implemented in a computer program written as a series of Matlab m-files (see Appendix 1 through 21 of the dissertation). The numerical integration algorithm is contained in the Matlab m-file called `inelasticMDOF.m`. This section of the dissertation includes a series of comparisons to demonstrate the accuracy of the algorithm for computing the response of linear and nonlinear MDOF shear building models with linear/nonlinear viscous and viscoelastic damping. Several benchmarking cases were developed and comparison between the responses computed using the present algorithm, theory, and other research-grade software is made. Finally, a five story shear building model with nonlinear springs and nonlinear viscous dampers is used to verify that all pertinent behaviors are correctly modeled in the program developed.

2.4.1 Linear Viscous Damping

Damping tends to reduce the amplitude of displacements and velocities in the structural system imparted through the earthquake hazard. In the simplest case, linear viscous damping forces may be mathematically modeled as being proportional to velocity as given below,

$$f^D(t) = c^S \dot{u}(t) \quad (2.16)$$

Consider the SDOF system shown in Figure 2.6. It includes inherent damping proportional to mass and stiffness and supplemental viscous or viscoelastic damping. The system is subjected to harmonic force given by $p(t) = p_0 \sin \bar{\omega}t$ and this harmonic force is translated to a harmonic ground acceleration, $\ddot{u}_g(t) = A_0 \sin \bar{\omega}t$.

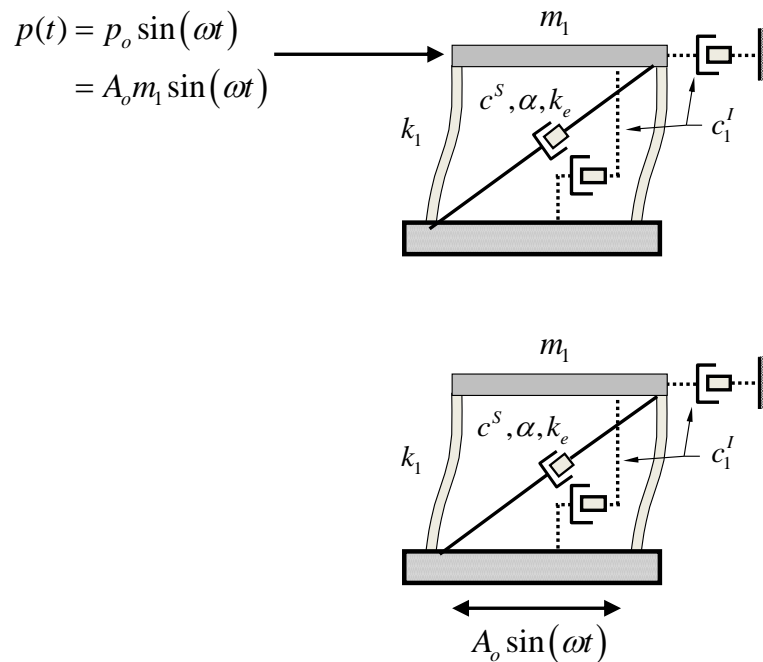


Figure 2.6 Single Degree of Freedom with Inherent Linear Viscous Damping and Equivalent Ground Acceleration.

The damping force in this system can be written as [2.4],

$$\begin{aligned}
 f^D &= c^s \dot{u}(t) = c^s \omega u_0 \cos(\omega t - \phi) \\
 &= c^s \omega \sqrt{u_0^2 - u_0^2 \sin^2(\omega t - \phi)} \\
 &= c^s \omega \sqrt{u_0^2 - [u(t)]^2}
 \end{aligned} \tag{2.17}$$

Equation (2.17) can be re-written as [2.4],

$$\left(\frac{u}{u_0} \right)^2 + \left(\frac{f^D}{c^s \omega u_0} \right)^2 = 1 \tag{2.18}$$

Equation (2.18) describes the hysteretic behavior (force versus displacement response) of the linear viscous damper. The hysteretic behavior follows an elliptical shape.

The SDOF system was given the characteristics are given in Table 2.1. It should be noted that the spring characteristics for this example are linear.

Table 2.1 Characteristics of the One-story Shear Building

m_1 ($k - s^2 / in$)	k_1 (k / in)	c^s ($k - s / in$)	c^l ($k - s / in$)
5	240	100	3.464 *

* -calculated on the basis of 5% of critical damping.

The harmonic (sinusoidal) forcing function was utilized to generate an equivalent horizontal harmonic ground motion acceleration given by,

$$\ddot{u}_g(t) = A_o \cdot \sin(\bar{\omega}t) = 0.25g \cdot \sin(\bar{\omega}t) \tag{2.19}$$

with the excitation frequency being taken as; $\bar{\omega} = 1 \text{ rad / sec.}$

The SDOF system subjected to harmonic forcing function and linear viscous damping has well known solutions for time history response. The parameters in Table 2.1 lead to the following conclusions regarding the system. The inherent damping coefficient and the supplemental damping coefficient lead to the following total damping coefficient for the system,

$$c^T = c^I + c^S = 103.46 \text{ k} \cdot \text{s} / \text{in}$$

The total damping ratio for the system is,

$$\zeta^T = \frac{c^T}{2\sqrt{k_1 \cdot m_1}} = \frac{103.46}{2\sqrt{240(5)}} = 1.49$$

The total damping ratio therefore, indicates that this system is overdamped and there will be very little transient response component for the system prior to it reaching the steady-state response. Using the harmonic loading frequency and natural frequency of the system computed as,

$$\omega = \sqrt{\frac{240}{5}} = 6.93 \text{ rad} / \text{s}$$

we can estimate the dynamic amplification factor as $D_f = 0.94$. Thus, the system parameters selected indicate that the harmonic loading and equivalent harmonic ground acceleration will cause peak displacements that are essentially equal to the magnitude of the static displacement. The amplitude of the forcing function is;

$$A_o m_1 = (0.25 \cdot 386.4) \cdot 5 = 483.0$$

and the static displacement for the system with this applied force is given by,

$$u_{static} = \frac{483}{240} = 2.01 \text{ in}$$

The peak dynamic displacement is therefore $u_{dynamic} = 0.94(2.01) = 1.89 \text{ in}$.

The steady-state elliptical damping response given by equation (2.18) is known as a hysteresis loop. The elliptical response takes on different shapes due to varying value of α as shown in Figure 2.3. In the case of $\alpha = 1.0$, the dampers have linear behavior.

The theoretical hysteretic response given by equation (2.18) is plotted together with the hysteretic response generated using the algorithms developed. This comparison is shown in Figure 2.7. The figure illustrates that the program developed for use in the present study is capable of doing a very good job simulating the response characteristics of linear viscous damping.

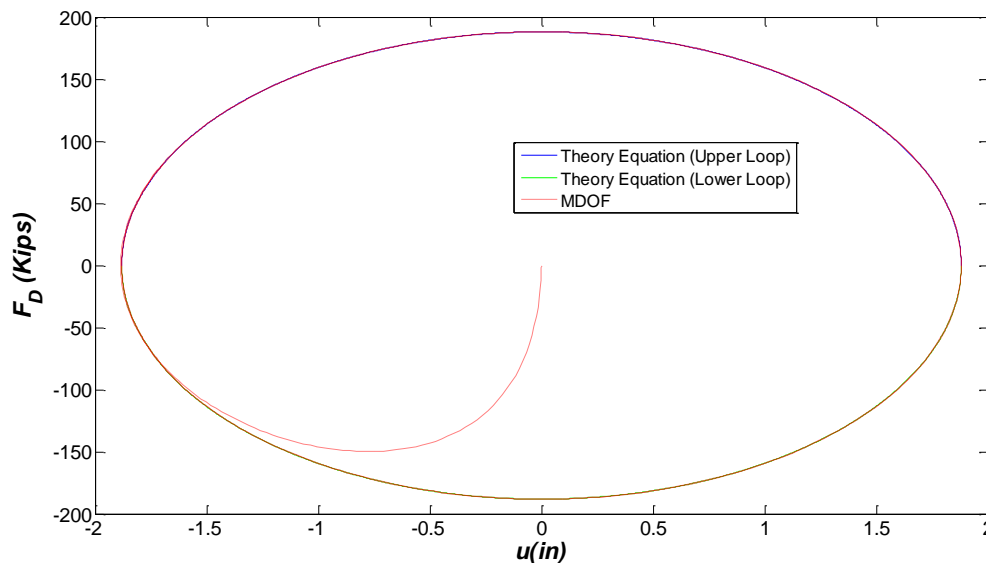


Figure 2.7 Hysteretic Response Comparison for SDOF System in Figure 2.6 with Linear Viscous Supplemental Damper.

The peak dynamic steady-state displacement shown in Figure 2.7 is approximately 1.87 inches. The peak dynamic displacement predicted using first principles approximations is 1.88 inches. Thus, the correlation is quite good and the solution methodology provides accurate results for the case of viscous supplemental dampers.

2.4.2 Linear Viscoelastic Damping

Viscoelastic dampers include elastic stiffness characteristics when subjected to deformation. Viscous materials resist forces as a function of the rate (velocity) at which strain is applied. Elastic materials strain when stretched and their response is independent of strain rate. The total resisting force in the SDOF system considered in the previous section (elastic stiffness generated and damping generated) can be written as,

$$\begin{aligned} f_s + f^D &= k_1 u(t) + k_d u(t) + c^S \dot{u}(t) \\ f^D &= k_d u(t) + c^S \omega \sqrt{u_0^2 - u(t)^2} \end{aligned} \quad (2.20)$$

The plot of f^D against u is the ellipse of Figure 2.3 rotated as shown in Figure 2.4 because of the $k_d u(t)$ term (elastic stiffness of the damper) in equation (2.20).

The accuracy and applicability of the algorithm developed for the present work for analyzing shear-building structures with linear viscoelastic (VE) damping is evaluated using the SDOF frame and equivalent sinusoidal ground motion shown in Figure 2.6 and equation (2.19). The SDOF system has the characteristics given in Table 2.1 and the linear elastic stiffness of the damper is $k_d = 50 \text{ kip} / \text{in}$.

The procedures found in Section 2.4.1 can again be used to estimate the dynamic displacement of the system with viscoelastic dampers. The natural frequency of the system can be approximated as,

$$\omega = \sqrt{\frac{k}{m}} = \sqrt{\frac{240 + 50}{5}} = 7.62 \text{ rad} / \text{s}$$

The total damping coefficient can be estimated as follows,

$$c^I = (0.05) \left[2\sqrt{(5)(290)} \right] = 3.81 \text{ k} \cdot \text{s} / \text{in}$$

$$c^T = c^I + c^S = 103.81 \text{ k} \cdot \text{s} / \text{in}$$

The total damping ratio is therefore,

$$\zeta^T = \frac{c^T}{2\sqrt{k \cdot m_1}} = \frac{103.81}{2\sqrt{290(5)}} = 1.36$$

This again indicates that the system is overdamped. The frequency ratio for the system is estimated as,

$$r = \frac{\bar{\omega}}{\omega} = \frac{1}{7.62} = 0.131$$

and the dynamic amplification factor can be computed as,

$$D_f = \frac{1}{\sqrt{(1-r^2)^2 + (2\zeta r)^2}} = \frac{1}{\sqrt{(1-0.131^2)^2 + (2(1.363)(0.131))^2}} = 0.956$$

The static displacement can be computed as,

$$u_{static} = \frac{483}{290} = 1.67 \text{ in}$$

The peak dynamic displacement is therefore $u_{dynamic} = 0.96(1.67) = 1.59 \text{ in}$.

Hysteretic response simulations generated using the present algorithm for the linear VE-damped SDOF frame subjected to the equivalent sinusoidal ground motion computed using equation (2.19) are plotted together in Figure 2.8. The simulation performed using the algorithm developed for the present study results in a hysteretic damper response that correlates nearly perfectly with the theoretical results. The peak dynamic displacement predicted using first principles is approximately 1.59 and this correlates quite favorably with the peak displacements given in Figure 2.8.

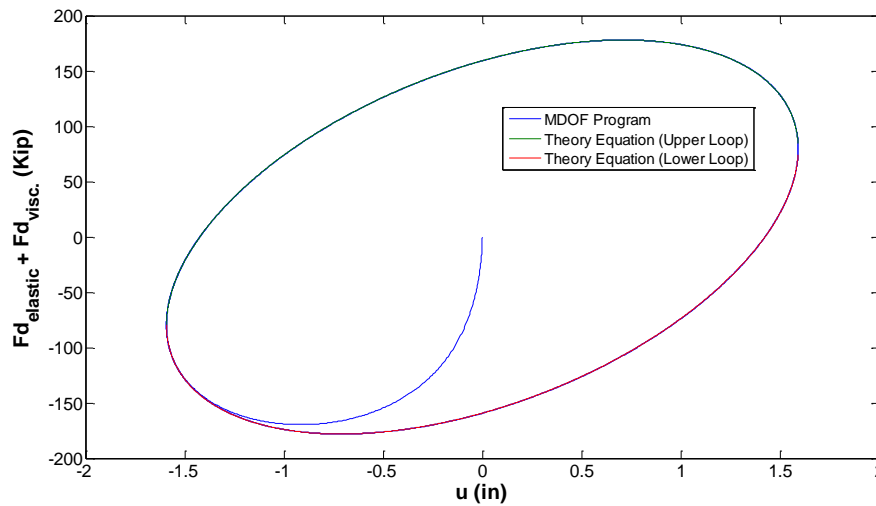


Figure 2.8 Hysteretic Response Comparison for SDOF System in Figure 2.6 with Linear Viscoelastic Damping.

The results of first principles analysis of the SDOF viscoelastically damped system and the results generated using the algorithm and program developed for use in this thesis correlate quite favorably and the programs developed are accurately modeling linear viscoelastic and viscous systems.

2.4.3 Nonlinear Viscous Damping

The force and velocity relationship for a nonlinear viscous damper can be characterized as,

$$f^D = c^s V^\alpha \quad (2.21)$$

Where V is the relative velocity across the damper and α is a constant exponent which can be any value within a typical range of 0.30 to 1.95. The exact value for α depends on the shape of the piston head. The best values ranges from 0.3 to 1.0 for structural applications [2.5]. In the case of $\alpha = 1.0$, the dampers have linear behavior. The

manufacturer determines the velocity at which the dampers can displace and the maximum displacement that the shafts of the piston can undergo. The most common values for V are between 0.6 - 1.50 in/s. The practical range for the damper coefficient, c^s , is 100 - 200 lb-s/in [2.5], but the range can expand.

Let's again assume that the linear elastic (stiffness) SDOF system shown in Figure 2.6 is subjected to the harmonic force: $p(t) = p_0 \sin \bar{\omega}t$. The equation of motion for a system with nonlinear viscous or viscoelastic damping can be expressed as,

$$m_1\ddot{u} + c^l\dot{u} + c^s\dot{u}^\alpha + k_1u + k_du = p_0 \sin \bar{\omega}t \quad (2.22)$$

where all terms in equation (2.22) have been defined previously. If viscous damping is considered, equation (2.22) reduces to,

$$m_1\ddot{u} + c^l\dot{u} + c^s\dot{u}^\alpha + k_1u = p_0 \sin \bar{\omega}t$$

The SDOF shear building model with nonlinear viscous damping characteristics was again used to compute system response when subjected to sinusoidal ground motion accelerations. The SDOF system characteristics are given in Table 2.1.

The displacement time history and the hysteretic loops computed using the simulation algorithm generated in this study and those computed by solving Eq. (2.22) using MATLAB ODE45 solver [2.6]. The default options for ODE45 were initially utilized. Relative tolerance settings were altered from the default values as well. The nonlinear viscous damping problem could not be solved without generating real and complex components to the displacement time histories. While not ideal, plotting the real component of the ODE45 solution allows a qualitative comparison of the solution generated by ODE45 and the program written for the present study. As a result, the

quality of the solutions generated by the algorithms generated for later use in this thesis can be evaluated.

The velocity exponent chosen for comparison was 0.50. Figure 2.9 illustrates the displacement time histories for the ODE45 solver and the MDOF program.

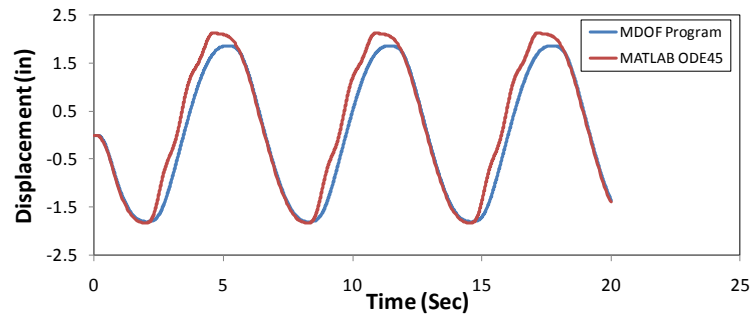


Figure 2.9 Displacement Comparison for SDOF System in Figure 2.6 with Nonlinear Viscous Damping, $\alpha = 0.5$.

Only the real component of the displacement is plotted. The overdamped system has the expected response that includes nearly immediate migration to the steady-state response with a period equal to that of the harmonic ground motion or force (6.28 s). Figure 2.10 illustrates the hysteretic response of the supplemental damper.

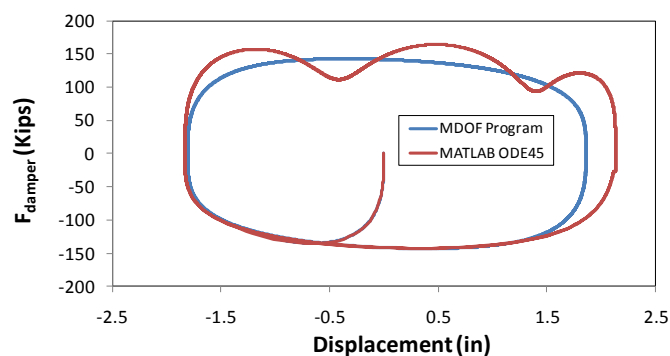


Figure 2.10 Hysteretic Response Comparison for SDOF System in Figure 2.6 with Nonlinear Viscous Damping, $\alpha = 0.5$.

The steady-state damper response includes the expected elliptical hysteresis for the velocity exponent chosen. Only the real component of the displacement response computed by ODE45 is included in Figure 2.10. As a result, there is deviation from the solution generated by MDOF, but the hysteresis shape is preserved. The m-files used as the basis for MDOF generated are able to numerically solve this difficult nonlinear differential equation very effectively. In fact, the MDOF solution can be considered as a benchmark solution for this problem.

2.4.4 Nonlinear Viscoelastic Damping

The final condition used in the algorithm validation for SDOF systems is one that includes nonlinear viscoelastic damping. The same SDOF frame and sinusoidal ground motion in Figure 2.6 is considered and the equation of motion is given by equation (2.22). The linear elastic stiffness of the damper in the system used as the basis for comparison was defined as $k_d = 50kip/in$. The damping coefficient, the linear elastic spring stiffness, and the SDOF system mass are given in Table 2.1 and the velocity exponent was taken as 0.50.

The displacement time history for the system in Figure 2.6 was computed using the algorithm developed for this thesis work and the response of the system was also determined using the MATLAB ODE45 solver [2.6]. Figure 2.11 illustrates the displacement time histories for both solutions. Only the real components of the displacements are plotted. The response is similar to that illustrated in Figure 2.9. The system is overdamped in both cases and the main difference in the response is the peak dynamic displacement magnitude (less in Figure 2.11). The viscoelastic stiffness of the

damper in this case serves to reduce the dynamic displacement from that seen in the previous system.

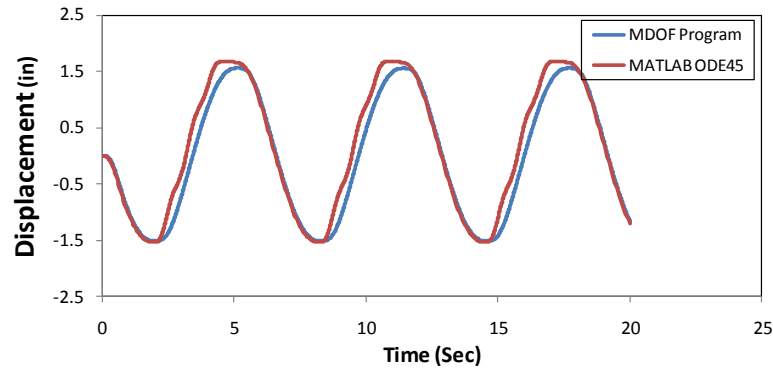


Figure 2.11 Displacement Time History Response Comparison for SDOF System in Figure 2.6 with Nonlinear Viscoelastic Damping, $\alpha = 0.5$.

The hysteretic loop (steady-state response) computed using the algorithm developed for current use (MDOF program) is plotted in Figure 2.12. The solution generated using ODE45 was similar to that shown in Figure 2.11 and the hysteretic response qualitatively followed that of the MDOF program.

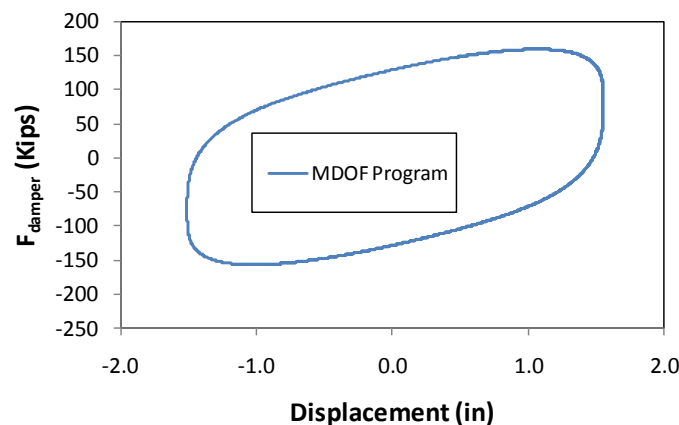


Figure 2.12 Hysteretic Response for SDOF System in Figure 2.6 with Nonlinear Viscoelastic Damping, $\alpha = 0.5$, $k_d = 50 \text{ k/in}$.

The steady-state damper hysteresis generated by the MDOF program shows the expected tilted, flattened, elliptical shape expected for a viscoelastic damper with the parameters used.

The time history response and the hysteretic behavior of the supplemental damper illustrates that the MDOF program is capable of generating accurate solutions to dynamic systems with nonlinear viscoelastic and viscous supplemental damping. The comparisons given in Figures 2.9 through 2.12 indicates the algorithm developed is capable of simulating the response quite well and the methodology developed for the present study is a suitable tool for analyzing building structures with supplemental nonlinear viscous or viscoelastic dampers.

2.4.5 Energy Dissipation

The final SDOF system comparison that was made to evaluate the computer algorithm used to simulate the ground motion response of 2D shear building systems with supplemental linear/nonlinear viscous/viscoelastic damping was based upon energy dissipation characteristics of the damper systems. The area within the damper force hysteresis loop gives the energy dissipated by dampers in the system. In the case of $\alpha = 1.0$, the area enclosed by the hysteretic ellipse is [2.4],

$$E_D = \int f^D du = \int_0^{2\pi/\bar{\omega}} (c^S \dot{u}) \dot{u} dt = \int_0^{2\pi/\bar{\omega}} c^S \dot{u}^2 dt = \pi c^S \bar{\omega} u_0^2 \quad (2.24)$$

It should be noted that equation (2.24) is for one cycle of deformation for vibrations in the steady state. The peak dynamic displacement is u_o .

The SDOF system parameters for a system with linear viscous dampers are given in Table 2.2. The energy dissipated by the dampers in the solution generate by the

MDOF program was determined through numerical integration of the damper force versus relative displacement response for one hysteretic cycle of vibration in the steady state. The period for this is 6.28 seconds. Because the system is overdamped, the response in any 6.28 second cycle can be chosen.

Table 2.2 Dynamic Properties of One – Story Shear Building (SDOF system)

Mode	ω (rad/s)	c^s (k-s/in)	$\bar{\omega}$ (rad/s)	\bar{T} (sec)	u_0 (in)	ED (kips-in)
1	6.928	100	1	6.28	1.8810	1111.5

The accumulated energy dissipated by the dampers computed using the m-files developed for use in this thesis work (MDOF) for various damper types is shown in Figure 2.13.

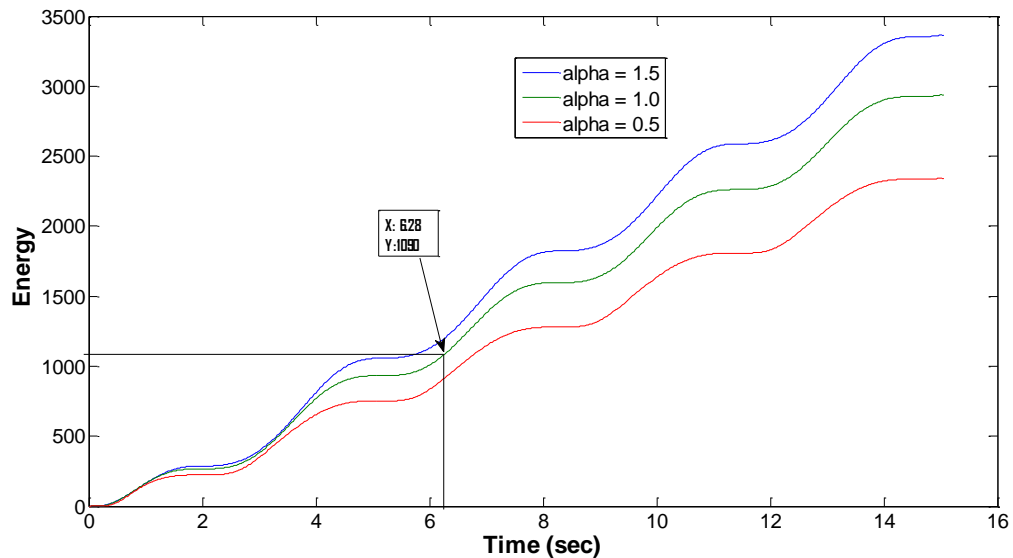


Figure 2.13 Energy Dissipated by Dampers in One Cycle of Steady-State Vibration.

The energy dissipated in any one cycle in the steady state can be numerically integrated using the response shown in Figure 2.13. As mentioned earlier, any cycle can

be chosen because the system is overdamped. The present analysis utilized the first cycle in the response and therefore, there is slight error introduced into the numerical integration. The parameters in Table 2.2 lead to the energy dissipated by the damper computed using equation (2.24) being 1,112 k-in. Numerical integration of the first 6.28 seconds of response shown in Figure 2.13 leads to the energy dissipated being equal to 1,097 k-in. The comparison is excellent and it demonstrates that the numerical simulation is capable of preserving the damper energy dissipation.

2.5 Case Study Comparisons with OpenSees

The Open System for Earthquake Engineering Simulation (OpenSees) [2.1] is being developed by the Pacific Earthquake Engineering Research Center (PEER) for the research and professional communities and it is open-source “object-oriented framework for finite element analysis” [2.1]. The goal of OpenSees is to improve modeling and computational simulation in earthquake engineering through open-source development. Structures in OpenSees can be modeled in 2D or 3D including linear damping and may include elements with degrading stiffness. OpenSees was an option for the present research effort as dynamic analysis software. However, it was not selected because it is under development and it is not able to model nonlinear viscous and nonlinear viscoelastic damping.

The 3-story shear building shown in Figure 2.1 was used as the basis for further comparison of the MDOF program. The motivation for these comparisons was to evaluate the present algorithm’s capabilities with respect to modeling multi-story shear-

building system behavior with/without supplemental dampers and with/without diagonal bracing.

The OpenSees computer program is not designed for shear building analysis and the model used in OpenSees had to be modified to simulate shear building-type behavior. As outlined earlier, the algorithm formulated for simulations in this dissertation assumes shear building behavior.

The following outlines the planar 3-story model used in OpenSees. Columns and beams were steel material with Young's modulus equal to 29,000 ksi. Flexurally rigid beams were desired and $I_g = 100000 \text{ in}^4$, and $A_g = 100000 \text{ in}^2$ was used. The length of beams in the model topology was $L_{beam} = 144 \text{ in}$. The characteristics of the model and ground motion input are summarized in Table 2.3.

Table 2.3 3–Story Building Model Characteristics.

Story	m_i ($k - s^2 / in$)	Columns		
		I_i (in^4)	k_i (k / in)	H_i (in)
1	15	1,710	398.6	144
2	10	1,710	398.6	144
3	5	1,710	398.6	144
$k_i = 2 \left[\frac{12EI}{H^3} \right]_i = 398.6 \frac{k}{in}$ Earthquake Input Record: 1940 El Centro				

Three cases of damping were considered in the comparisons. c_i^I is defined as the inherent damping coefficient at any story, and c_i^S is the supplemental damping coefficient at any story, which is introduced by adding dampers to the system. k_i is the story (spring) stiffness resulting from column members, and k_{di} is the additional linear-elastic stiffness introduced through dampers. α_i is a constant velocity exponent corresponding to the supplemental dampers and m_i is the mass at story i . Comparison of the simulations computed with those generated using OpenSees [2.1] and the present algorithm are described in the following sections.

2.5.1 Case 1 - No Supplemental Damping Devices or Braces

The first model considered includes no added dampers in the system: $c_i^S = 0$, $k_{di} = 0$.

The system was analyzed with the Matlab m-files (denoted as MDOF or Matlab) and OpenSees [2.1]. The fundamental (1st) and 3rd modal frequencies were used to calculate Rayleigh proportional (inherent system) damping constants a, b with equations (2.25), and (2.26) [2.4],

$$a = \zeta \frac{2\omega_i\omega_j}{\omega_i + \omega_j} \quad (2.25)$$

$$b = \zeta \frac{2}{\omega_i + \omega_j} \quad (2.26)$$

The parameters within equations (2.25) and (2.26) are defined as follows: $i = 1$, $j = 3$, and the inherent damping ratio ζ is a target value of 5%.

Figure 2.14 shows the displacement time-histories for the 3rd floor (roof level) when the model was subjected to the El Centro 1940 earthquake ground acceleration. The two analysis results plotted in this figure illustrate excellent correlation.

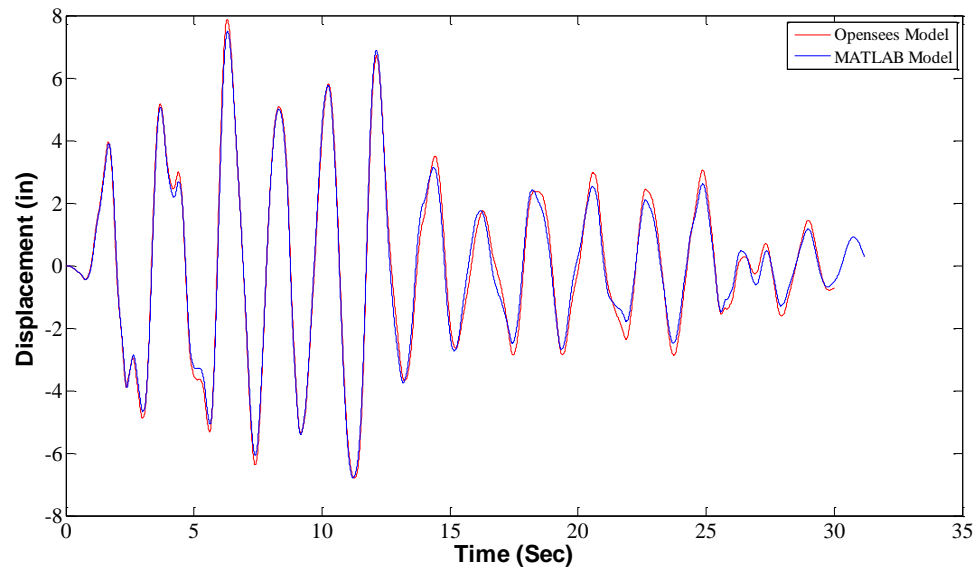


Figure 2.14 The 3rd Floor (Roof Level) Displacement Time Histories.

There is slight deviation in the response histories late in the response after 15 seconds results from implementation of the damping model, but overall the comparison is very, very good.

2.5.2 Case 2 - Elastic Diagonal Braces and No Dampers

The second model considered includes the addition of elastic diagonal braces to the previous case. The elastic braces provide additional linear elastic stiffness at each story. The cross-sectional area of the braces, A , was taken as 20 in^2 . Using frame topology (bay width equal to 144 inches and story height equal to 144 inches, the length of braces can be computed as 203.65 inches based upon an angle, θ , made between the diagonal brace

and horizontal beam. The added horizontal stiffness component resulting from the diagonal braces can be computed using,

$$k_{ei} = \frac{AE}{L} \cos^2 \theta \quad (2.27)$$

If we assume that the material modulus is taken as 29,000 *ksi*, this horizontal stiffness is equal to 1,424 *kips/in*.

A comparison of the computed time histories when the system is subjected to the El-Centro 1940 ground motion are given in Figure 2.13. The results indicate that the computed response histories match nearly perfectly.

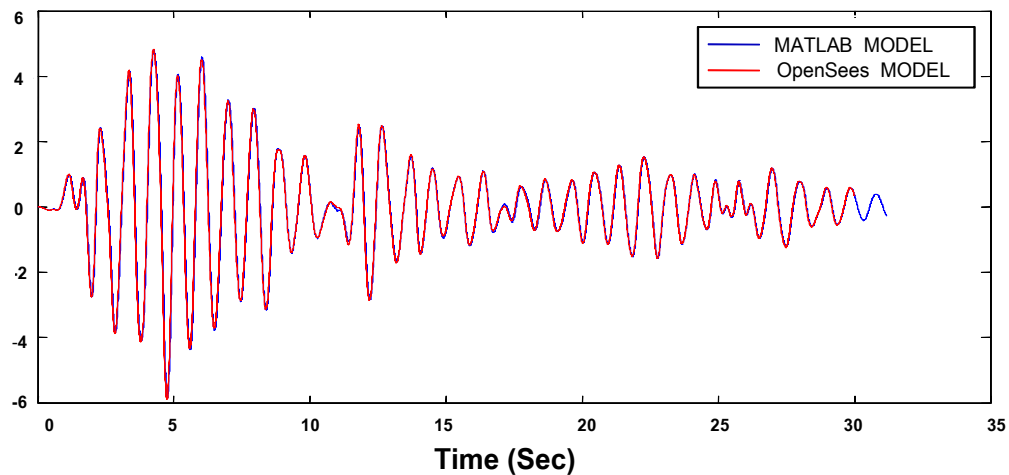


Figure 2.15 The 3rd Floor (roof) Displacement Time Histories for Case 2.

2.5.3 Case 3 and 4 - Supplemental Linear Viscous Dampers

These cases are based on the steel frame (with no braces) from case 1, but now include supplemental linear viscous dampers. Stiffness contribution from the supplemental damping device was not considered, so $k_{ei} = 0, \forall i = 1, 2, 3$ and the systems in these cases

can be considered to have supplemental linear viscous damping with the following characteristics:

$$\text{Case 3: } c_i^S = 100.0 \text{ k-s/in}, \alpha_i = 1.0 \forall i = 1, 2, 3$$

$$\text{Case 4: } c_i^S = 10.0 \text{ k-s/in}, \alpha_i = 1.0 \forall i = 1, 2, 3$$

The inherent damping characteristics remained Rayleigh damping computed for a target of 5% of critical in modes 1 and 3 as outlined in equations (2.25) and (2.26). Ground motions applied as base acceleration again was based in the El Centro 1940 record.

Figures 2.16 and 2.17 include the response time-histories for cases 3 and 4, respectively.

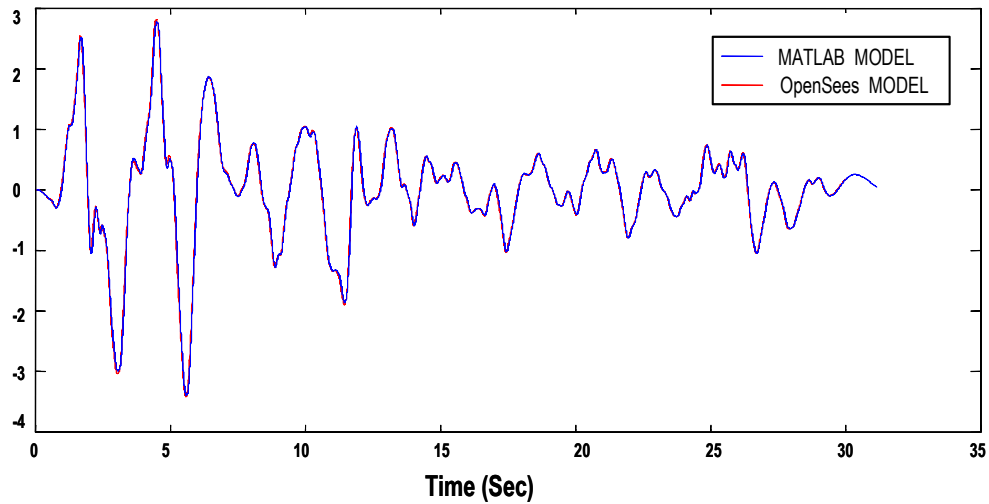


Figure 2.16 The 3rd Floor Displacement Time Histories for Case 3.

The figures illustrate that the time histories computed using both programs essentially lie on top of one another and therefore, the comparison is excellent. Thus, one can conclude that the MDOF program and OpenSees are capable of accurately simulating the response of shear building systems with supplemental linear viscous damping.

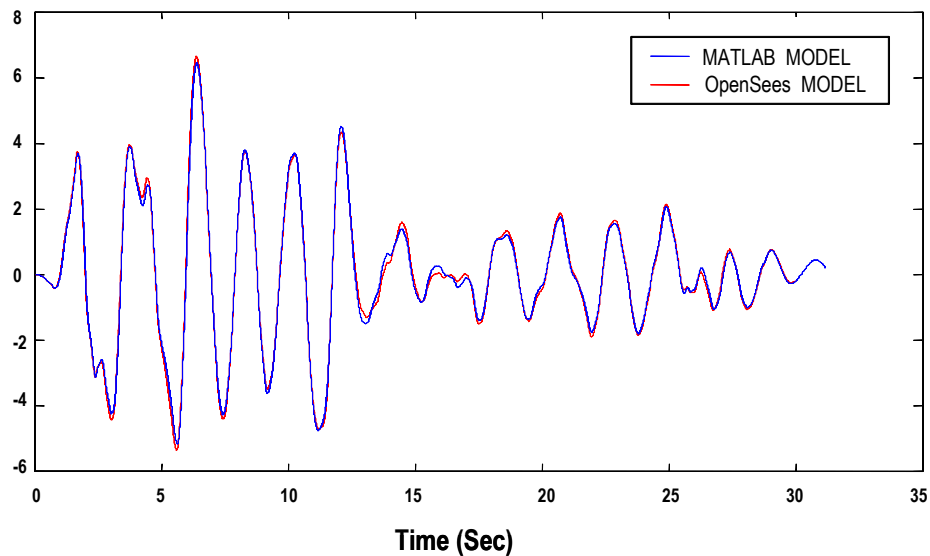


Figure 2.17 The 3rd Floor Displacement Time Histories for Case 4.

2.5.4 Case 5 – Various Supplemental Devices

Another case (composed of many different brace and damper configurations) was studied to validate the MDOF program's capability to accurately simulate system response when linear or nonlinear viscoelastic supplemental dampers exist at various levels throughout the system. The input ground motion acceleration time history was again the El-Centro 1940 record.

Five different shear building configurations were considered in this evaluation case. Inherent (Rayleigh) damping was considered at 5% of critical damping and the first and third modal frequencies were used to establish Rayleigh damping coefficients. The linear-elastic braces and the linear-elastic stiffness component of the viscoelastic damper are based upon a cross-sectional area of 20 square inches and steel material and a diagonal length of the brace or damper, L , in equation (2.27), taken as 203.6 inches. If a steel brace was used, the elastic modulus was set to 29,000 ksi. All dampers had

proportionality coefficients equal to 100 k-s/in and three cases of velocity exponents were evaluated.

The three-story shear building parameters for the three story frame considered in this final evaluation are given in Table 2.4. Figure 2.18 illustrates the time-history response computed using the MDOF computer program developed for use in this dissertation work for a variety of brace and damper configurations.

Table 2.4 System Parameters for the Three-Story Shear Buildings in Case 5.

Story	m ($k \cdot s^2 / in$)	I_g (in^4)	H (in)	k (k / in)	k_e or k_d (k / in)	c^s ($k \cdot s / in$)
1	15	1,710	144	398.6	150	100
2	10	1,710	144	398.6	150	50
3	5	1,710	144	398.6	150	10

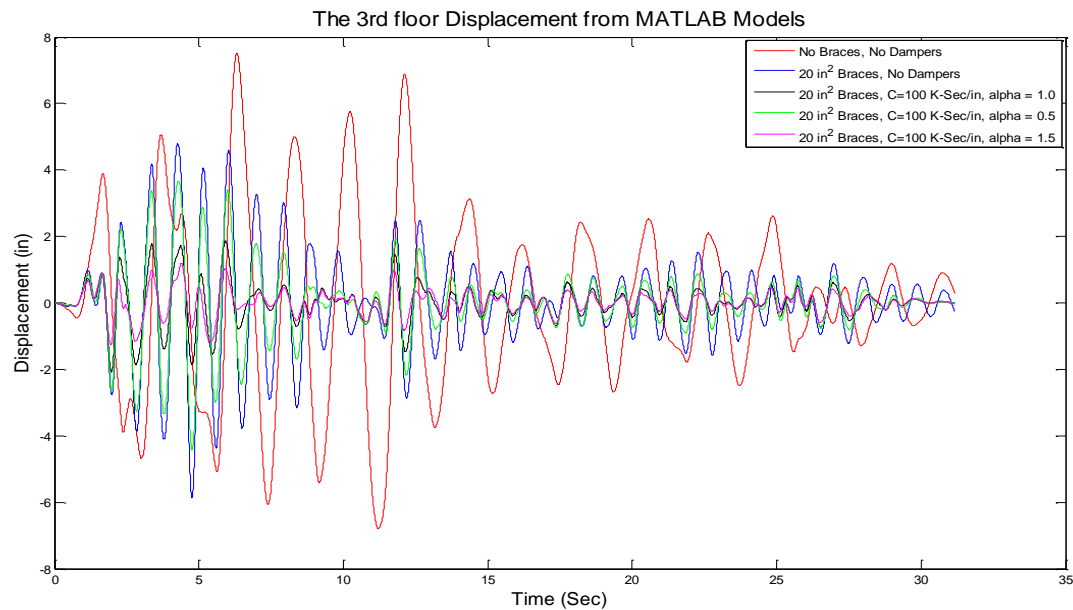


Figure 2.18 The 3rd Floor Displacement Time Histories for Case 5 Systems.

As expected, the presence of supplemental dampers significantly reduces the horizontal displacement at the roof (top floor) level. It appears the greatest reduction in horizontal displacement comes from the velocity exponent being equal to 1.50. However, the roof displacement for all damper configurations is relatively consistent with one another with exceptions occurring relatively early in the systems response to the El Centro record (10 seconds or earlier in the response). Frame configurations with added dampers undergo considerably reduced amplitude of vibration in comparison to the structure without the energy dissipation system when subjected to the same ground motion record. Overall, the behavior of the systems followed expected response characteristics.

A slight modification to the framework described in the data found in Table 2.4 in which different damper velocity exponents exist at each level in the frame was used as a follow-up evaluation to ensure that the programming of the nonlinear damper characteristics were correct. The damper velocity exponents at the first through third stories were 0.5, 1.0, and 1.5, respectively.

Figure 2.19 illustrates a comparison of the force-relative-velocity response for the three different types of viscoelastic dampers at each of the stories in the three story system. It is clearly seen that the linear viscoelastic damper has the expected linear response in force-relative-velocity space. The nonlinear viscoelastic dampers also exhibit the expected behavior. This is an important check of the programming to ensure that correct damping behavior is seen in the system response.

The response illustrated in Figure 2.19 also gives an understanding of the solution increment size needed to accurately trace the force-velocity response characteristics of

the supplemental dampers in the system. If the nonlinear response characteristics did not follow the smooth curves implied by the nonlinear response, one could argue the time steps used for the solution were not small enough. The response in Figure 2.19 indicates that adequate solution time increments were used.

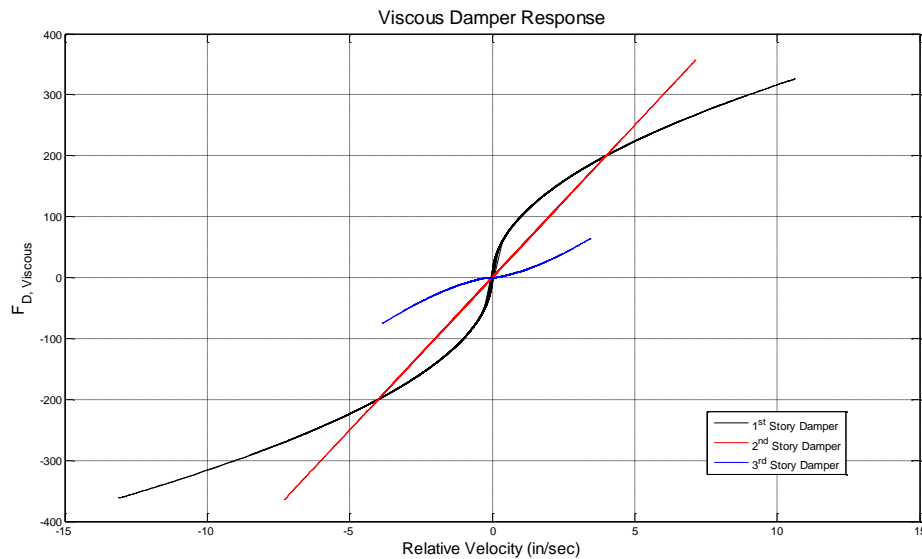


Figure 2.19 Force-Velocity Response for Nonlinear Viscoelastic Dampers in Three-Story Shear Building with Parameters in Table 2.4.

Figures 2.20, 2.21 and 2.22 illustrate the hysteresis loops for the dampers added at each of the three stories computed when the three-story frame is subjected to the El-Centro 1940 ground motion. As expected, the loops are elliptical in shape, but the input ground motion results in some waviness in the shapes and a growth and retraction tendency indicating that the relative displacements imparted through the ground motion are increasing and decreasing during the response. The hysteretic behavior in these loops illustrates expected characteristics consistent with those outlined and discussed earlier in the chapter.

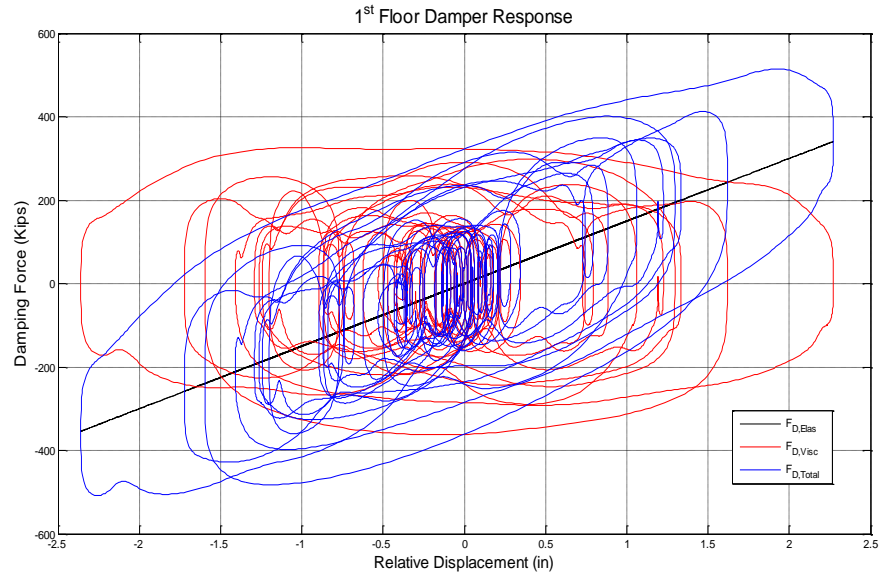


Figure 2.20 Hysteresis Loops of Dampers at Story 1 in Three Story Frame.

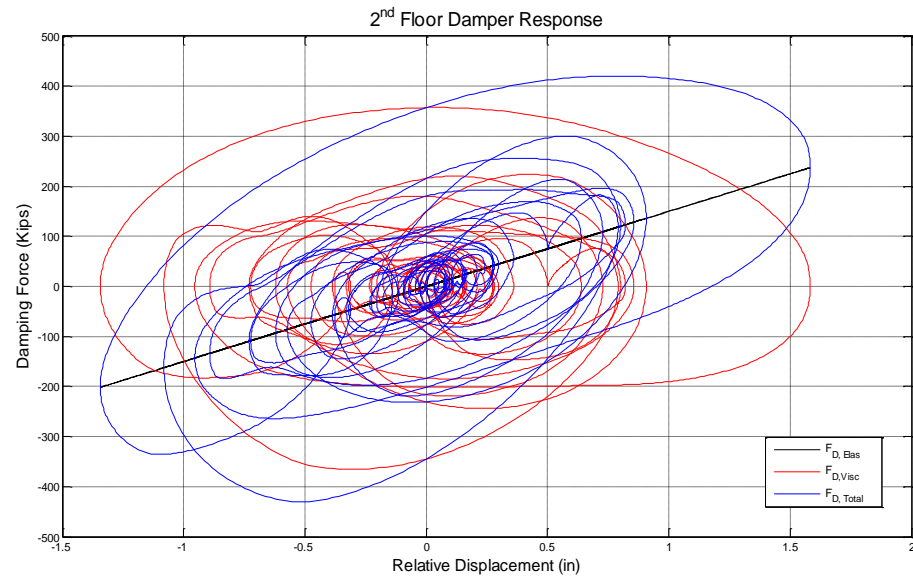


Figure 2.21 Hysteresis Loops of Dampers at Story 2 in Three Story Frame.

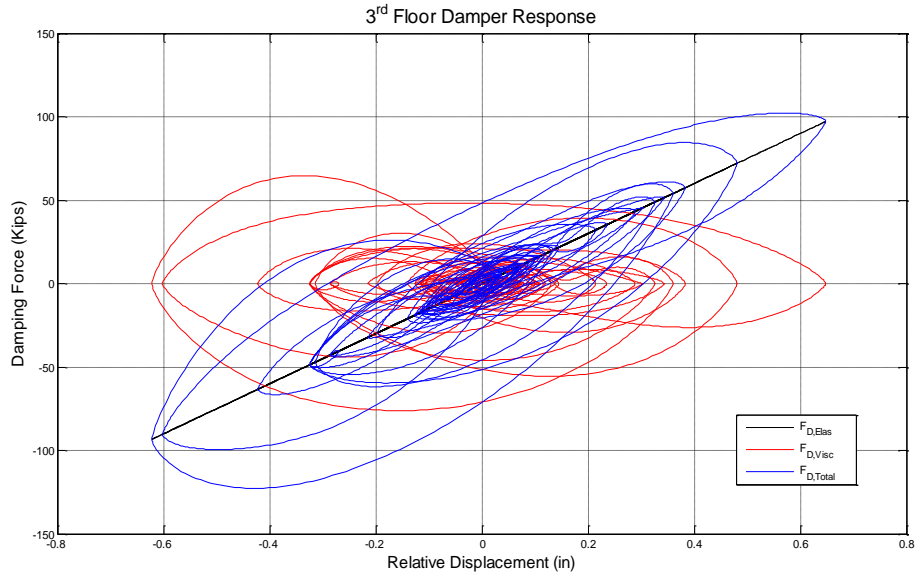


Figure 2.22 Hysteresis Loops of Dampers at Story 3 in Three Story Frame.

It should also be noted that the damper force plotted in components include: (a) elastic stiffness contribution; and (b) viscous damping contribution. The first story damper response is as expected and consistent with the modeling assumptions and theory upon which the present algorithm is based. Linear viscoelastic damper response (i.e. second story damper response) is shown in Figure 2.21. Response characteristics of the components and total damper force response are again consistent with the assumptions and theoretical basis. The pinched hysteretic behavior of the stiffening damper is present in the response shown in Figure 2.22. The significant difference in energy dissipation among the three cases is as expected in the responses shown in these three figures.

2.6 Additional Evaluation

The behavior of an idealized five-story shear building frame, as shown in Figure 2.23 [2.4], was used as a final evaluation the present algorithm's modeling capabilities with

respect to simultaneous nonlinear material behavior and nonlinear viscous damper behavior. The 5-story frame is a shear building. The characteristics of the model are summarized in Figure 2.23 and the ground motion applied to the system was the El Centro earthquake that occurred in 1940 [2.4].

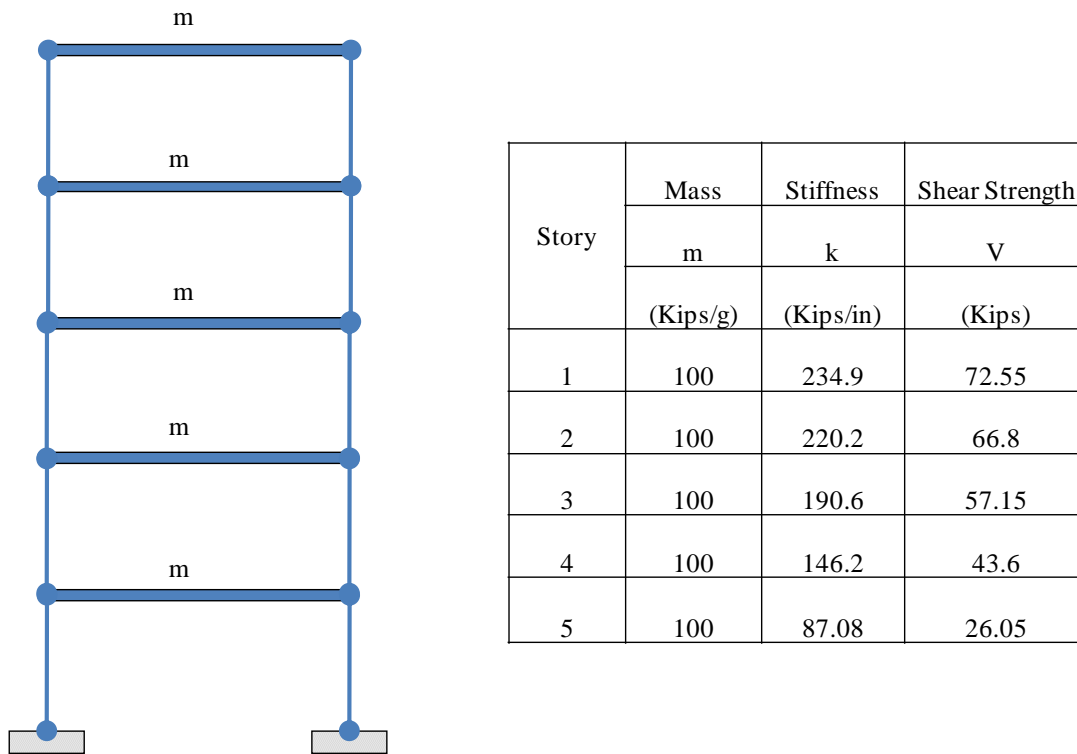


Figure 2.23 Five-Story Shear Building Frame [2.4].

The inherent viscous damping in the structure is defined by Rayleigh proportional (classical) damping. The first and third ($i = 1, j = 3$) natural vibration modes and constant damping ratio $\zeta = 5\%$ were used to calculate Rayleigh proportional damping constants a, b with equations (2.25), and (2.26).

Figure 2.24 shows the displacement time-histories for the 5th floor when the model subjected to the El Centro earthquake. The peak displacement at the 5th floor is 3.203 in from Choprs's book as shown in Figure 2.24.

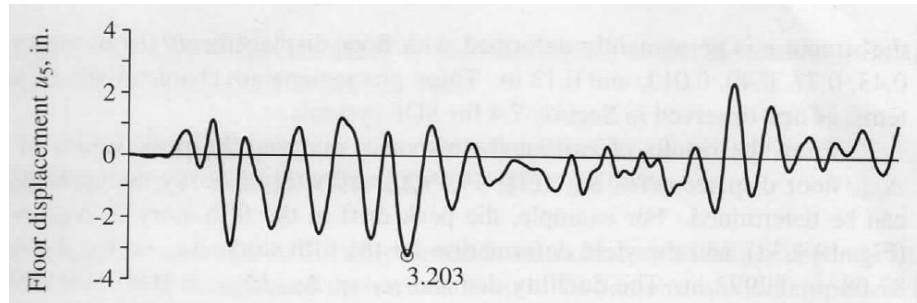


Figure 2.24 The 5th Floor Displacement for the Five-Story Shear Building Described in Figure 2.23 [2.4].

Yielding in the stories causes the system to drift from its initial position in to a position of permanent deformation [2.4]. As a result, the system does not oscillate always about its initial un-deformed position. The system oscillates around a new deformed position when it is shifted by episodes of yielding [2.4].

Figure 2.25 was generated by the program developed for later use in the dissertation (MDOF). The maximum displacement at the 5th floor computed using the programs and algorithms for the present study is 3.22 inches at 5.44 sec. The comparison to earlier work [2.4] is excellent and nonlinear material is modeled correctly.

Figure 2.26 shows the relation between story shear V_j and the inter-story drift Δ_j as the structure goes through several cycles of oscillation. The figure shows elastoplastic relation between the shear force V_j and interstory drift.

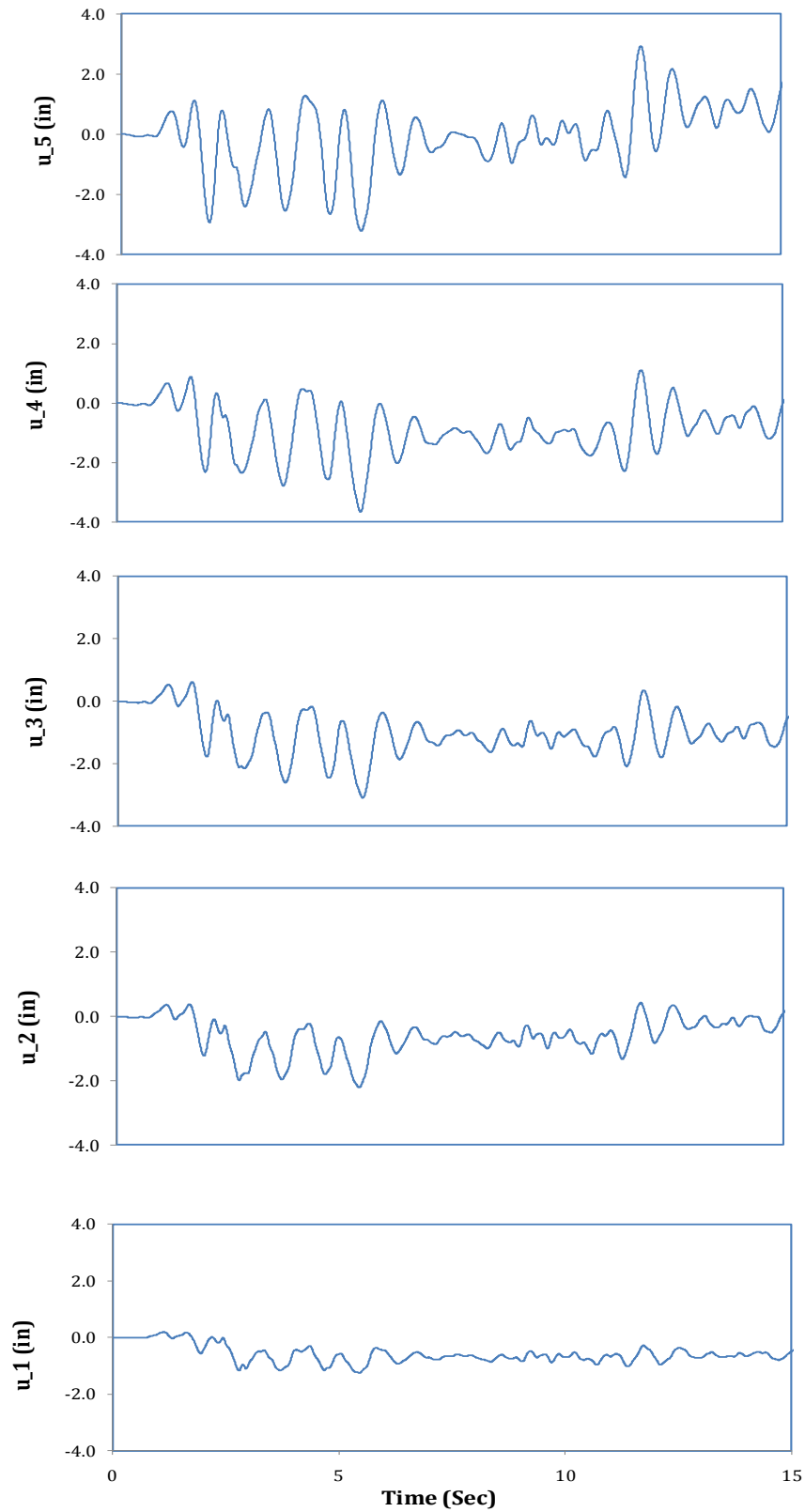


Figure 2.25 Displacement Time History at Each Level Computed Using MDOF.

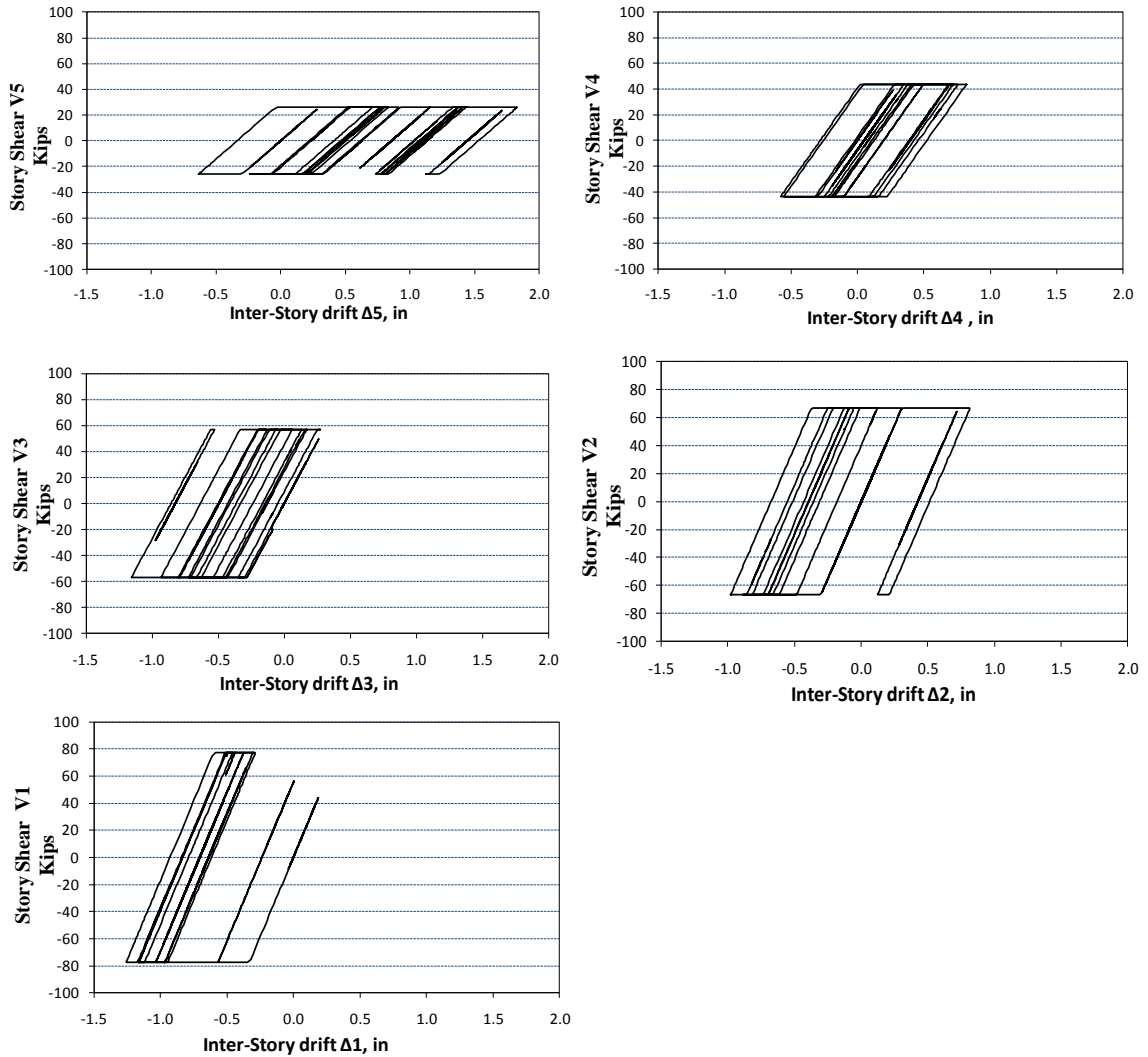


Figure 2.26 Story Shear at Each Story Computed Using MDOF.

The nonlinear spring hysteretic response behavior seen in Figure 2.26 indicates that the modeling of elasto-plastic spring behavior is being adhered to and the program generated is performing as intended. Values of initial stiffness, yielding and the hardening model assumed earlier are preserved in the system response.

A second topology included identical nonlinear ($\alpha = 1.5$) viscous dampers at each story with $c = 10 \text{ kips} - \text{sec}/\text{in}$. This frame was studied to evaluate the behavior of

nonlinear dampers and nonlinear springs in all five stories of the frame. The shear yield strengths at each story were reduced to keep the system in plastic stage when subjected to ground motions. The characteristics of the model are listed in Figure 2.24 and the ground motion applied to the system was the El Centro earthquake that occurred in 1940 [2.4].

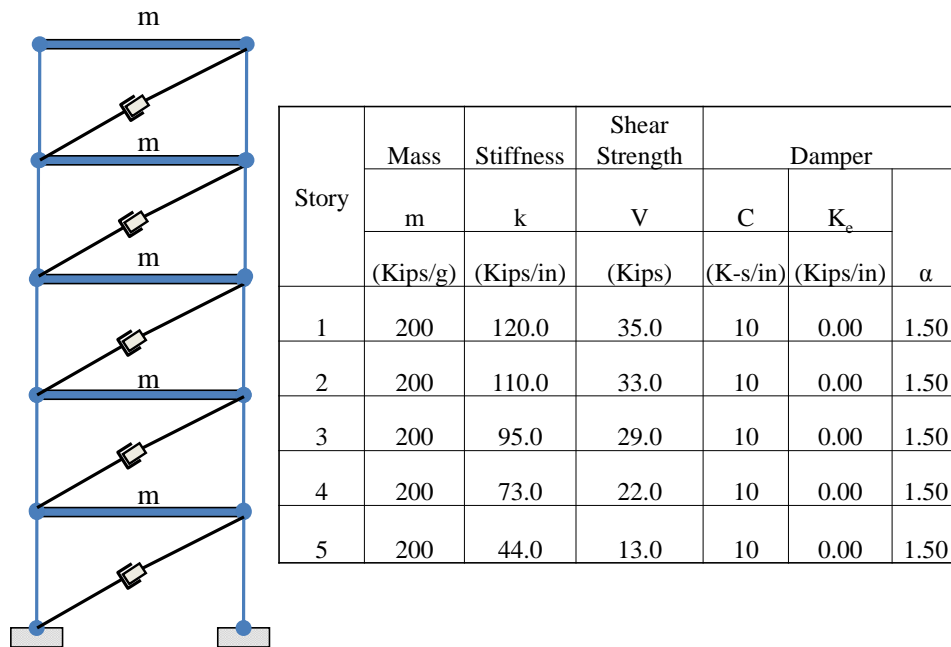


Figure 2.27 Five Story Shear Building Frame with Nonlinear Viscous Dampers.

Figures 2.28 through 2.31 show the displacement histories of building, the relation between story shear and story drift, the relation between damper force and story drift and the relation between damper force and relative velocity, respectively. The response results present in Figures 2.28 through 2.31 are organized as follows: (a) the top (5th) story; (b) the 4th story; (c) the 3rd story; (d) the 2nd story; and (e) the 1st story.

Figure 2.29 shows elastoplastic relation between the shear forces at each level V_j and story drift, $\Delta_j = u_j - u_{j-1}$. The relations between damper forces and relative velocities

and the damper force and the inter-story drift illustrate the dampers are also modeled correctly in the MDOF program.

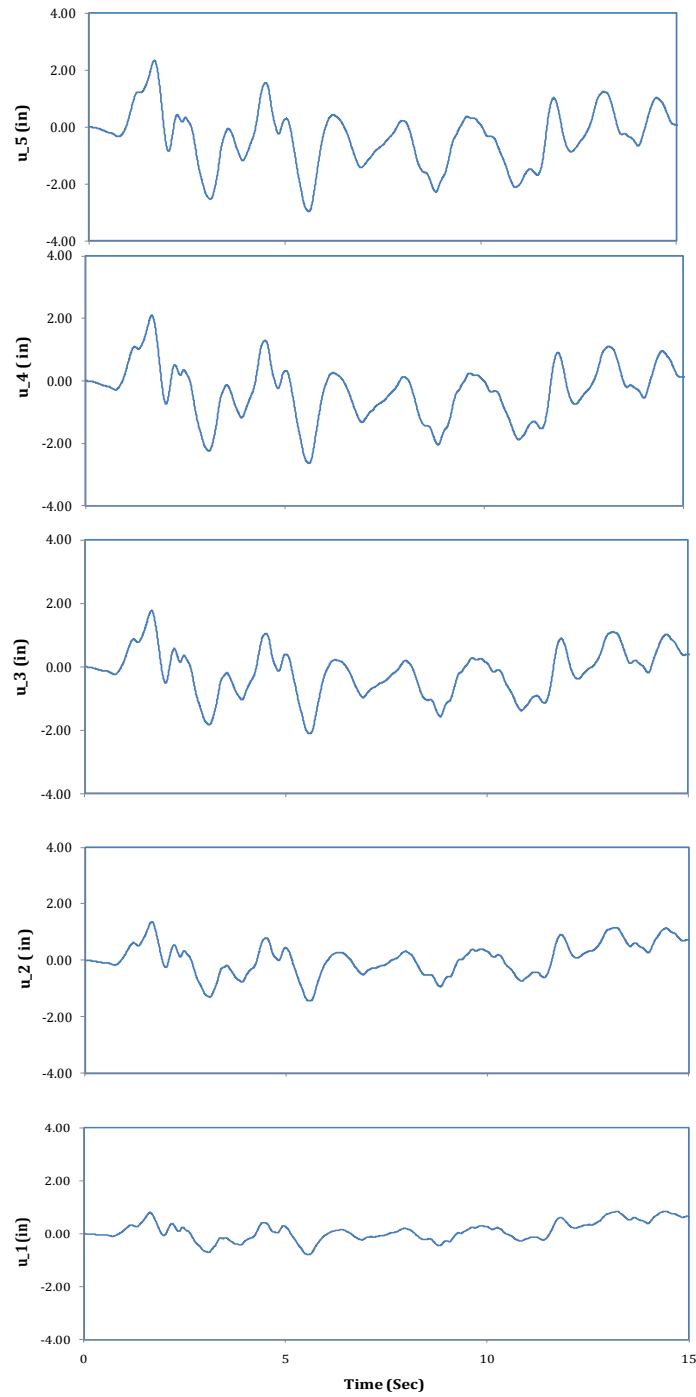


Figure 2.28 Displacements at Each Story

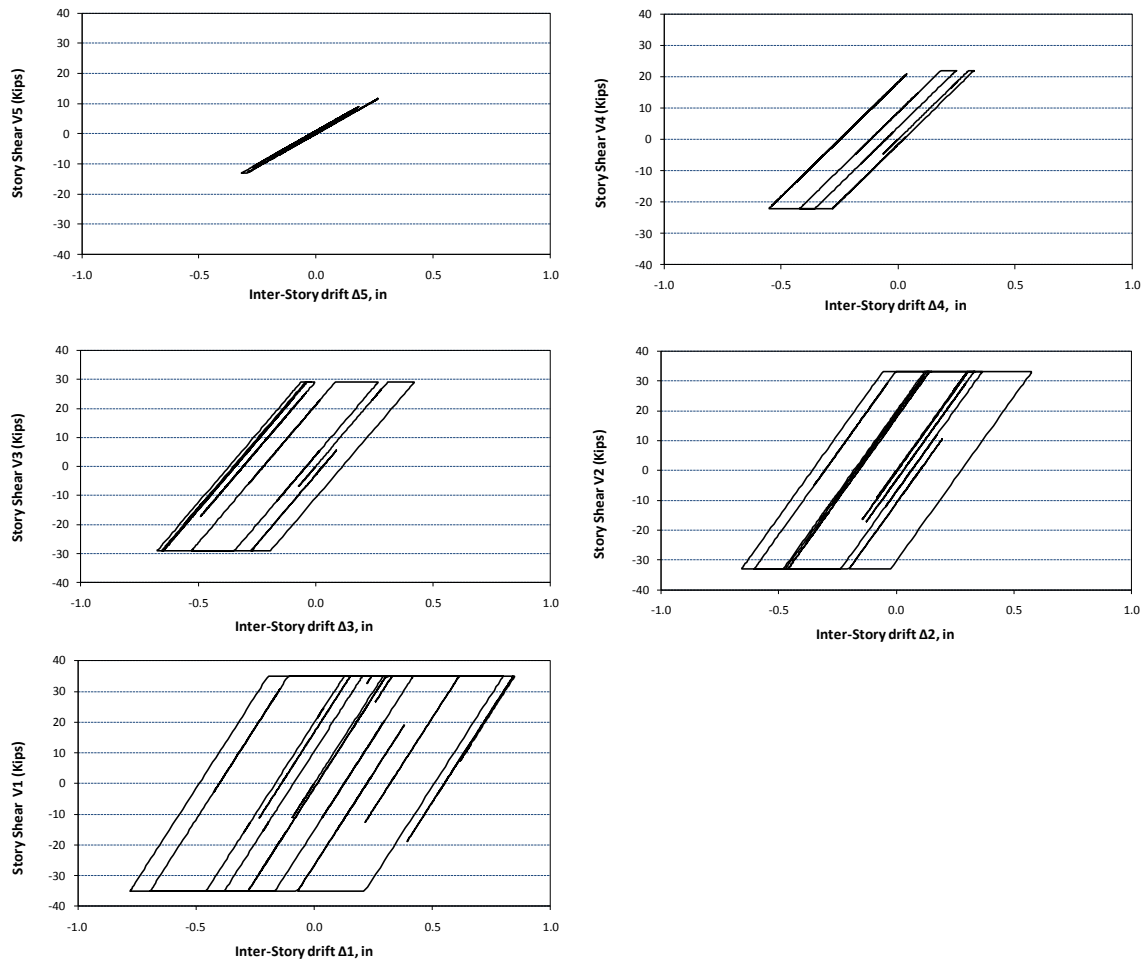


Figure 2.29 Story Shear Forces vs. Inter-Story Drift at Each Story

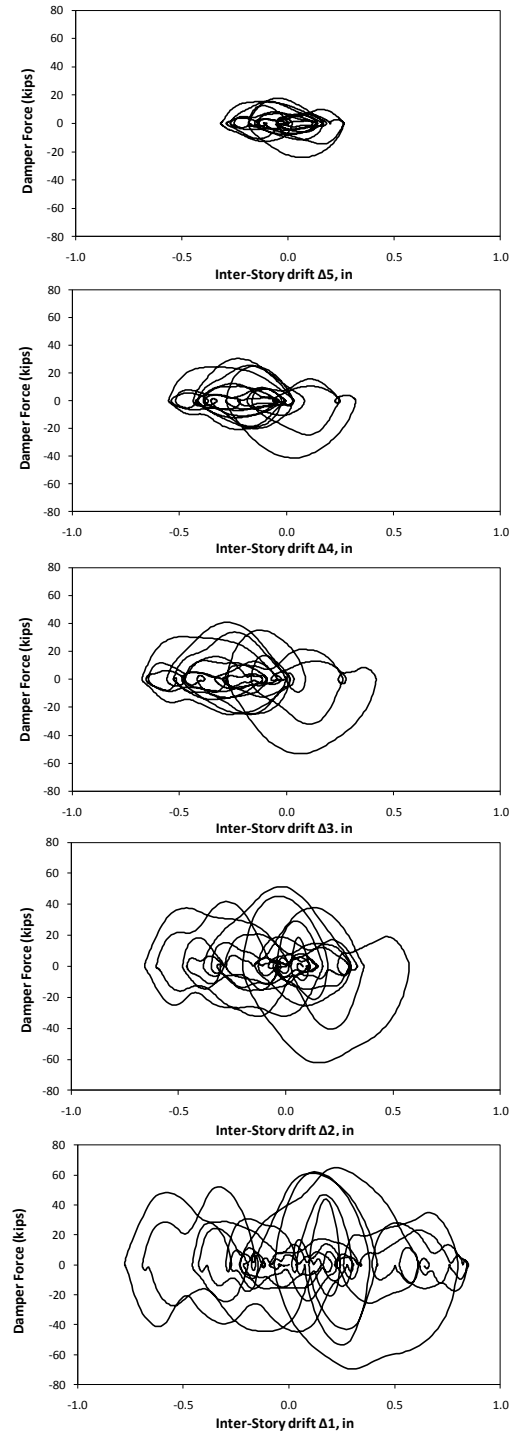


Figure 2.30 Damper Forces vs. Inter-Story Drift at Each Story

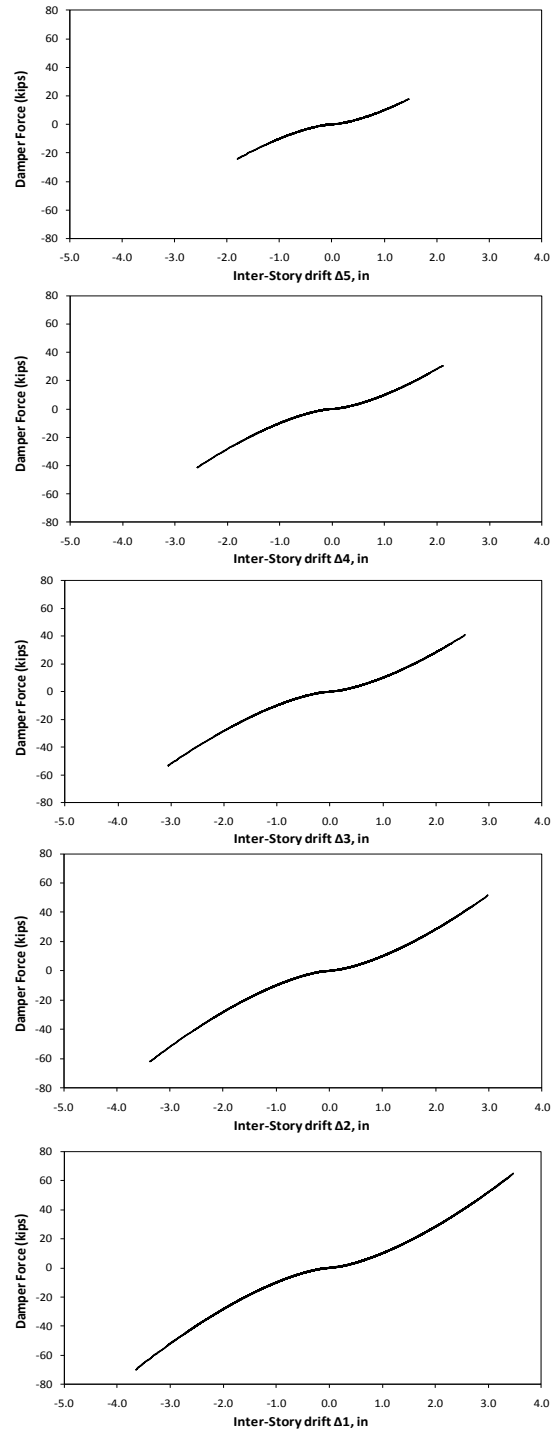


Figure 2.31 Damper Forces vs. Relative Velocity at Each Story

2.7 Concluding Remarks

This chapter in the thesis included discussion of many comparative cases designed to illustrate that the MDOF program written for use in this dissertation is able to correctly simulate the behavior of shear buildings with a variety of supplemental damping devices (elastic, viscous or viscoelastic) when subjected to ground acceleration records and sinusoidal ground accelerations consistent with harmonic loading.

Comparison of simulation results for test cases using theoretically based solution, research-grade software solutions (*e.g.* OpenSees), and the MDOF system program written indicates that it can be used to provide reliable dynamic analysis that can be used as the basis for the risk-based optimized design algorithms to follow. In fact, the case studies examined can serve as benchmark solutions for complicated nonlinear dynamic behavior.

Chapter 3

Risk-Based Seismic Design Optimization of Steel Building Systems with Supplemental Damping Devices

3.1 Introduction

In the past ten years, estimated losses due to seismic hazard were twenty times larger than in the previous 30 years combined [3.1]. FEMA's expenditures related to earthquake losses have become an increasing percentage of its disaster assistance budget [3.1]. A typical expected service life for a building is 50-70 years. For purposes of this dissertation, there are two costs associated with a building system. The initial construction cost and the cumulative expected losses (cost) associated with damage resulting from seismic activity. Initial construction cost includes costs for fabrication and erection of the structural framing system. It is recognized that initial construction cost associated with the framing system are a small fraction of the total building cost, but the framing system is the entity with the most ability to control loss due to seismic hazard. A building's life-cycle cost also includes losses resulting from damage due to natural hazards: earthquakes, tornados, and hurricanes. A risk-based design optimization should include these losses in order to help builders choose the most suitable building system that can balance initial construction cost with the expected losses resulting from natural hazards.

Building codes have historically required that structures be built to meet a minimum level of life safety to protect building occupants. Current building codes do not directly consider loss resulting from damage due to ground motions. Performance or risk-based design is a methodology that seeks to more accurately predict risk of seismic

damage in buildings and offer the structural engineer and owner a means to include this risk in the design of the structural system. When performance levels are tied to probable losses within a reliability-based design framework, the building design process can be tied into an owner's long-term capital planning strategies, as well as numerical life-cycle cost models [3.1]. The current research effort is geared toward development of automated risk-based design methodologies to optimize structural system performance to reduce expected annual losses due to seismic hazard and reduce initial construction costs for structural steel systems with passive damping devices.

3.2 Structural Optimization Fundamentals

As discussed earlier in this dissertation, many algorithmic approaches to solving optimal design problems include design variable representations that are discrete rather than continuous in nature (e.g. wide-flange column sections, passive damper configurations). This dissertation assumes discrete design variables and seeks to attack a multiple-objective structural optimization problem using a genetic algorithm. The present section seeks to provide more details regarding structural optimization and the algorithms that are used to solve them and develop algorithms for automatically selecting structural system components. This discussion will introduce the multiple objective optimization problem tackled in this dissertation as well as provide background and justification for the genetic algorithm as the method to attack the problem.

The traditional form of a structural optimization problem includes a statement of objective(s) and constraints. The classical form of the optimization problem statement is given in the following:

$$\begin{aligned}
 \text{Minimize:} \quad & f(x) \\
 \text{Subject to:} \quad & g_j(x) = 0, & j = 1, \dots, p \\
 & h_k(x) \leq 0, & k = 1, \dots, m \\
 & x_i^L \leq x_i \leq x_i^U & i = 1, \dots, n
 \end{aligned}$$

Therefore, any algorithm suitable for automating a design will seek to define a vector of design variables, x , within an upper bound x_i^U and a lower bound x_i^L that satisfies all equality constraints $g_j(x)$, and inequality constraints $h_k(x)$, while minimizing the objective function, $f(x)$.

There are many methods to solve optimization problems such as these. These algorithms have been discussed extensively in the literature [3.2, 3.3, 3.4, 3.5]. The design variable representations can generally take two forms: (a) continuous; and (b) discrete. In general, discrete variable optimization problems usually require more computational effort compared to the continuous variable problems even though the number of feasible points with discrete variables is finite, but are infinite with continuous variables. The reason for this is that continuous-variable optimization problems can allow very efficient search of the design space as a result of mathematical gradients being defined for constraints and objective functions.

Stochastic, gradient-based, and direct-search algorithms can be used as the basis for powerful search and optimization tools. Direct-search methods are point-to-point search algorithms that use objective function and constraint values to guide the search through feasible decision space [3.2]. A Genetic Algorithm (GA) is a popular stochastic search technique that simulates natural phenomena related to genetic evolution. Gradient-

based methods use derivatives of objective functions and constraint equations to guide the search. Convergence of these algorithms depends upon selection of an initial solution for subsequent modification through iteration and design variable changes. However, the algorithm can be stuck in sub-optimal regions of the decision space due to poor initial design selections.

The structural engineering optimization problem considered in this dissertation includes multiple objectives, discrete design variables, and inequality constraints.

Therefore, the formal definition of the optimal design problem considered is;

$$\begin{aligned} \text{Minimize:} \quad & F_1(x) \text{ and } F_2(x) \\ \text{Subject To:} \quad & h_k(x) \leq 0 \quad k = 1, \dots, m \\ & x^L \leq x_i \leq x^U \quad i = 1, \dots, n \end{aligned}$$

There are two objectives considered: initial construction cost and expected annual loss due to ground motion hazard. The inequality constraints formulated include strength constraints normally associated with structural steel design. The design variables considered will be discrete wide-flange member cross-sections found in steel construction and parameters associated with defining the response characteristics of a supplemental damping device.

A genetic algorithm will be used as the basis for the automated design variable selection. Therefore, fitness functions for each objective considered need to be formulated. The optimal design problem also needs to be re-cast into one that is unconstrained. Therefore, constraints need to be considered as penalties tied to the objectives (or fitness). The following sections provide details related to re-casting the optimal design problem into one that is suitable for application of a genetic algorithm.

3.3 Fitness Function for Initial Construction Cost

Estimating initial cost for a steel building with supplemental damping devices is complicated, because there are a large number of variables that go into any project. For example, a building in Chicago is required to support relatively large snow loads when compared to a building in Phoenix. Furthermore, seismic hazard variability across different regions can affect the expected loss and the types and locations of supplemental damping systems within the structure.

The initial construction cost of a building system often includes: (a) the material cost of structural members such as beams, columns, and bracing; (b) the fabrication cost including the material costs of connection elements, bolts, welding electrodes, and the labor cost; (c) the cost of transporting the fabricated pieces to the construction site; (d) the erection cost; and (e) the cost of the foundation. The weight of a steel structure is most-often used as the basis for defining initial construction cost of a steel framing system without supplemental damping devices. The weight can be used as the basis for the cost of the steel framing system if a proportional multiplier is introduced. Therefore, the costs of (a), (b), (c), and (d) above can be related to the initial weight of the elements in the structural framing system. These costs are included in this dissertation, but the foundation cost and transportation costs are ignored.

As discussed earlier, two objectives are included in the optimal design problem statement considered in this dissertation. The first is initial construction cost. The initial construction cost is re-cast to fitness using the weight of the structural framing system components. The initial construction cost is approximated using the following,

$$C_1 = 1.20 \cdot (WT) \quad (\text{in dollars}) \quad (3.1)$$

where: WT is the weight of steel components (wide-flange cross-section members) in the framing system; and the multiplier (1.20) is a factor that includes the cost for material, fabrication, and erection.

This dissertation assumes that wide-flange steel members are utilized. These members are often cataloged using weight per linear foot [3.5]. Therefore, the cost of the wide flange member components in the framing system can be re-written as,

$$C_1 = 1.20 \cdot \sum_{k=1}^N L_k (wt_k) \quad (3.2)$$

where: wt_k is the weight of the component on a per foot basis (tabulated), L_k is the length of the component, and N is the number of wide-flange components in the framing system.

The additional cost of supplemental damping devices is also included in the initial cost to the structural framing system. The price of a supplemental damping device is related to the maximum force expected in the damper during a seismic event and the maximum stroke required from the damper during the seismic events considered. The peak damper force is used to define the diameter of the supplemental damping device and the maximum stroke expected defines the length of the damper.

Supplemental damping devices in typical structures often have strokes on the order of +/- 3 to 4 inches. Smaller buildings (low rise, or low mass) often include dampers with peak force magnitudes in the range of 30-75 tons. Larger buildings or those with larger mass often include larger dampers with capacities in the 70-200 ton force range.

Engineers at Taylor Devices (<http://www.taylordevices.com>) were contacted to gain input with regard to formulating a rational cost estimate for supplemental damping

devices. Table 3.1 lists cost estimates for a 4-ft long Taylor damping device which includes a clevis and spherical bearing at one end and a square plate at the other end to attach to an extender. The cost of the extenders is not included in this dissertation.

Table 3.1 Supplemental Damper Device Costs

Peak Force (Tons)	Cost Per Damper (Dollars)
25	3,200
50	3,600
80	4,400
100	6,400
150	8,700
200	11,000

Therefore, if the peak force expected during seismic events is known, Table 3.1 provides a means with which to define the cost of the damper associated with that peak force.

Interpolation and extrapolation of values in Table 3.1 are used in this dissertation to define costs. Thus, the damper contribution to the initial construction cost can be written as,

$$C_2 = \sum_{j=1}^{N_d} C_j(f_{\max}^D) \quad (3.3)$$

where: $C_j(f_{\max}^D)$ is the cost of damper j , which is a function of the peak damper force,

$F_{d,\max}$, and N_d is the number of dampers in the system.

The total initial construction cost for the framing configuration or system considered is then a sum of the two components. This is conveniently written as,

$$C = C_1 + C_2 \quad (3.4)$$

Two objectives are included in the optimization statement and as a result, the fitness function related to initial construction cost objective is,

$$F_1 = C = C_1 + C_2 \quad (3.5)$$

3.4 Fitness Function for Expected Annual Loss (EAL)

Earthquakes can result in damage to both structural and non-structural components within a building system depending upon the severity of the ground motion, the type of structural system used in the building, and the building's contents and their susceptibility to deformation-induced and acceleration-induced damage. Damage can be classified as being in one of five discrete damage states: no damage, slight damage (SLT), moderate damage (MOD), extensive damage (EXT), or complete damage (COM) using fragility curves for specific building occupancy classes and their corresponding expected repair costs for a defined building structural system and its non-structural components and contents [3.10].

This dissertation uses fragility curves and repair cost percentages developed for low-rise structural steel moment resisting frames categorized as SIL for building occupancy class COM4, which is office buildings housing professional or technical services [3.10]. It is recognized that both braced and unbraced moment resisting frameworks are considered in the dissertation research. However, the present work constitutes a framework under which risk-based optimized seismic design can be undertaken. As a result, any suitable fragility curve can be implemented.

Table 3.2 provides fragility function parameters for structural system (SS), nonstructural drift-sensitive (NSD) components and nonstructural acceleration-sensitive (NSA) components used in the dissertation research.

Table 3.2 Fragility Curve Parameters for Structural and Non-Structural Components (S1L Building System and COM4 Occupancy Class) [3.10].

Component	Fragility Curve Parameter	Damage State			
		SLT	MOD	EXT	COM
SS	\overline{ISDA}_{ds}	0.004	0.008	0.020	0.0533
	β_{ds}	0.50	0.50	0.50	0.50
NSD	\overline{ISDA}_{ds}	0.004	0.008	0.025	0.050
	β_{ds}	0.50	0.50	0.50	0.50
NSA	$\overline{PFA}_{ds}(g)$	0.30	0.60	1.20	2.40
	β_{ds}	0.60	0.60	0.60	0.60

The relative percentage of total building replacement cost allocated to structural and non-structural components is derived from Means of component breakdowns for a building's occupancy class [3.10]. Table 3.3 shows the values for the expected repair cost (expressed as a percentage of the building replacement value) of the structural system (SS), nonstructural acceleration sensitive (NSA) components and nonstructural drift sensitive (NSD) components. Acceleration sensitive nonstructural components include hung ceilings, mechanical and electrical equipment, and elevators. Drift sensitive components include partitions, exterior wall panels, and glazing.

Table 3.3 Repair Costs Expressed as Percentage of Building Replacement Cost (S1L Building System and COM4 Occupancy Class) [3.10].

Component	Damage State			
	SLT	MOD	EXT	COM
SS	0.40	1.90	9.60	19.2
NSD	0.70	3.30	16.4	32.9
NSA	0.90	4.80	14.4	47.9

The expected losses L (in percentage of building replacement cost) resulting from earthquake damage to structural components (SS) or nonstructural components (NSA or NSD) for a given ground motion intensity measure, IM , can be written as

$$E[L^Y | IM] = \sum_1^5 P[DS^Y = ds | EDP] * RC_{ds}^Y \quad (3.6)$$

RC_{ds}^Y is the repair cost for building component Y being in damage state ds , which is defined as being one of the following: 1 (no damage); 2 (SLT); 3 (MOD); 4 (EXT); and 5 (COM). $P[DS^Y = ds | EDP]$ is the probability of building component Y being in damage state, ds , given the engineering demand parameter, EDP , used to characterize damage of building component Y . This probability is calculated using fragility functions given by equations (1.3) and (1.4) using parameters defined in Table 3.2.

The total expected loss for a given building structure type and occupancy class is the summation of loss due to structural and nonstructural component damage,

$$E[L_T | IM] = E[L^{SS} | IM] + E[L^{NSD} | IM] + E[L^{NSA} | IM] \quad (3.7)$$

where $E[L^Y | IM]$ is the expected loss for component Y given a ground motion intensity measure, IM . It should be noted that equation (3.7) includes the earthquake intensity measure, IM , and losses must be aggregated over all earthquake intensities considered at the building site. The earthquake intensity measure most often considered in past research efforts is the peak ground acceleration (PGA). PGA magnitude is often given probabilities of occurrence on an annualized basis, or a probability of recurrence given a building's exposure period (*e.g.* 2% chance of exceedence in 50 years).

Computing the expected annual loss (EAL) requires that different intensities of earthquake motion and their annual probability be considered. The annual average

probability, \bar{p} of an earthquake intensity measure, IM , being exceeded can be computed using the assumption that ground motion recurrence follows a Poisson probability distribution. If this is the case, annual average probabilities of occurrence of ground motion intensity measures can be defined with 2%, 10% and 50% probabilities of exceedence during a defined exposure period. The annual probability of a specified ground motion intensity measure being exceeded given that intensity measure's probability of being exceeded, p , within an exposure period of t years can be computed using the Poisson model [3.11],

$$\bar{p} = (-1/t) * \ln(1 - p) \quad (3.8)$$

Table 3.4 lists the annual probability of different earthquake intensities corresponding to exceedence probabilities of 2/50, 10/50 and 50/50.

The expected annual loss (EAL) resulting from all potential ground motion intensities can then be computed using the individual losses determined using equation (3.5) and the annual probabilities found in Table 3.4. This computation is given below,

$$EAL = E[L_T | IM_{2/50}] * \bar{p}_{2\%} + E[L_T | IM_{10/50}] * \bar{p}_{10\%} + E[L_T | IM_{50/50}] * \bar{p}_{50\%} \quad (3.9)$$

The second objective fitness then follows from equation (3.7),

$$F_2 = EAL \quad (3.10)$$

3.5 Genetic Algorithm Constraint Formulation

A building must be designed and constructed according to the provisions of a building code, which is a legal document containing requirements related to structural safety.

Design specifications give guidance for the design of structural members and their

connections and present criteria that enable a structural engineer to achieve the objectives mandated by a building code. In this research, the American steel design specifications [3.5] are used to formulate constraints needed for designs to meet strength requirements set forth by building codes.

Table 3.4 Annual Probabilities for Earthquake Intensities Considered.

Earthquake Exceedence Probability	Annual Probability of Occurrence
2% in 50 years	$\bar{p}_{2\%} = -\left(\frac{1}{50}\right) * \ln(1-0.02) = 0.000404$
10% in 50 years	$\bar{p}_{10\%} = -\left(\frac{1}{50}\right) * \ln(1-0.1) = 0.002107$
50% in 50 years	$\bar{p}_{50\%} = -\left(\frac{1}{50}\right) * \ln(1-0.5) = 0.013863$

The genetic algorithm implementation requires that optimization problems be posed as unconstrained. Therefore, the constraints defined must be re-formulated as penalties that are applied to individual fitness. Penalty multipliers or scaling factors are also formulated. The present section discusses the constraints formulated for the design problem considered in this dissertation and method used to define penalty factors and scaling factors suitable for the constraint application within the context of the genetic algorithm formulated.

3.5.1 Strength

Strength limit states are related to safety and load-carrying capacity of the structural framing system and its members or components. Load combinations for assessing the

strength for buildings and their components are available [3.5, 3.12]. The load and resistance factor design (LRFD) provisions should be followed in the research to ensure that the strength limit state is not exceeded when the structure is subjected to all appropriate design load combinations. The basic safety check in LRFD may be expressed mathematically as

$$\sum \gamma_i Q_i \leq \phi R_n \quad (3.11)$$

where, γ_i = a load combination factor; Q_i = a load effect (a force or a moment); ϕ = a resistance factor; and R_n = the nominal resistance, or strength, of the component under consideration.

The following load combinations are used in this research to assess the strength limit states are,

$$1.0(D_F + D_S) + 1.0(L_r) \quad (3.12)$$

$$1.0(D_F + D_S) + 1.0(L_r) \pm 1.0E \quad (3.13)$$

As a result, the applied ultimate load ration, γ_u , must satisfy the constraint $\phi_{\gamma U}$.

$$\gamma_u = \frac{\phi R_n}{\sum \gamma_i Q_i} \quad (3.14)$$

$$\phi_{rU} = \frac{1}{\gamma_u} \leq 1.0 \quad (3.15)$$

Where, D_F = the floor dead load; D_S = the self-weight; L_r = the live load present when ground motion occurs. The load combinations are similar to those found in ASCE-7 [3.12], but the combination factors have been simplified. It should be noted that any load combination and associated factors can be implemented.

3.5.2 Local and Member Instability

It is assumed that the axial and flexural strength of the members within the frames considered in this research are not affected by local buckling of the web or flanges within the cross sections. Wide flange members subjected to plastic hinging resulting from combined flexure and axial compression should be compact with width-thickness ratios for the webs in the cross-section satisfying the following:

$$\left(\frac{h}{t_w}\right)_{Limit} \leq 3.76 \sqrt{\frac{E}{F_y}} \left(1 - \frac{2.75 P_u}{\phi_b P_y}\right) \quad \text{for } \frac{P_u}{\phi_b P_y} \leq 0.125 \quad (3.16)$$

$$\left(\frac{h}{t_w}\right)_{Limit} \leq 1.12 \sqrt{\frac{E}{F_y}} \left(2.33 - \frac{P_u}{\phi_b P_y}\right) \quad \text{for } \frac{P_u}{\phi_b P_y} \geq 0.125 \quad (3.17)$$

where, P_u is the required axial strength, P_y is the yield strength, F_y is the yield stress of the steel, and ϕ_b is the resistant factor for flexure (assumed equal to 1.0). The flange slenderness must satisfy,

$$\left(\frac{b_f}{2t_f}\right)_{Limit} \leq 0.30 \sqrt{E/F_y} \quad (3.18)$$

Therefore, web and flange slenderness constraints can be formulated for the optimization problem. The constraint corresponding to the web slenderness ratio, $\frac{h}{t_w}$, can be expressed as,

$$\phi_{h/t_w} = \frac{h/t_w}{(h/t_w)_{Limit}} \leq 1.0 \quad (3.19)$$

The constraint corresponding to flange width-thickness ratio, $\frac{b_f}{2t_f}$, can be expressed as,

$$\phi_{b_f/2t_f} = \frac{b_f/2t_f}{\left(b_f/2t_f\right)_{Limit}} \leq 1.0 \quad (3.20)$$

Any cross-section within a framework that does not satisfy the web-slenderness constraints will be penalized. These slenderness ratios for the members are taken from the manual of steel construction databases of shapes [3.5].

3.5.3 Beam-Column Strength

The members within the frames considered will be subjected to flexural and well as axial loads. In other words, the members are treated as beam columns. The following two constraints are set up for steel members subjected to axial force and flexure [3.5],

(a) For $\frac{P_r}{P_c} \geq 0.2$

$$\phi_{B-C} = \frac{P_r}{P_c} + \frac{8}{9} \left(\frac{M_{rx}}{M_{cx}} \right) \leq 1.0 \quad (3.21)$$

(b) For $\frac{P_r}{P_c} < 0.2$

$$\phi_{B-C} = \frac{P_r}{2P_c} + \left(\frac{M_{rx}}{M_{cx}} \right) \leq 1.0 \quad (3.22)$$

where, P_r is required axial compressive strength; P_c is available axial compressive strength; M_r is required flexure strength; M_c is available flexure strength; x is subscript relating symbol to strong axis bending.

Additional axial loads resulting from the presence of a damper is included on the columns adjacent to the dampers. The vertical component of damper axial forces is added

to the axial column loads when they cause column compression. However the tension force introduced into the columns is conservatively ignored. Effective length factors for major-axis flexural buckling and minor-axis flexural buckling are taken as 1.0.

3.5.4 Damper Stiffness

The frames considered in this dissertation can be considered as dual systems where any bay that contains a diagonal damper compression member acts together with moment-resisting frame bays to resist seismic loading. It should also be noted that the columns within the bay that includes diagonal dampers (i.e. bracing members) are assumed to have flexural stiffness. This means that the braced bay is actually a combination of axial-flexural members and diagonal bracing members (i.e. dampers).

In order to prevent the dampers from becoming the dominant lateral load resisting component in the framing system thereby placing large and currently not quantified demands on the connections at the ends of the damper, the damper elastic stiffness was restricted. This prevents large elastic stiffness magnitudes from dominating the definition of the damper and prevents the damper elastic stiffness from becoming the dominant source of lateral load resistance in the shear building models considered.

The damper elastic stiffness, k_e , at any story level is selected from a range of discrete values ranging from 0 to 100 k/in with increment equal to 10 k/in . The upper bound equal to 100 k/in is defined as the summation of flexural stiffness for all columns at the same level. The column stiffness is calculated using,

$$k_{Col} = \frac{12 * E * I_x}{H^3} \quad (3.23)$$

The lightest and heaviest columns possibly being selected from AISC steel shape database are W6x9 and W14x342 respectively at any story level considered. Therefore, the minimum column stiffness is 1.5 k/in and maximum column stiffness is 224.6 k/in when $h = 156 \text{ in}$ (story height assumed in the frames considered). A damper elastic stiffness constraint at any level i is therefore, defined as follows,

$$\Phi_{\text{Damper}} = \frac{k_{ei}^D}{0.3 * k_{Col_i}} \leq 1.0 \quad (3.24)$$

This constraint ensures that the elastic stiffness of the damper is 30% or less than the stiffness of the story in which it is placed. This helps to maintain the damper systems as being supplemental and not the sole source of lateral load stiffness and strength in the framing system considered.

3.5.5 Designer Preference

Good structural engineering and economical steel erection practice suggests that column sizes either remain the same cross-sectional shape for as long as possible as one rises through a building frame. If shape changes do occur along vertical column runs within a building, larger dimension shapes will be below shapes that are supported. In other words, nominal depths should decrease as one rises through the frame and nominal weights should reduce as one rises through the framework.

Therefore, a design preference or shape constraint is established to guide automatic selection of columns from AISC steel shape database. The shape constraint requires that a column have the same or a larger nominal depth than the column immediately above it. This constraint is similar to that used by Foley and Schinler [3.13].

The AISC designation for a W-shape includes the nominal depth and unit weight. (*i.e.* a W14x48 has a nominal depth of 14 inches and a weight of 48 pounds per linear foot). The shape constraint is therefore, set up as follows,

$$\Phi_{shp} = \left\{ \begin{array}{l} \frac{d_i^{upper}}{d_i^{lower}} \leq 1.0 \\ \frac{wt_i^{upper}}{wt_i^{lower}} \leq 1.0 \end{array} \right\} \quad (3.25)$$

where, d_i^{lower} and d_i^{upper} are the nominal depth of lower and upper columns respectively; wt_i^{lower} and wt_i^{upper} are the weight of the lower and upper columns; and i is the index of the columns.

3.6 Penalty Functions

A genetic algorithm is used in the present research effort to solve the optimization problem established earlier. The GA requires that optimization problems be re-cast as unconstrained optimization problems and as a result, the constraints discussed earlier must be re-formulated as penalties.

The unconstrained objective fitness function f is expressed as the product of the original multi-objective fitness involving initial construction cost and expected annual loss and penalties which reflect violations of the problem constraints expressed in equations (3.15), (3.19), (3.20), (3.21), (3.22), (3.24) and (3.25).

The unconstrained objective function is expressed as the product of the fitness and penalties,

$$F = (F_1 + F_2) \cdot \prod_{i=1}^{n_p} \Phi_i \quad (3.26)$$

where, $F_1 + F_2$ is the multiple objective fitness given by equations (3.5) and (3.10), Φ_i is the penalty corresponding to i^{th} constraint, and n_p is the number of constraints for the problem. This form of individual fitness has been used in previous research [3.6], [3.7], [3.13].

The penalty multipliers, Φ_i , contained in (3.26) are formulated for each of the constraints considered above by taking the product of the scaled constraint violations for each component and each load case. This is illustrated with the following generic expression,

$$\Phi_i = \prod_{r=1}^{N_r} \prod_{j=1}^{N_j} (p_i)_{j,r} \quad (3.27)$$

where, N_r is the total number of load cases, N_j is the total number of components, and p_i is the scaled constraint violation associated with the i^{th} constraint. The scaled constraint violations are established via scaling functions [3.8], [3.9]. Linear and quadratic scaling functions are included in the proposed algorithm using,

$$p_i = 1.0 + k_i (q_i - 1)^n \quad (3.28)$$

where, n is the degree of the scaling function (1 for linear, 2 for quadratic), k_i is the scaling rate, and q_i is the scaling switch defined as,

$$q_i = \begin{cases} 1.0 & \text{if } \Phi_i \leq 1.0 \\ \Phi_i & \text{if } \Phi_i > 1.0 \end{cases} \quad (3.29)$$

In other words, q_i ensure only constraints that are violated (i.e. $\Phi \geq 1.0$) contribute to the penalty.

Figure 3.1 demonstrates the effect of the scaling rate, k_i and the type of scaling function (linear or quadratic) on the scaled constraint violations.

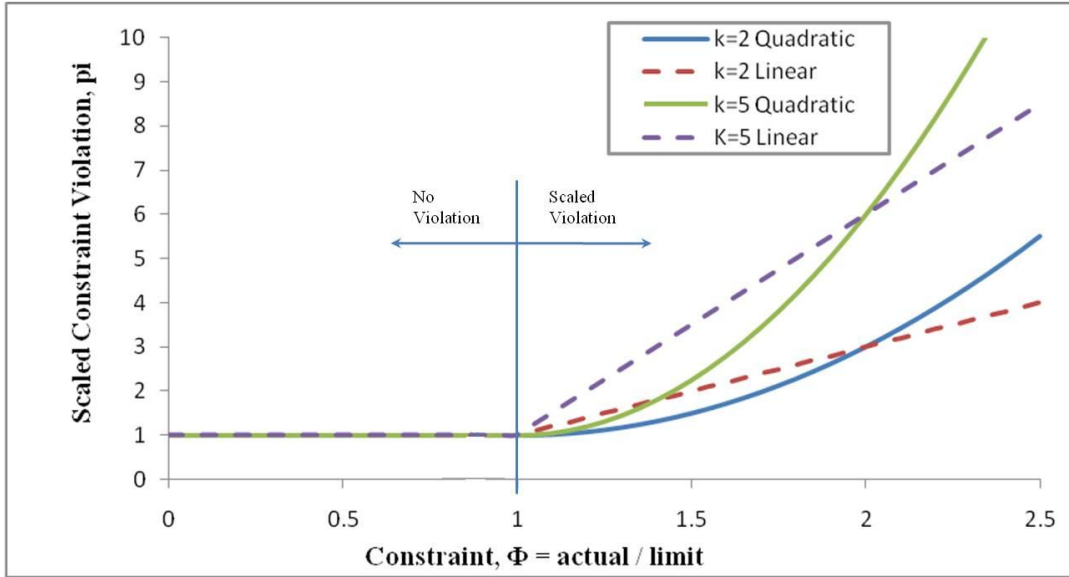


Figure 3.1 Scaling Functions Used for Penalty Multipliers.

Each constraint requires a penalty multiplier with scaling factor. The expressions for penalty multipliers corresponding to each of constraints are written below:

- 1.) The penalty multipliers for not attaining the ultimate load levels

$$\Phi_{\gamma_U} = \prod_{r=1}^{N_u} (p_{\gamma_U})_r \quad (3.30)$$

where, N_u is the number of factored load cases.

- 2.) The penalty multiplier for column web local buckling, out-of-plane flexural buckling, and lateral torsion buckling, respectively, are computed using,

$$\Phi_{h/t_w} = \prod_{r=1}^{N_u} \prod_{k=1}^{N_{col}} \left(p_{h/t_w} \right)_{k,r} \quad (3.31)$$

$$\Phi_{b_f/2t_f} = \prod_{r=1}^{N_u} \prod_{k=1}^{N_{col}} \left(p_{b_f/2t_f} \right)_{k,r} \quad (3.32)$$

where, N_{col} is the number of columns in the framework.

- 3.) The penalty multiplier for the Beam-Column design criteria is computed using,

$$\Phi_{B-C} = \prod_{r=1}^{N_u} \prod_{k=1}^{N_{col}} \left(p_{B-C} \right)_{k,r} \quad (3.33)$$

- 4.) The penalty multiplier for the designer defined damper design criteria is computed using,

$$\Phi_{Damper} = \prod_{r=1}^{N_u} \prod_{k=1}^{N_{Damper}} \left(p_{Damper} \right)_{k,r} \quad (3.34)$$

where, N_{Damper} is the number of dampers in the framework.

- 5.) The penalty multiplier for the designer preference criteria (shape) is computed using,

$$\Phi_{shap} = \prod_{k=1}^{N_{col}} \left(p_{shap} \right)_k \quad (3.35)$$

3.7 GA Optimization Statement and Basic Flowchart

Three different earthquake intensity levels are assumed in the design problems considered in this research. The suite of earthquakes corresponding to each intensity

level is assumed to cause direct economic losses and damage to a given building. The three sets of ground motion records are 2%, 10% and 50% probabilities of exceedance in 50 years (2/50, 10/50 and 50/50, respectively) are used. The ground motions are selected from the records developed by the SAC steel project for the city of Los Angeles, California [4.7]. Each intensity level group (*i.e.* 2/50) includes 6 ground motion acceleration records which are used as ground motion input to the inelastic seismic analysis program MDOF described in chapter 2 to compute the median of peak response quantities (*i.e.* ISDA, PFA) for the risk-based design optimization considered. These ground motions will be discussed in Chapter 4.

The risk-based design optimization problem considered in this dissertation research can be stated in words as follows:

- 1.) Minimize the total initial construction cost described in equation (3.2) for structures without supplemental dampers or equation (3.5) if the analyzed structures include supplemental viscoelastic dampers.
- 2.) Minimize the Expected Annual Loss (EAL) described in equation (3.10).
- 3.) Subject to constraints ensuring system strength under ASCE-7 load combinations, constraints preventing local buckling of the elements within the cross-section, constraints ensuring column members have sufficient strength, constraints restricting the viscoelastic stiffness of the supplemental damper at any story level; and constraints ensuring design preference.

The application of the genetic algorithm is depicted in the flowchart shown in Figure 3.2. An initial population (possible designs) is generated randomly from the search space which is the database of steel w-shapes. For each set individual design

variables, a nonlinear dynamic analysis is conducted using the algorithm, “MDOF”, described in Chapter 2 of the dissertation. This evaluation is conducted to find the peak (maximum) engineering demand parameter (e.g. interstory drift, floor acceleration) at each story level for each ground motion record. The median value of the maximum engineering demand parameter for each set of ground motions is then determined.

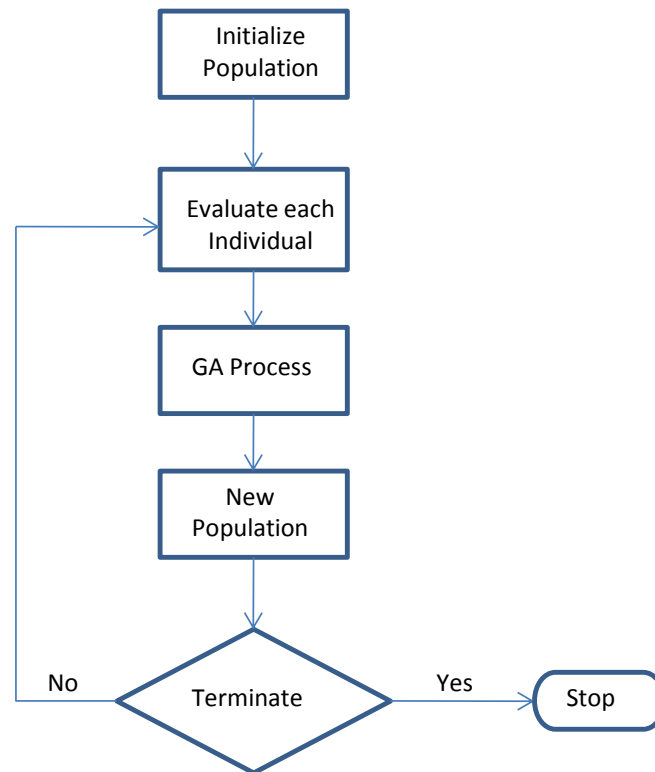


Figure 3.2 Flowchart of Genetic Algorithm Implemented.

The fitness component of individual in the population related to expected annual loss is determined using the peak engineering demand parameter for all stories considered, fragility functions, and the repair cost percentages found in Tables 3.2 and 3.3. The cost ratios expressed as a percentage of building replacement cost for Structural

System components (SS), acceleration sensitive non-structural (NSA), and drift sensitive non-structural (NSD) components in buildings are listed in Table 3.2 and 3.3. The fitness component related to initial construction cost is determined using equation (3.2), equation (3.3) and the tabular data found in Table 3.1.

The GA then continues in traditional fashion until a termination criterion is reached. It should be noted that the following chapter will highlight further details related to implementation of the genetic algorithm on a personal computer cluster and further details related to the algorithm parameters and scaling factors used in the definition of penalties.

Chapter 4

Application of the Genetic Algorithm to Optimized Design of Steel Framing Systems

4.1 Introduction

The primary objectives of this chapter are to introduce the concept of distributed computing applied within the context of evolutionary computation; to illustrate how the present evolutionary algorithm incorporates distributed computing on a desktop computer cluster; to demonstrate the ability of the proposed evolutionary algorithm to obtain practical designs within the context of performance-based structural engineering for systems subjected to seismic loading; and to evaluate the performance of the algorithm. Assessment is carried out through brief discussions and observations of the results.

The focus of the chapter is on a steel framed building system with fixed topology. The design scenarios considered include structural systems with and without supplemental dampers with viscous and viscoelastic properties. The evolutionary algorithm developed in earlier chapters and the performance-based engineering philosophy for seismic design constitute the automated engineering design system implemented in this chapter.

The frame design cases formulated are based upon a three-story building frame considered in previous research [1.23]. The 3-story, 4-bay steel building frame is modeled using the shear-building approach. As a result, beam members are considered flexurally rigid with respect to the column members and they are also considered inextensible. Design variables in the frame scenarios considered include damper parameters and column sizes.

The computational expense that the evolutionary algorithm brings required that alternate computational architectures be investigated for use in the dissertation. This dissertation utilizes distributed computing to execute the genetic algorithm. As a result, the present chapter outlines how this is accomplished and how the Matlab distributed computing toolbox and engine [1.32] is utilized.

4.2 Introduction to Distributed Computing

It is well known that evolutionary algorithms can be computationally expensive [4.1]. Test runs of the present evolutionary algorithm on the three story framework considered, indicated that run times on single processor computers were on the order of 24 hours for design scenarios that included the bare minimum number of design variables. Larger frames and those that include more design variables took even longer. As a result, it was decided to implement distributed computing to speed up the evolutionary algorithm developed. In simple terms, distributed computing is the technique of distributing computational tasks to multiple processors within a computing system (most often a networked cluster of computers).

The concepts of parallel and distributed computing are not new. There have been applications in structural engineering for many decades including applications in inelastic analysis of structural steel systems [4.2, 4.3, 4.4]. There are many types of computing systems suitable for implementing parallel and distributed computing and there are two types of computers capable of distributing computational cycles: (a) shared memory computers; and (b) distributed memory computers. Shared memory computers utilize more than one processor and share a single memory pool for the results of computations.

Distributed memory computers have processors that include their own memory for the results of computations.

The following is a brief discussion of the major classifications commonly found in the high-performance computing arena. Parallel Vector Processors (PVP's) utilize limited numbers of vector processors within a single machine. Compilers most often utilized on these machines optimize a calculation automatically by breaking the innermost loops into blocks of N (64, etc) elements in size. Each element processor, functioning in a pipeline mode, operates on all elements within a single clock cycle. So vector processors could work on large vectors of data in parallel (simultaneously). The PVP computer architecture is relatively expensive (vector processors are often expensive and cooling the processors is not trivial) and these machines have often been historically referred to as supercomputers. PVP's have historically been very powerful and very expensive and no longer are in the mainstream of computing. Such machines (Cray Y-MP 64) have been used for conducting inelastic collapse-load analysis of large-scale steel buildings [4.4].

Shared-Memory multi-Processor (SMP) parallel systems have multiple processors which share a common memory pool and data bus. Generally, each processor has its own local memory (cache) which can save data temporarily while the data bus is used by other processors. These computing systems can suffer from bottlenecks in data flow and as a result, the data bus should be fast enough to transfer data through all processors [4.5]. These computer architectures often involve relatively inexpensive processors with low levels of on-board memory. Each processor in this computing architecture is sometimes referred to as a "node".

Distributed memory computing systems often include many processors where each includes its own local memory. These systems will often require a head or master node that orchestrates computations and assembles the results of the computing effort. The main difference between distributed and shared memory machines is the presence so significant levels of memory that comes along with the distributed processors. If this memory level is significant, this is referred to as distributed memory. In reality, both distributed and shared memory computers require head or master computers (often called nodes) to orchestrate computations. Distributed memory architectures also include reference to processors as nodes.

The advent of relatively inexpensive personal computers and computing networks has lead to an extension of the distributed memory computing architecture. The modern implementation of distributed-memory computing architecture is the networked computing cluster. A computing cluster is most often composed of many identical computers which are assembled together (often in racks). These computers are then networked together with one another using high-speed data bus network connections and a network switch facilitating communications among each other. Heterogeneous computers within a common network can also be used to form a computer cluster. This is often referred to as network/internet-based distributed computing. This differs from a cluster in that these heterogeneous computers can be geographically separated personal computer workstations. Internet-based network traffic can be slow relative to local network connectivity and therefore Network/Internet distributed computing can be successfully implemented under limited scenarios (e.g. fast network speeds).

The present dissertation utilizes a form of network distributed computing to economically execute the genetic algorithm developed for optimized design of steel framing systems for seismic loading. A four-node networked computer cluster was developed for the present research effort. A schematic of the cluster architecture is shown in Figure 4.1. The four networked computers are connected via a 10 M Byte/Sec network and each has its own network interface card (NIC) attached to its own peripheral component interconnect (PCI), which is a 10 MB/s bus. The cluster developed for this dissertation work was constructed using spare personal computers. A 10 MB/s network switch was included in the cluster configuration. The cluster was made accessible to the outside world through the Internet and all runs were conducted remotely. The architecture described can be defined as a distributed memory computational architecture that utilizes local area network connectivity.

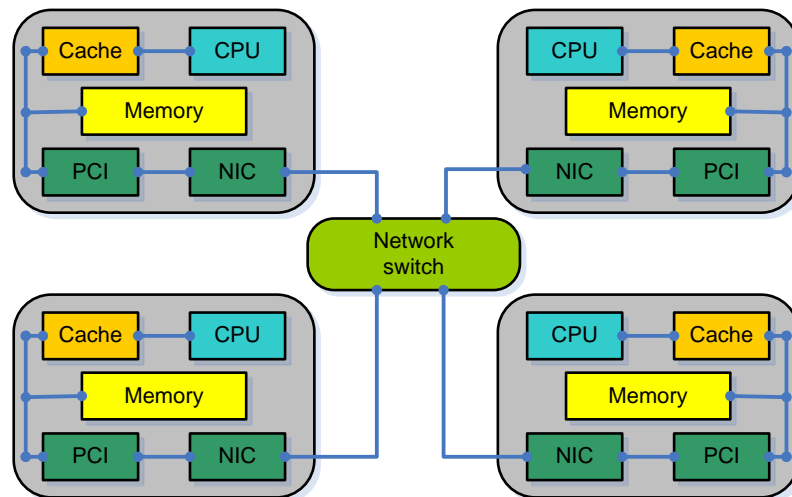


Figure 4.1 Computer Cluster with 4 Workers.

4.3 Distributed Computing Implementation of GA Using MATLAB

Assembling the computer hardware (e.g. computers, cabling, and switches) is relatively easy, but orchestrating the four computers to perform computational tasks can be relatively difficult. As a result, distributed memory computing architectures often include head nodes and worker nodes with job schedulers. An engineer interested in distributing computations within a distributed memory architecture would have to program these job schedulers and orchestrate the distribution of computations using software written by him or herself. This can be a very daunting task and as a result, there is very limited application of distributed computing in structural engineering.

The present dissertation work utilizes the Matlab Parallel Computing Toolbox and Distributed Computing Engine [4.3] to orchestrate the distributed computing implementation of the genetic algorithm written for optimized design of steel framing systems subjected to seismic loading. The Optimization Toolbox [1.32] also contains a distributed computing option and this is used to facilitate distribution of computing tasks within the genetic algorithm implemented.

The Genetic Algorithm and Direct Search Toolbox [1.32] can automatically distribute the evaluation of objective function and nonlinear constraint functions associated with a genetic algorithm population to multiple processors within a distributed computing network [1.32]. There are two options to use the inherent parallelism in optimization problems to reduce the time to get a solution.

Option 1, using the parallel computing option in Optimization Toolbox™ and no code modification required. To use the parallel computing capability in Optimization Toolbox, one needs to do the following:

- add the following command-line to change the “UseParallel” option from the default ‘Never’, to ‘Always’,
- `options = optimset('UseParallel', 'Always');`
- enable the desired number of computer nodes with `matlabpool` command,
- `Matlabpool open 2`
- Run the optimization solver as before [4.3],
- `[x, fval,exitflag] = ga(@GA_fitness, NumberOfVariables, options)`

For Optimization Tool, set Options > User function evaluation > Evaluate fitness and constraint functions > parallel.

Option 2, if each run is independent in a serial approach as shown in Figure 4.2, and therefore can benefit from parallel computation. Using *parfor* (parallel for loop) to replace the for loop construct can speed up the objective function evaluation time because the objective statements inside the *parfor* loop can run in parallel.

Both of these two options need Parallel Computing Toolbox and MATLAB Distributed Computing Server [1.32]. Option 1 is selected for the present research effort. The parallel computing option in the Optimization Toolbox [1.32] can be used to automatically distributed computations and no code modification is required provided a working cluster is defined and the installation of MATLAB and all toolboxes is done properly. A schematic illustrating the administrative structure for MATLAB’s orchestration of distributed computations is given in Figure 4.3. The scheduler or job manager is resident on the head node on the computer cluster and computations are distributed to worker nodes according to tasks defined by the scheduler. The present

cluster includes four computers and therefore, there is a single master node and three worker nodes.

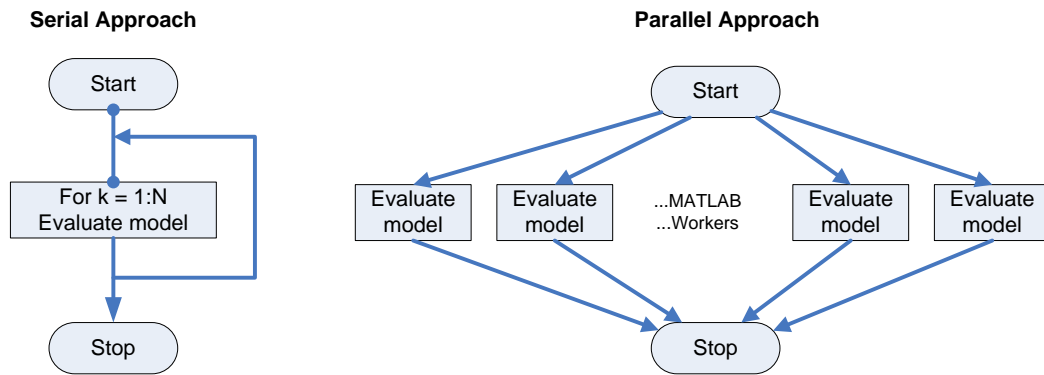


Figure 4.2 Serial Approach vs. Parallel Approach [1.32].

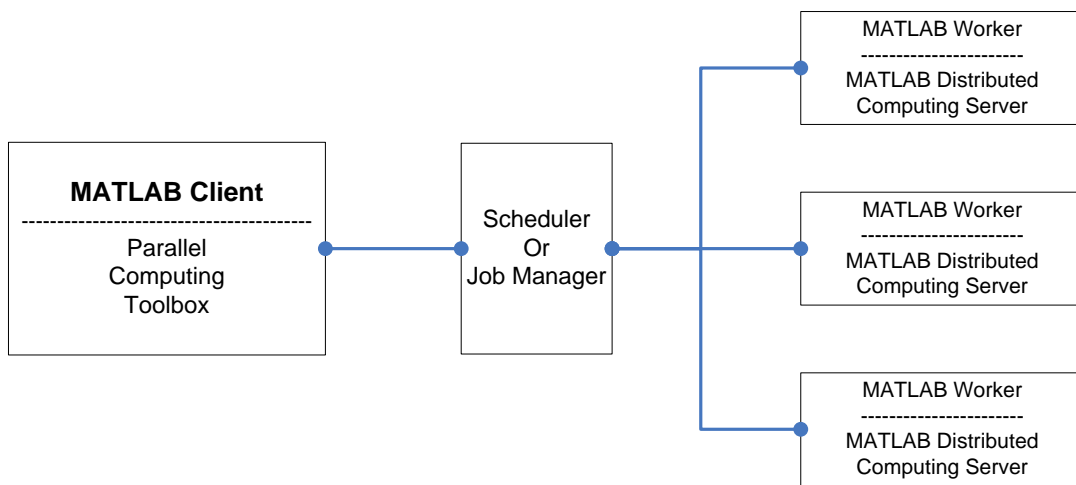


Figure 4.3 A MATLAB Administration System for Parallel and Distributed Computing

Parallel computing genetic algorithm with multiple objective functions works almost exactly the same as with single objective GA [1.32]. The only difference is to run

optionally a hybrid function, `fgoalattain`, after `gamultiobj` finishes its run. Each individual on Pareto curve in each generation becomes the starting point for an optimization using function `fgoalattain`. The optimization could be done in parallel and the number of processors involved is the smaller of the number of individuals or the number of working nodes which were regulated with command `matlabpool`.

The following command lines [1.32] need to be added to the program to run function `fgoalattain` in parallel.

```
fgoalopts = optimset('UseParallel', 'always')
gaoptions = gaoptimset('HybridFcn' , {fgoalattain,
fgoalopts})
```

There is a limitation to use Function `fgoalattain` - the objectives must be continuous. Function `fgoalattain` was not used though multiple objectives need to be optimized. However the objectives are discontinuous in the present research effort.

4.4 Frame Design Case Studies

A base frame topology was chosen to evaluate the evolutionary algorithm's ability to generate frame designs. A shear building model is implemented for structural analysis purposes and design variables in the optimization analysis include wide-flange column shapes and nonlinear viscous and visco-elastic damper parameters.

The 3-story, 4-bay frame topology used in the FEMA/SAC project [1.23] was converted to the shear-building model used in the present study. The topology of the revised frame model is shown in Figure 4.4. As outlined earlier in the dissertation, wind loads are not considered in this research. The structural steel which composes the wide-flange shapes is assumed to have a modulus of elasticity of 29,000 ksi and yield strength

of 50 ksi (elasto-plastic material response is assumed). The frames are spaced every 30 feet [1.23]. The floor dead load is taken as 96 lb/ft^2 ($D_F = 96 \text{ lb/ft}^2$) and the reduced live load present when ground motion occurs is taken as 20 lb/ft^2 ($L_r = 20 \text{ lb/ft}^2$). The self-weight of the steel framing is taken as 13 lb/ft^2 ($D_s = 13 \text{ lb/ft}^2$) and this is assumed to be consistent for all designs generated during the evolution. The seismic mass of the structure at the roof level and floor levels were taken to be: roof- $70.9 \text{ kip sec}^2/\text{ft}$; and floors- $65.53 \text{ k. sec}^2/\text{ft}$. The masses at each floor level are lumped and have a magnitude of $0.591 \text{ k. sec}^2/\text{in}$ on the roof level and a magnitude of $0.546 \text{ k. sec}^2/\text{in}$ on the 2nd and 3rd floor.

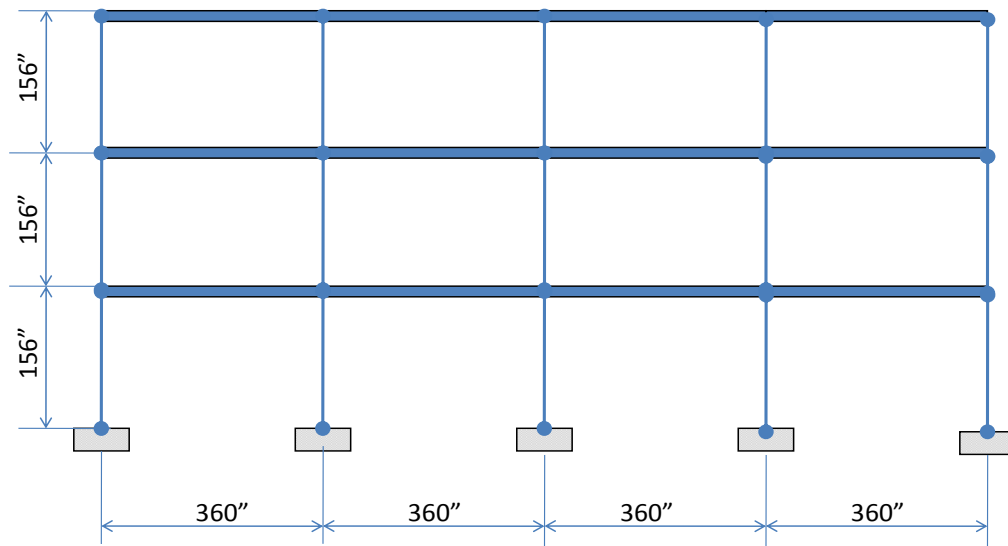


Figure 4.4 Basic Frame Topology Used for Design Studies

The structural frame without damping system could be modeled using various numbers of design variables. The wide-flange shape for any column member in the frame is considered a design variable. The number of column shapes chosen by the design algorithm varies depending upon how often the engineer seeks to change shapes within the frame topology. For example, the exterior columns shapes can be considered as a single design variable. Furthermore, the interior columns can be considered a common design variable. The engineer may also wish to allow the column shape to change over the height of the frame and as a result, the three story frame may have three design variables for each column line.

In addition to the column design variables, the dampers within the framing system (if present) include three design variables to describe the nonlinear, viscous and visco-elastic properties of the damper. The design variables for the dampers are: linear damping coefficient; elastic stiffness; and nonlinear characterizing parameter. The location of the viscoelastic dampers within the three-story, four-bay frame is considered fixed. Dampers are located in the second bay from the left within the frame topology.

The computer software package MDOF discussed earlier in this dissertation is utilized for the nonlinear response history analysis of structural systems. The program models hysteretic yielding of the steel member components and the linear/nonlinear characteristics of any viscous/viscoelastic dampers present in the framework. The MDOF analysis algorithms formulated in this dissertation are used as the basis for evaluating system response parameters needed to assess the expected annual loss quantity that is a foundational objective in the design optimization.

There are fifteen ground motions used to assess expected annual loss. These ground motions have various probabilities of exceedence within a common recurrence interval (50 years). The ground motions are characterized using peak ground acceleration (PGA). There are three ground motions for each of three probabilities of exceedence: 2% in 50 years; 10% in 50 years; and 50% in 50 years. The fifteen ground motions are given in Figure 4.5 [4.6].

Floor accelerations (relative to the ground) and interstory drift are engineering demand parameters used to define expected annual loss within the performance-based design environment discussed earlier in Chapter 3. The five ground motions for each intensity measure shown in Figure 4.5 are used to define the median floor maximum acceleration and the median level maximum drift corresponding to each intensity measure.

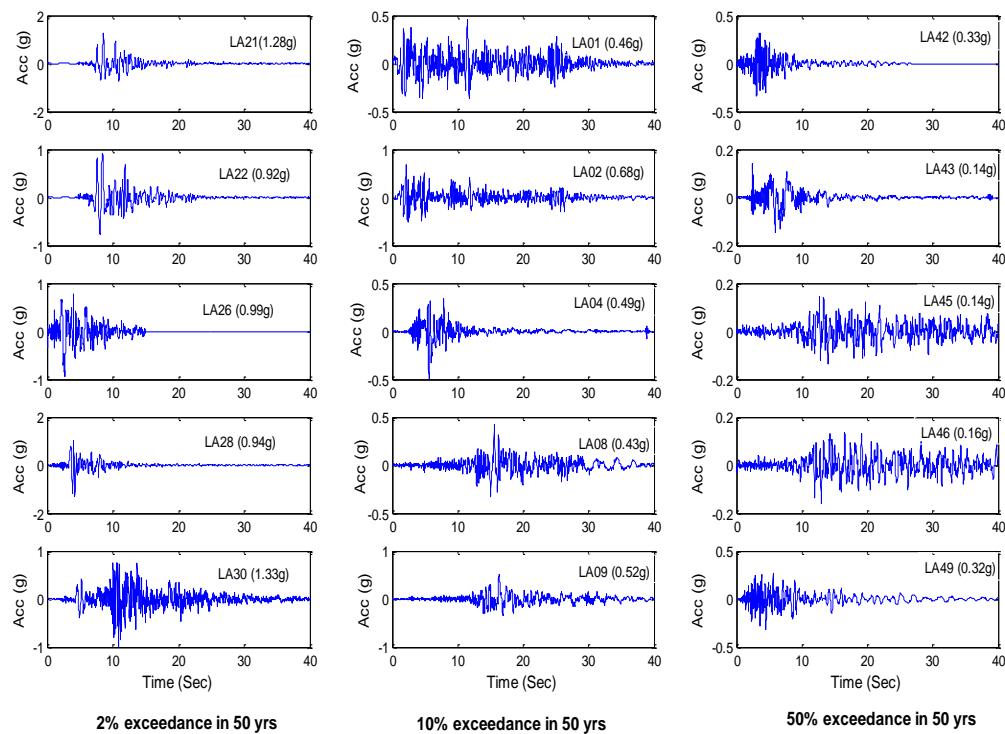


Figure 4.5 Ground Motion Record Suite Used for Frame Designs

The engineering demand parameters are then used in conjunction with fragility functions to evaluate damage to the structural system (SS), non-structural drift-sensitive components (NSD), and non-structural acceleration-sensitive components (NSA). These damage magnitudes are then used to define loss using each intensity measure. The annual probabilities of occurrence for each intensity measure are then assigned and equation (3.8) is used to establish the expected annual loss for any given design. This is then one of the two objectives considered in the optimized design statement.

4.4.1 Genetic Algorithm Parameters

Genetic Algorithm (GA) and Direct Search Toolbox built-in MATLAB [1.32] are used to operate optimization design in this research. The parameters for Genetic Algorithm were defined and listed in the Table 4.1. The Pareto fraction option limits the number of individuals on the Pareto front. The default population size used by `GAMULTIOBJ` is '15*Design Variables'. To set the Parameters of Population size and Pareto fraction to 0.9 and 100, would generate 90 individual points on the Pareto front in the last generation. There three different criteria to determine when to stop the solver running GA program. The solver stops when any one of the stopping criteria is met. It stops when the maximum number of generations is reached; 200 for the present research. The solver also stops if the average change in the spread of the Pareto front over the 'StallGenLimit' generations (default is 100) is less than tolerance specified in options 'TolFun'. The third criterion (not used in the present research) is the maximum time limit in seconds (default is ∞). The stopping criteria for GA in this research were defined to “no

improvement in the best fitness value for an interval of time in seconds specified by Stall time limit” or a maximum generation number of 200 is reached.

Table 4.1 Genetic Algorithm Parameters:

Design Variables	Varies with cases
Fitness Functions	2, Total initial construction cost and Expected Annual Lost (EAL)
Population type	“custom”, discrete integer,
Max. generation	200
Population size	100
Pareto Fraction	0.9
StallGenLimit	100
TolFun	1e-4

4.4.2 Fragility Curve Parameters and Repair Cost Ratios

The parameters listed in Table 4.2 are assigned to the fragility functions given in equations (3.4) and (3.5) to evaluate the damage and loss to the structural system and non-structural components. ISDA represents the interstory drift angle and PFA represents the peak floor acceleration. ISDA and PFA are used to characterize the response of SS, NSD, and NSA components during an earthquake. The numbers in Table 4.2 present the median values of ISDA and PFA used to define the fragility curve(s). β_{ds} is the damage-state lognormal standard deviation. The fragility curves used in the present study correspond to high-code seismic levels and a building type S1L (steel moment-frame) in the HAZUS model [1.24]. High-code seismic level refers to lateral force design requirements of seismic Zone 4 according to 1994 UBC code.

The repair cost ratios are listed in Table 4.3 and equation (3.4) are used to estimate the losses due to the damage to structural and non-structural components. Only direct economic loss is considered in this dissertation. The methodology developed can be extended to estimate casualty and downtime (indirect) losses using different repair

cost ratio parameters. The values in Table 4.3 are picked from Table 3.2, Table 3.3, and Table 3.4 in Chapter 3, assuming that a commercial building provides Professional/Technical/Business Services.

Table 4.2: Fragility Curve Parameters for Structural and Non-Structural Components in SIL building and High-Code Design Level.

Component	Fragility Curve Parameter	Damage State			
		Slight	Moderate	Extensive	Complete
SS	\overline{ISDA}_{ds}	0.004	0.008	0.020	0.0533
	β_{ds}	0.50	0.50	0.50	0.50
NSD	\overline{ISDA}_{ds}	0.004	0.008	0.025	0.050
	β_{ds}	0.50	0.50	0.50	0.50
NSA	$\overline{PFA}_{ds}(g)$	0.30	0.60	1.20	2.40
	β_{ds}	0.60	0.60	0.60	0.60

Table 4.3: Repair Cost Ratios in % of Building Replacement Cost for Structural and Non-Structural Components.

Component	Damage State			
	Slight	Moderate	Extensive	Complete
SS	0.4	1.9	9.6	19.2
NSD	0.7	3.3	16.4	32.9
NSA	0.9	4.8	14.4	47.9

4.4.3 Optimal Design Statements for Case Studies

Two of the major objectives of the dissertation are to evaluate the ability of the genetic algorithm and optimal design algorithm formulated to generate feasible and realistic designs for practically sized frameworks; and to evaluate the influence of supplemental damper systems on the performance of frames and expected annual losses when subjected to seismic loads.

Six design case studies are considered in this dissertation. Each case study corresponds to a unique combination of design variables involving wide-flange column arrangements and passive supplemental damper parameters for the three-story, four-bay frame shown in Figure 4.4. The cases considered and the objective of their comparison to other cases is described in the following.

Design Cases 1:

The frame topology and design variables considered for Design Case 1 are shown in Figure 4.6.

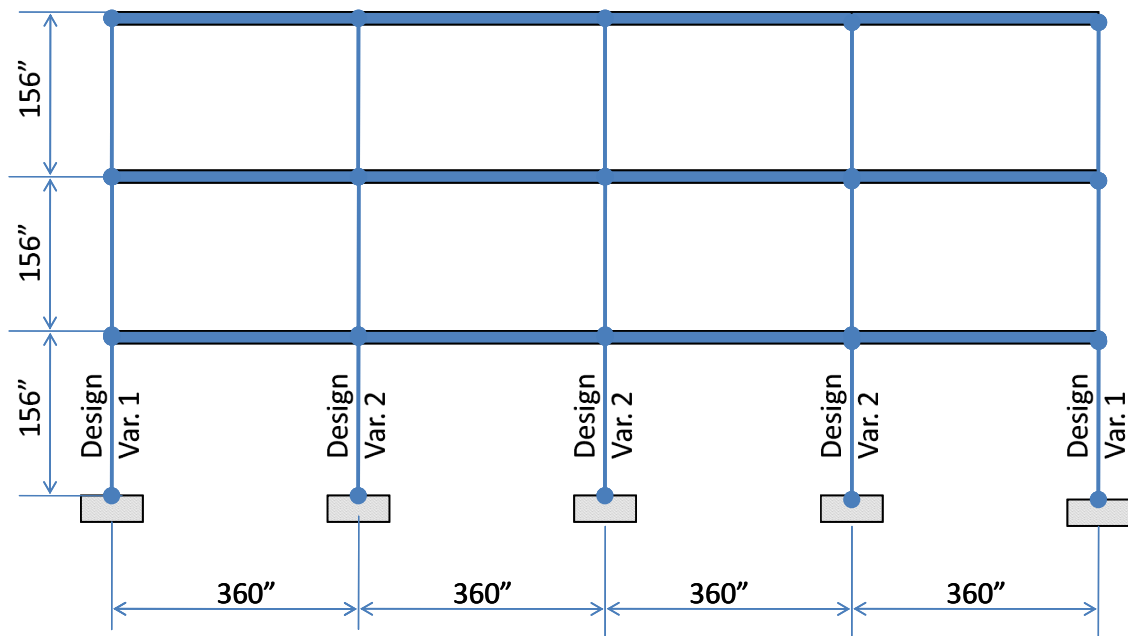


Figure 4.6 Topology for Frame Design Case 1.

This design case includes the bare minimum number of design variables considered practical for the present framework. Two design variables are considered: interior column shape and exterior column shape. There are no supplemental dampers or

diagonal bracing elements in this design case. The column shape is assumed to extend through all three stories. Column shapes come from the standard wide-flange shapes found in the *AISC Steel Construction Manual* [3.5]. A reduced database of wide-flange shapes is used and it is given in Appendix 22.

The motivation for this case is to evaluate expected annual loss and initial construction cost when the frame is constructed without supplemental damping devices and diagonal bracing elements. The results generated by the algorithm for this design case can facilitate comparison with the results for other design cases. This will allow the engineer to explore how defining the parameters of the damper can affect expected annual loss and initial construction cost.

Design Cases 2, 3, and 4:

The frame topologies and design variables for design cases 2, 3, and 4 are shown in Figures 4.7, 4.8, and 4.9, respectively. These three design cases involve passive supplemental damping devices located in the second bay from the leftmost bay. There are three design variables for column sizes in each frame. The column shapes are assumed to extend from the ground story to the third story. Column shapes adjacent to the diagonal bracing are assumed to be the same.

The main difference among these three design cases is in regard to the type of passive dampers allowed in the design. Case 2 includes linear dampers with the damper exponent, α equal to 1.0. Case 3 includes what can be termed as softening dampers where response in force-velocity space asymptotically approaches a limiting value

(Figure 2.3). Design Case 4 includes super linear dampers where force-velocity space behavior exponentially increases.

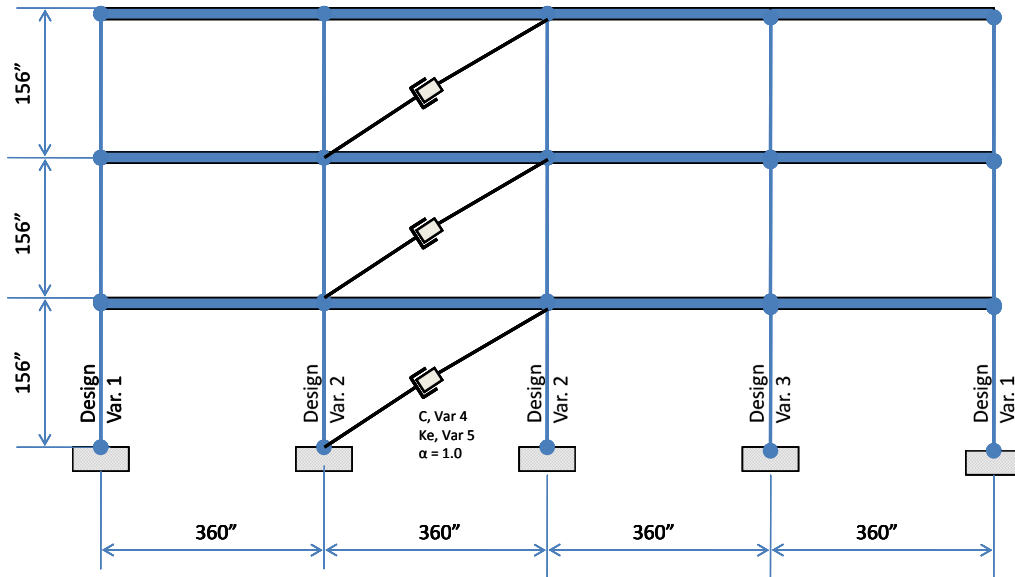


Figure 4.7 Frame Design Case 2, 5 Design Variables, Linear Dampers

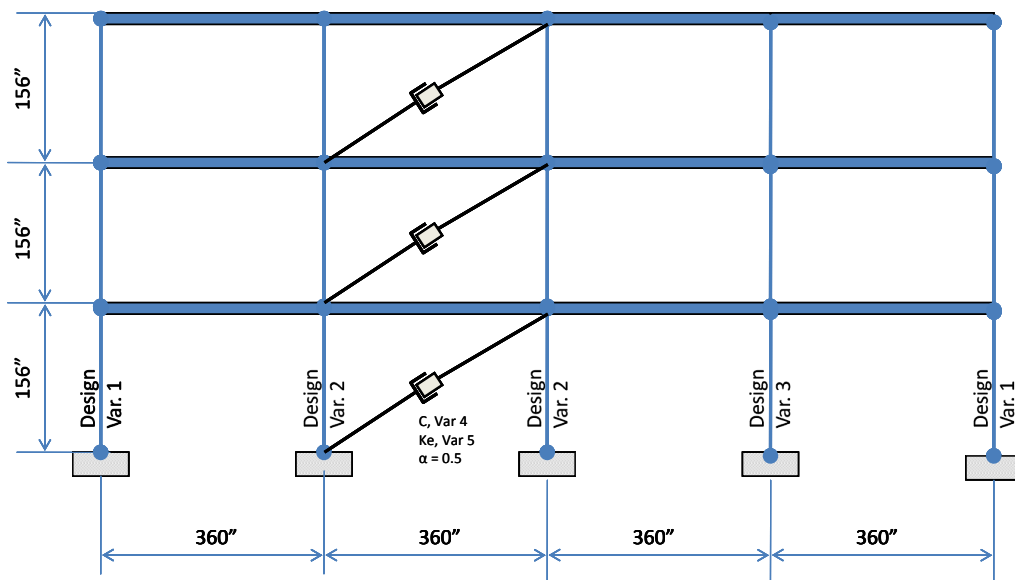


Figure 4.8 Frame Design Case 3, 5 Design Variables, Nonlinear Dampers, $\alpha = 0.5$

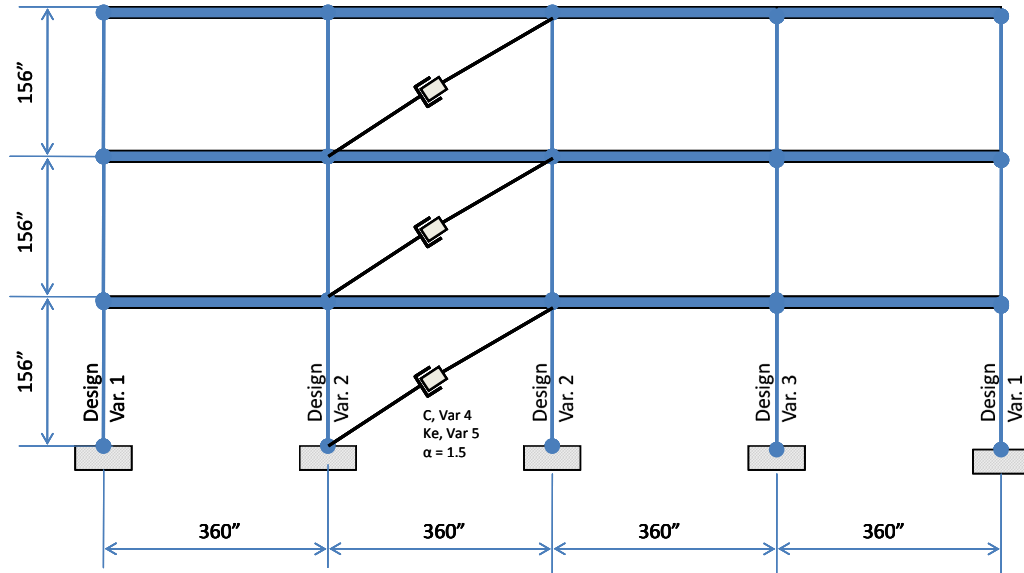


Figure 4.9 Frame Design Case 4, 5 Design Variables, Nonlinear Dampers, $\alpha = 1.5$

Design variables in each of these three design cases include two parameters defining damper characteristics: the proportionality factor, c^S ; and the visco-elastic stiffness parameter, k_e . The damping coefficient, c^S is typically selected from a range of discrete values from 0 to 100 ($k - s / in$) with increasing spacing 10 ($k - s / in$). The constraints to damper stiffness, k_e and the cost of dampers are described in Chapter 3. It should be noted that the dampers at all three levels are the same passive damper. In other words, there are three dampers placed in the framework, each with the same damper characteristics (two of which are assigned by the design algorithm developed).

The motivation for these three cases is to evaluate the designs that result when specific damper types are forced: linear viscoelastic; super-linear viscoelastic; and asymptotic viscoelastic dampers. Column sizes may be affected by these variations in damper types as well as the proportionality and viscoelastic stiffness parameters.

Comparison of results from these three cases also facilitates evaluation of how damper characteristics affect expected annual loss and the resulting impact on initial construction cost. Furthermore, these cases will help to identify the most appropriate damper type.

Design Cases 5 and 6:

The frame topologies and design variable orientations for design cases 5 and 6 are given in Figures 4.10 and 4.11, respectively. Three linear supplemental damping devices are assumed in Case 5. Dampers are allowed to be different at each level in the frame. Case 6 allows all three damper parameters at all three levels within the frame to be defined by the automated design algorithm. The relative velocity exponents, α is selected from a range of discrete values from 0.5 to 1.5 with increasing spacing 0.25. Damping coefficient, c^s is selected from a range of discrete values from 0 to 100 ($k - s / in$) as in Cases 2, 3, and 4. The number of design variables for the column sizes remains as defined in the previous design cases which have damping devices. Design Case 6 will allow the most flexibility with regard to the algorithm selecting damper characteristics. As a result, the engineer can see what the ground motions and frame topology demand as the best damper arrangement at all locations within the frame.

4.5 Case Study Results and Discussion

Each of the six design cases was run using the objectives of minimizing expected annual loss (EAL) and minimizing initial construction cost. These objectives are defined in equations (3.2) for frames without dampers, equation (3.3) for frames with dampers, and

equation (3.8). Design constraints transformed to penalties thereby generating an unconstrained optimization problem are defined in Section 3.2 of the dissertation.

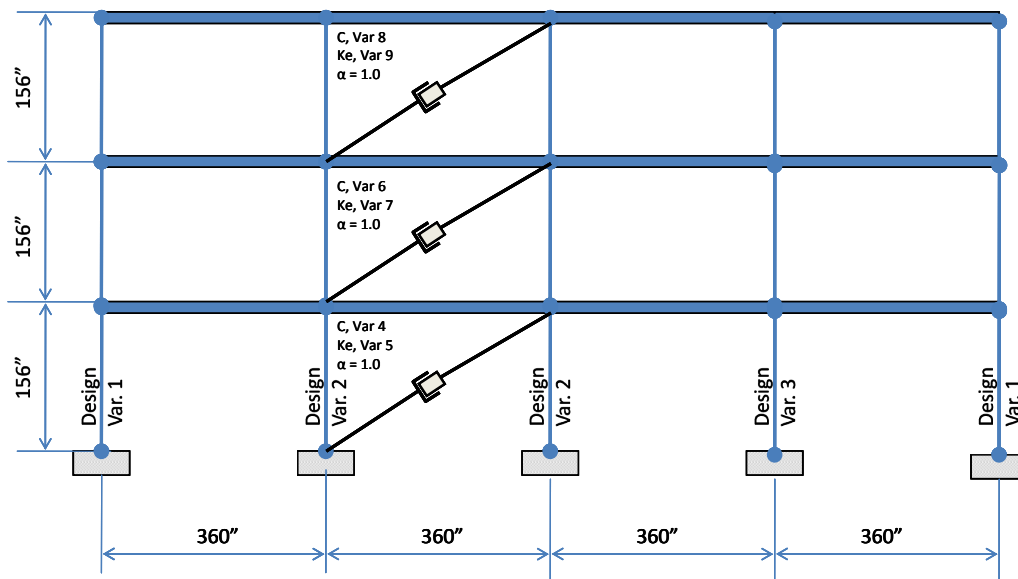


Figure 4.10 Frame Design Case 5, 9 Design Variables, Linear Dampers, $\alpha = 1.0$

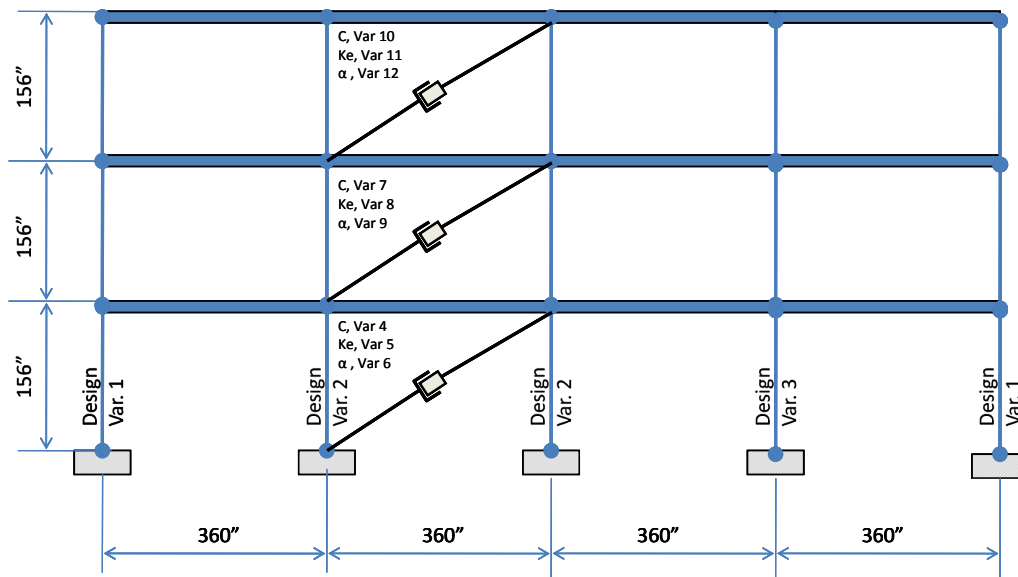


Figure 4.11 Frame Design Case 6, 12 Design Variables.

Genetic algorithm parameters were defined in Table 4.1 and the stopping criteria described earlier in this chapter. The optimization design results for the steel shear building models with/without viscoelastic dampers will be discussed in this section. Three (3) individual designs, which represent minimum initial cost, minimum expected annual loss (EAL), and the median point in the last generation Pareto fronts are included in the synthesis of the design results.

All design results included in the Pareto fronts are feasible designs (*i.e.* all design constraints are satisfied). The feasibility of the designs was gauged by checking constraint penalty factors. All penalty factors for the designs considered and discussed are less than or equal to 1.1 (*i.e.* there is a 10% violation of constraints allowed).

Each design case will be discussed in the following. Comparisons will also be made among design cases to explore how various design variable selection schemes as well as damper inclusion/exclusion affects initial construction costs and expected annual losses for the steel frame topology examined.

4.5.1 Design Case 1

Design Case 1 is the first to be considered. The genetic algorithm was run and many feasible designs in objective space were developed. As discussed earlier, two objectives were present in the optimization problem formulated: (a) minimum expected annual loss as a percentage of initial construction cost; and (b) minimum total initial construction cost (dollars).

Design Case 1 included a framework with two design variables (see Figure 4.6). Figure 4.12 illustrates potential feasible designs plotted in objective space.

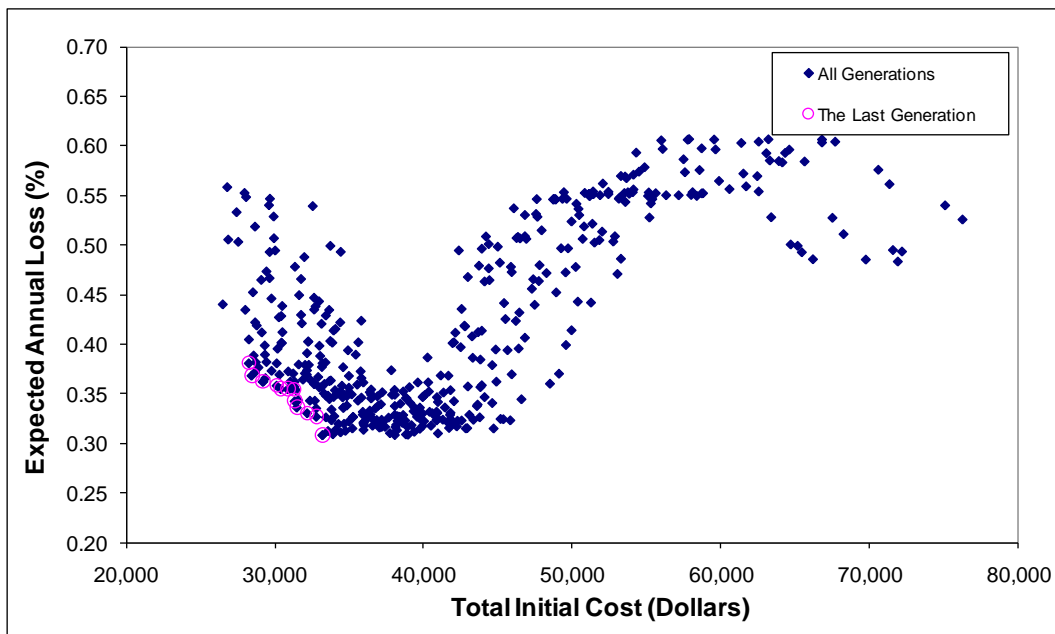


Figure 4.12 Pareto Front for Frame Design Case 1

The solid diamonds in the plot are feasible designs generated throughout all generations in the genetic algorithm. The circled diamonds indicate the designs oriented along the Pareto front at the last generation. As indicated in the figure, there are many, many potential feasible designs that the structural engineer may consider. The Pareto front includes designs that dominate all potential feasible solutions in at least one of the two objectives.

Table 4.4 includes the feasible designs on the Pareto front in Figure 4.12. These designs are better than all designs generated throughout the evolution in at least one of the two objectives. If both objectives are weighted equally (*i.e.* no designer preference), there are twelve potential designs to consider at the end of the evolution. The Pareto front designs range in initial construction cost from \$28,300 to \$33,200. The expected annual loss (EAL) resulting from the suite of ground motions considered ranges from 0.38% to 0.31% of the building replacement cost. Thus, an engineer can select the

magnitude of EAL that is desired and then understand the associated cost of additional construction cost to meet that loss level. This is performance-based engineering.

Table 4.4 Design Variables in the Last Generation, Case 1

Designs	1st Story		2nd Story		3 Story		Cost (\$)	EAL (%)
	Variable 1	Variable 2	Variable 1	Variable 2	Variable 1	Variable 2		
1 *	W14X283	W14X48	W14X283	W14X48	W14X283	W14X48	33200	0.31
2	W14X283	W12X45	W14X283	W12X45	W14X283	W12X45	32800	0.33
3	W14X233	W14X74	W14X233	W14X74	W14X233	W14X74	32200	0.33
4	W14X257	W14X53	W14X257	W14X53	W14X257	W14X53	31500	0.34
5	W14X233	W14X68	W14X233	W14X68	W14X233	W14X68	31400	0.34
6 **	W12X96	W14X159	W12X96	W14X159	W12X96	W14X159	31300	0.36
7	W14X132	W14X132	W14X132	W14X132	W14X132	W14X132	30900	0.36
8	W14X257	W10X45	W14X257	W10X45	W14X257	W10X45	30400	0.36
9	W14X211	W14X74	W14X211	W14X74	W14X211	W14X74	30100	0.36
10	W14X48	W14X176	W14X48	W14X176	W14X48	W14X176	29200	0.36
11	W14X193	W14X74	W14X193	W14X74	W14X193	W14X74	28500	0.37
12 ***	W14X233	W10X45	W14X233	W10X45	W14X233	W10X45	28300	0.38

*, The minimum EAL design

**, The median point of Pareto Front in the last generation

***, The minimum initial cost

Three designs are noted in Table 4.4. The first is the design with the minimum EAL (0.31%). The second is the design median design on the Pareto front (*i.e.* one-half the designs have lower initial construction cost, but greater EAL and one-half the designs have higher initial construction cost, but lower EAL). This median design can be said to have equal preference in meeting the minimization objectives. The final noted design is the one which has the minimum initial construction cost (\$28,300).

The column sizes follow a relatively predictable pattern with weight reducing as one rises through the frame, nominal depth reducing as one rises through the frame, and the exterior columns being slightly larger than the interior. Overall, the wide-flange

shapes selected by the algorithm are shapes expected. It should be re-emphasized that a reduced database of shapes (Appendix 22) was used (see earlier discussion).

Design Case 1 has the same cross-section shape running from the ground floor level to the roof. It should be noted that the economy of repetition is not addressed in the definition of lower initial construction costs. In other words, while changing member sizes over the height of a three-story frame may result in lower weight, there is more fabrication-related expense in allowing this variation. As a result, it may actually cost less to construction a design using the design variable arrangement used in Design Case 1. This additional fabrication-related expense could be interjected into the present definition of cost, but it was not done in this dissertation.

The distribution of expected annual loss among the structural and nonstructural components in the building system for Design Case 1 is shown in Table 4.5.

Table 4.5 The Distribution of Losses, Case 1

Designs	Seismic Losses	Distribution of Repair Cost (%)									Total EAL (%)
		2% in 50 yrs			10% in 50 yrs			50% in 50 yrs			
		SS	NSD	NSA	SS	NSD	NSA	SS	NSD	NSA	
1	EAL (%)	2.46E-03	3.41E-03	2.95E-02	1.23E-03	2.12E-03	4.30E-02	2.50E-03	4.36E-03	2.20E-01	3.09E-01
	Distribution	0.80	1.10	9.56	0.40	0.68	13.91	0.81	1.41	71.21	
2	EAL (%)	2.80E-03	3.85E-03	3.60E-02	1.51E-03	2.59E-03	4.87E-02	3.08E-03	5.37E-03	2.23E-01	3.27E-01
	Distribution	0.86	1.18	10.99	0.46	0.79	14.90	0.94	1.64	68.28	
3	EAL (%)	2.56E-03	3.55E-03	3.05E-02	1.99E-03	3.38E-03	5.09E-02	3.53E-03	6.15E-03	2.28E-01	3.31E-01
	Distribution	0.77	1.07	9.21	0.60	1.02	15.38	1.07	1.86	68.95	
4	EAL (%)	3.05E-03	4.23E-03	3.54E-02	1.96E-03	3.33E-03	5.09E-02	3.51E-03	6.11E-03	2.28E-01	3.36E-01
	Distribution	0.91	1.26	10.55	0.58	0.99	15.13	1.04	1.82	67.85	
5	EAL (%)	4.42E-03	6.24E-03	3.52E-02	2.41E-03	4.07E-03	5.04E-02	3.73E-03	6.49E-03	2.30E-01	3.43E-01
	Distribution	1.29	1.82	10.27	0.70	1.19	14.69	1.09	1.89	67.01	
6	EAL (%)	7.56E-03	1.20E-02	4.39E-02	3.43E-03	5.66E-03	6.19E-02	3.77E-03	6.57E-03	2.10E-01	3.55E-01
	Distribution	2.13	3.38	12.35	0.96	1.59	17.44	1.06	1.85	59.18	
7	EAL (%)	6.70E-03	1.03E-02	4.30E-02	3.38E-03	5.58E-03	5.45E-02	3.84E-03	6.69E-03	2.21E-01	3.55E-01
	Distribution	1.89	2.90	12.10	0.95	1.57	15.35	1.08	1.89	62.22	
8	EAL (%)	7.54E-03	1.19E-02	4.40E-02	3.46E-03	5.69E-03	5.62E-02	3.81E-03	6.64E-03	2.15E-01	3.55E-01
	Distribution	2.13	3.36	12.38	0.97	1.60	15.83	1.07	1.87	60.70	
9	EAL (%)	7.31E-03	1.15E-02	4.36E-02	3.32E-03	5.48E-03	5.34E-02	3.86E-03	6.72E-03	2.23E-01	3.59E-01
	Distribution	2.04	3.19	12.15	0.92	1.53	14.88	1.07	1.87	62.21	
10	EAL (%)	9.35E-03	1.53E-02	4.65E-02	3.42E-03	5.64E-03	6.12E-02	3.77E-03	6.58E-03	2.11E-01	3.62E-01
	Distribution	2.58	4.22	12.84	0.94	1.56	16.92	1.04	1.82	58.19	
11	EAL (%)	1.12E-02	1.89E-02	4.62E-02	3.43E-03	5.69E-03	6.49E-02	3.89E-03	6.78E-03	2.08E-01	3.69E-01
	Distribution	3.03	5.12	12.52	0.93	1.54	17.60	1.06	1.84	56.27	
12	EAL (%)	1.32E-02	2.26E-02	4.81E-02	4.29E-03	6.96E-03	6.52E-02	4.35E-03	7.57E-03	2.07E-01	3.79E-01
	Distribution	3.48	5.96	12.69	1.13	1.84	17.21	1.15	2.00	54.60	

Most of the total losses come from the losses of non-structural acceleration-sensitive (NSA) components. When the seismic level is not severe, such as 50/50 ground motions, the contribution to losses from damage of NSA components was almost 70% for all designs. Tables 4.4 and 4.5 illustrate that losses move toward a more even balance among SS, NSD and NSA components as the initial construction cost is reduced. Therefore, there is more damage to NSD and SS components as the initial construction cost reduces and there is little improvement with regard to the loss from NSA component damage.

4.5.2 Design Cases 2, 3, and 4

Design Case 2 includes a single damper configuration distributed over the height of the three-story framework located within the second bay from the left. The dampers in this case are linear or nonlinear and viscous or viscoelastic as determined by the algorithm (Figure 4.7).

The designs generated throughout the entire evolution plotted in objective space for Design Case 2 are shown in Figure 4.13. The final generation Pareto front is noted using diamonds enclosed by circles. Table 4.6 illustrates the design variables selected for the last generation in the evolution for Design Case 2. The use of passive supplemental damping systems has a significant impact on the column sizes required as a moment resisting framework is no longer the dominant lateral load resisting system. There is a relatively wide range of damping coefficients chosen 10 to 100 kips-sec/in. It is also interesting to note that relatively narrow viscoelastic stiffness property is selected (0 to 20

kips/in) by the algorithm. The range of EAL and total initial construction costs over the Pareto front is relatively narrow (\$49,211 to \$33,895).

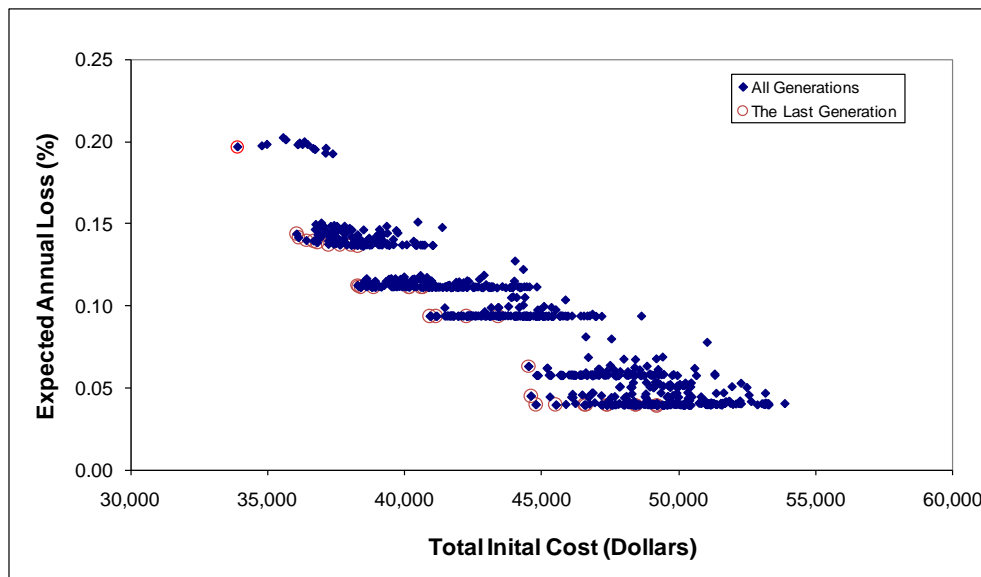


Figure 4.13 Pareto Front for Frame Design Case 2.

It is very interesting to note that the lowest construction cost (\$33,895) in Case 2 is very similar to the highest construction cost (\$33,200) in Case 1. However, the expected annual losses for all designs in Design Case 2 are less than 0.20% of building repair costs, where the lowest EAL in design case 1 was 0.31%. This suggests that the use of dampers, while adding initial construction expense, will result in lower expected annual losses due to ground motion. This supports the popularity of supplemental damping systems in seismic engineering.

The distribution of losses between structural (SS) and non-structural components (NSA, NSD) for each level ground motions from Case 2 is listed in Table 4.7. Most of the total losses in this design case again come from the losses due to damage to non-structural acceleration sensitive (NSA) components.

Table 4.6 Design Variables in the Last Generation, Case 2.

Designs	Columns			Dampers			Total Cost	EAL
	Exterior	Interior		C	K _e	α	(\$)	(%)
	Variable 1	Variable 2	Variable 3	kips-sec/in	kips/in			
1 *	W8X28	W10X112	W8X58	100	0	1.0	49211	0.04
2	W8X28	W10X112	W8X58	100	10	1.0	49196	0.04
3	W8X28	W10X112	W12X45	100	0	1.0	48439	0.04
4	W8X28	W10X112	W12X45	100	10	1.0	48421	0.04
5	W8X28	W12X96	W8X58	100	0	1.0	47386	0.04
6	W8X28	W12X96	W8X58	100	10	1.0	47365	0.04
7	W8X28	W12X96	W12X45	100	0	1.0	46598	0.04
8	W8X28	W12X96	W12X45	100	10	1.0	46573	0.04
9	W8X28	W10X60	W8X58	100	0	1.0	45514	0.04
10	W8X28	W10X60	W12X45	100	0	1.0	44783	0.04
11	W8X28	W10X60	W12X45	90	0	1.0	44602	0.05
12	W8X28	W10X60	W12X45	70	0	1.0	44515	0.06
13	W8X28	W10X112	W12X45	40	0	1.0	43415	0.09
14	W8X28	W12X106	W8X58	40	0	1.0	42254	0.09
15	W8X28	W12X106	W12X45	40	0	1.0	41131	0.09
16	W8X28	W12X96	W12X45	40	10	1.0	40925	0.09
17	W8X28	W12X96	W12X45	40	0	1.0	40917	0.09
18 **	W12X96	W12X106	W12X45	30	20	1.0	40667	0.11
19	W12X96	W12X106	W12X45	30	10	1.0	40589	0.11
20	W12X96	W12X96	W12X45	30	20	1.0	40172	0.11
21	W12X96	W12X96	W12X45	30	10	1.0	40147	0.11
22	W10X45	W12X106	W12X45	30	20	1.0	38859	0.11
23	W8X28	W12X106	W12X45	30	20	1.0	38398	0.11
24	W8X28	W12X106	W12X45	30	10	1.0	38310	0.11
25	W8X28	W12X106	W12X45	30	0	1.0	38280	0.11
26	W8X40	W10X112	W12X96	20	10	1.0	38273	0.14
27	W8X28	W10X112	W12X96	20	20	1.0	38045	0.14
28	W12X96	W12X106	W12X45	20	10	1.0	37637	0.14
29	W8X28	W10X112	W12X96	20	10	1.0	37633	0.14
30	W8X28	W10X112	W12X96	20	0	1.0	37213	0.14
31	W10X45	W12X106	W12X96	20	20	1.0	36803	0.14
32	W10X45	W12X106	W12X96	20	10	1.0	36676	0.14
33	W8X28	W12X106	W12X96	20	20	1.0	36410	0.14
34	W8X28	W12X106	W12X96	20	10	1.0	36121	0.14
35	W8X28	W12X106	W12X96	20	0	1.0	36053	0.14
36 ***	W10X45	W10X112	W12X96	10	10	1.0	33895	0.20

*, The minimum EAL design

**, The median point of Pareto Front in the last generation

***, The minimum initial cost

Table 4.7 Distribution of Losses, Case 2

Designs	Seismic Losses	Distribution of Repair Cost (%)									Total EAL (%)
		2% in 50 yrs			10% in 50 yrs			50% in 50 yrs			
		SS	NSD	NSA	SS	NSD	NSA	SS	NSD	NSA	
1	EAL (%)	5.26E-04	8.73E-04	2.21E-03	1.68E-04	2.94E-04	5.97E-03	4.85E-05	8.48E-05	2.93E-02	3.94E-02
	Distribution	1.34	2.21	5.60	0.43	0.75	15.14	0.12	0.22	74.26	
2	EAL (%)	5.25E-04	8.71E-04	2.21E-03	1.66E-04	2.89E-04	5.98E-03	4.81E-05	8.41E-05	2.93E-02	3.95E-02
	Distribution	1.33	2.21	5.61	0.42	0.73	15.13	0.12	0.21	74.27	
3	EAL (%)	5.25E-04	8.71E-04	2.22E-03	1.65E-04	2.89E-04	5.98E-03	4.80E-05	8.40E-05	2.93E-02	3.95E-02
	Distribution	1.33	2.20	5.61	0.42	0.73	15.13	0.12	0.21	74.29	
4	EAL (%)	5.24E-04	8.69E-04	2.22E-03	1.63E-04	2.84E-04	5.99E-03	4.74E-05	8.30E-05	2.94E-02	3.96E-02
	Distribution	1.32	2.19	5.61	0.41	0.72	15.12	0.12	0.21	74.30	
5	EAL (%)	5.24E-04	8.69E-04	2.22E-03	1.62E-04	2.84E-04	5.99E-03	4.74E-05	8.29E-05	2.94E-02	3.96E-02
	Distribution	1.32	2.19	5.62	0.41	0.72	15.12	0.12	0.21	74.31	
6	EAL (%)	5.22E-04	8.66E-04	2.23E-03	1.59E-04	2.78E-04	6.00E-03	4.66E-05	8.15E-05	2.95E-02	3.97E-02
	Distribution	1.31	2.18	5.62	0.40	0.70	15.11	0.12	0.21	74.31	
7	EAL (%)	5.22E-04	8.66E-04	2.23E-03	1.59E-04	2.78E-04	6.00E-03	4.65E-05	8.13E-05	2.95E-02	3.97E-02
	Distribution	1.31	2.18	5.62	0.40	0.70	15.12	0.12	0.20	74.33	
8	EAL (%)	5.20E-04	8.63E-04	2.24E-03	1.56E-04	2.72E-04	6.01E-03	4.55E-05	7.97E-05	2.96E-02	3.98E-02
	Distribution	1.31	2.17	5.63	0.39	0.68	15.11	0.11	0.20	74.33	
9	EAL (%)	5.25E-04	8.70E-04	2.13E-03	1.79E-04	3.12E-04	5.91E-03	4.35E-05	7.61E-05	2.87E-02	3.87E-02
	Distribution	1.36	2.25	5.50	0.46	0.81	15.28	0.11	0.20	74.07	
10	EAL (%)	5.26E-04	8.72E-04	2.14E-03	1.78E-04	3.11E-04	5.92E-03	4.54E-05	7.94E-05	2.88E-02	3.88E-02
	Distribution	1.36	2.25	5.52	0.46	0.80	15.26	0.12	0.20	74.13	
11	EAL (%)	6.54E-04	1.06E-03	2.48E-03	2.55E-04	4.46E-04	6.29E-03	7.81E-05	1.37E-04	3.19E-02	4.33E-02
	Distribution	1.51	2.46	5.73	0.59	1.03	14.53	0.18	0.32	73.73	
12	EAL (%)	1.06E-03	1.63E-03	3.36E-03	5.45E-04	9.47E-04	7.16E-03	2.40E-04	4.20E-04	4.11E-02	5.65E-02
	Distribution	1.87	2.89	5.94	0.96	1.68	12.68	0.43	0.74	72.76	
13	EAL (%)	2.73E-03	3.74E-03	6.02E-03	1.56E-03	2.67E-03	1.31E-02	8.88E-04	1.55E-03	6.14E-02	9.37E-02
	Distribution	2.91	3.99	6.42	1.67	2.85	14.03	0.95	1.66	65.50	
14	EAL (%)	2.74E-03	3.76E-03	5.85E-03	1.44E-03	2.46E-03	1.34E-02	7.04E-04	1.23E-03	6.22E-02	9.38E-02
	Distribution	2.92	4.01	6.23	1.53	2.63	14.31	0.75	1.31	66.27	
15	EAL (%)	2.71E-03	3.72E-03	5.88E-03	1.39E-03	2.39E-03	1.35E-02	6.43E-04	1.12E-03	6.25E-02	9.38E-02
	Distribution	2.89	3.96	6.27	1.48	2.54	14.39	0.69	1.20	66.59	
16	EAL (%)	2.71E-03	3.72E-03	5.87E-03	1.43E-03	2.45E-03	1.34E-02	6.89E-04	1.20E-03	6.22E-02	9.37E-02
	Distribution	2.89	3.97	6.26	1.52	2.61	14.34	0.73	1.28	66.42	
17	EAL (%)	2.72E-03	3.72E-03	5.83E-03	1.47E-03	2.52E-03	1.34E-02	7.47E-04	1.31E-03	6.20E-02	9.36E-02
	Distribution	2.90	3.98	6.22	1.57	2.69	14.27	0.80	1.40	66.20	
18	EAL (%)	2.71E-03	3.73E-03	8.22E-03	1.36E-03	2.34E-03	1.78E-02	2.63E-04	4.61E-04	7.45E-02	1.11E-01
	Distribution	2.44	3.36	7.41	1.23	2.11	15.99	0.24	0.42	67.11	

Table 4.7 Distribution of Losses, Case 2 (continued)

Designs	Seismic Losses	Distribution of Repair Cost (%)									Total
		2% in 50 yrs			10% in 50 yrs			50% in 50 yrs			EAL
		SS	NSD	NSA	SS	NSD	NSA	SS	NSD	NSA	(%)
19	EAL (%)	2.83E-03	3.89E-03	8.14E-03	1.41E-03	2.41E-03	1.79E-02	2.82E-04	4.94E-04	7.41E-02	1.11E-01
	Distribution	2.55	3.51	7.33	1.27	2.17	16.11	0.25	0.44	66.77	
20	EAL (%)	2.87E-03	3.95E-03	8.18E-03	1.44E-03	2.47E-03	1.80E-02	3.00E-04	5.24E-04	7.38E-02	1.12E-01
	Distribution	2.57	3.53	7.30	1.29	2.21	16.05	0.27	0.47	65.90	
21	EAL (%)	3.03E-03	4.18E-03	7.92E-03	1.49E-03	2.55E-03	1.81E-02	3.22E-04	5.63E-04	7.34E-02	1.12E-01
	Distribution	2.71	3.73	7.07	1.33	2.28	16.13	0.29	0.50	65.57	
22	EAL (%)	3.53E-03	4.85E-03	7.64E-03	1.90E-03	3.22E-03	1.82E-02	6.08E-04	1.06E-03	7.06E-02	1.12E-01
	Distribution	3.15	4.33	6.82	1.69	2.87	16.24	0.54	0.95	63.05	
23	EAL (%)	3.67E-03	5.03E-03	7.46E-03	2.06E-03	3.48E-03	1.79E-02	7.79E-04	1.36E-03	6.97E-02	1.11E-01
	Distribution	3.30	4.53	6.72	1.85	3.14	16.16	0.70	1.23	62.80	
24	EAL (%)	3.86E-03	5.33E-03	7.18E-03	2.12E-03	3.58E-03	1.78E-02	8.56E-04	1.49E-03	6.94E-02	1.12E-01
	Distribution	3.45	4.76	6.41	1.89	3.20	15.91	0.76	1.33	61.95	
25	EAL (%)	3.94E-03	5.46E-03	7.03E-03	2.18E-03	3.68E-03	1.77E-02	9.41E-04	1.64E-03	6.91E-02	1.12E-01
	Distribution	3.52	4.87	6.28	1.95	3.29	15.78	0.84	1.47	61.67	
26	EAL (%)	5.40E-03	7.84E-03	9.32E-03	3.38E-03	5.55E-03	2.49E-02	1.02E-03	1.78E-03	7.74E-02	1.37E-01
	Distribution	3.94	5.72	6.80	2.47	4.05	18.19	0.74	1.30	56.49	
27	EAL (%)	5.48E-03	7.97E-03	9.43E-03	3.37E-03	5.54E-03	2.50E-02	1.01E-03	1.76E-03	7.74E-02	1.37E-01
	Distribution	4.00	5.81	6.88	2.46	4.04	18.21	0.73	1.28	56.53	
28	EAL (%)	4.21E-03	6.06E-03	1.03E-02	2.35E-03	3.96E-03	2.56E-02	3.90E-04	6.82E-04	8.36E-02	1.37E-01
	Distribution	3.07	4.42	7.51	1.72	2.89	18.71	0.28	0.50	61.02	
29	EAL (%)	5.63E-03	8.25E-03	9.21E-03	3.47E-03	5.68E-03	2.47E-02	1.11E-03	1.95E-03	7.70E-02	1.37E-01
	Distribution	4.11	6.02	6.72	2.53	4.15	18.00	0.81	1.42	56.22	
30	EAL (%)	5.71E-03	8.33E-03	8.98E-03	3.56E-03	5.82E-03	2.43E-02	1.24E-03	2.17E-03	7.66E-02	1.37E-01
	Distribution	4.17	6.08	6.56	2.60	4.25	17.76	0.91	1.58	55.92	
31	EAL (%)	4.75E-03	6.83E-03	9.98E-03	2.77E-03	4.62E-03	2.61E-02	5.52E-04	9.65E-04	8.08E-02	1.37E-01
	Distribution	3.46	4.98	7.28	2.02	3.37	19.02	0.40	0.70	58.97	
32	EAL (%)	4.98E-03	7.25E-03	9.71E-03	2.86E-03	4.75E-03	2.60E-02	5.98E-04	1.04E-03	8.03E-02	1.37E-01
	Distribution	3.64	5.29	7.09	2.08	3.47	18.98	0.44	0.76	58.59	
33	EAL (%)	5.00E-03	7.22E-03	9.72E-03	3.01E-03	4.99E-03	2.58E-02	6.92E-04	1.21E-03	7.94E-02	1.37E-01
	Distribution	3.65	5.27	7.09	2.20	3.64	18.83	0.51	0.88	57.93	
34	EAL (%)	5.18E-03	7.50E-03	9.47E-03	3.10E-03	5.12E-03	2.56E-02	7.56E-04	1.32E-03	7.89E-02	1.37E-01
	Distribution	3.78	5.47	6.91	2.26	3.74	18.71	0.55	0.96	57.56	
35	EAL (%)	5.63E-03	8.37E-03	8.98E-03	3.19E-03	5.26E-03	2.54E-02	8.29E-04	1.45E-03	7.84E-02	1.38E-01
	Distribution	4.08	6.07	6.51	2.31	3.81	18.44	0.60	1.05	56.79	
36	EAL (%)	7.50E-03	1.17E-02	1.32E-02	6.06E-03	9.39E-03	4.35E-02	1.70E-03	2.97E-03	8.59E-02	1.82E-01
	Distribution	4.12	6.45	7.24	3.33	5.16	23.90	0.93	1.63	47.21	

When the seismic level is not severe, such as 50/50 ground motions, the contribution of losses from damage to NSA components is the most significant portion of the total EAL. Loss resulting from damage to NSA components increases to almost 70% as the construction cost increases. This suggests that the added stiffness generated by viscoelastic dampers and column sizes actually serves to increase the tendency for acceleration-related damage to nonstructural components. This makes sense because added stiffness will tend to move accelerations of the floor levels closer to those of the ground.

Higher damping coefficients lead to reduced overall loss due to seismic hazard, but result in loss from damage to NSA components becoming a larger percentage of the total EAL. As damping levels reduce, there is a tendency to have losses move toward equalization across all seismic hazards.

In general, higher magnitudes of damping coefficient and lower magnitudes of viscoelastic stiffness tend to result in lower EAL and higher initial construction costs when linear dampers are utilized.

Design Case 3 includes what has been termed a softening damper where the velocity exponent is 0.50. This damper configuration is used at each of three levels in the framework and the topology and design variable configuration is shown in Figure 4.8. The feasible designs generated during the evolution plotted in objective space are shown in Figure 4.14 and the design variables selected are given in Table 4.8.

The range of initial construction costs for Design Case 3 range from \$43,229 on the high end (EAL = 0.07%) to \$25,514 on the low end (EAL = 0.19%). The column shape design variables selected are similar in size and weight to those determined in

Design Case 2 at lower initial construction costs. However, the damper coefficient for this design case are larger through all designs on the Pareto front.

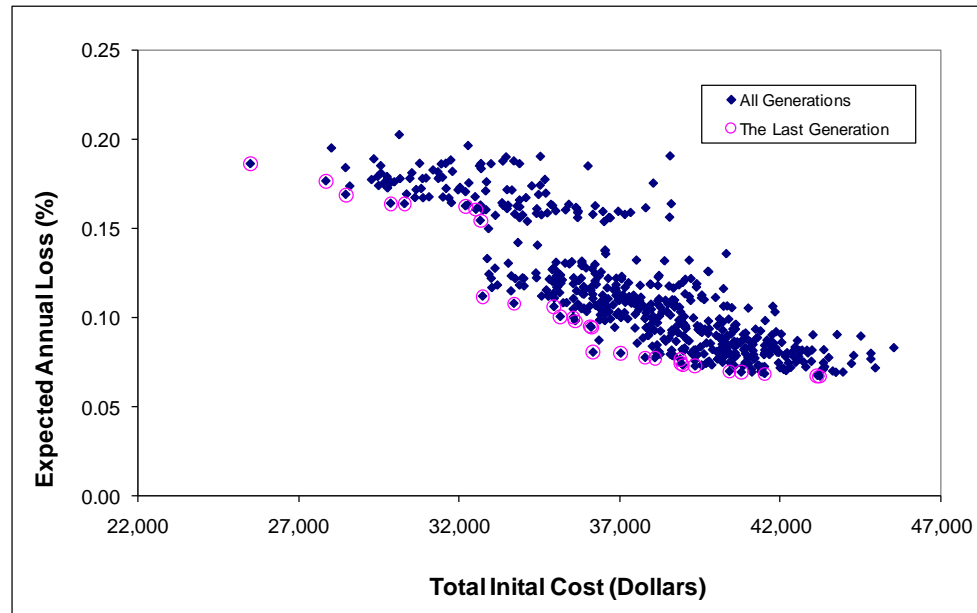


Figure 4.14 Pareto Front for Frame Design, Case 3.

In general, when softening dampers are utilized (velocity exponent equal to 0.5), very low viscoelastic stiffness was selected for the designs on the Pareto front in Design Case 3. This was coupled with overall larger magnitude damper coefficients selected.

As with linear dampers, the addition of softening dampers to the system results in an overall lowering of the expected annual loss. It also appears that linear dampers result in better loss performance when compared to softening dampers.

The Pareto front for Design Case 4 is shown in Figure 4.15. The variation in EAL along the Pareto front is similar in this case to that of Design Cases 2 and 3, but the initial construction costs are much greater. Table 4.9 contains the design variables selected. It should be pointed out that Design Case 4 includes superlinear dampers (velocity exponent equal to 1.5).

Table 4.8 Design Variables in the Last Generation, Case 3

Design1	Columns			Dampers			Total Cost	EAL
	Exterior	Interior		C	K _e	α		
	Variable 1	Variable 2	Variable 3	kips-sec/in	kips/in		(\\$)	(%)
1 *	W12X96	W12X87	W12X96	100	0	0.5	43229	0.07
2	W12X96	W12X106	W12X96	100	20	0.5	43150	0.07
3	W12X96	W12X106	W8X40	100	20	0.5	41508	0.07
4	W8X40	W12X106	W10X88	100	20	0.5	40783	0.07
5	W8X40	W12X106	W12X96	100	20	0.5	40416	0.07
6	W12X50	W10X88	W12X96	100	0	0.5	39349	0.07
7	W12X50	W12X106	W12X45	100	20	0.5	38967	0.07
8	W8X40	W12X106	W12X45	100	20	0.5	38913	0.07
9	W12X50	W12X106	W8X40	100	20	0.5	38884	0.08
10	W12X50	W12X106	W12X45	100	0	0.5	38098	0.08
11	W12X50	W12X87	W12X45	100	0	0.5	37795	0.08
12	W12X50	W12X106	W12X45	90	20	0.5	37035	0.08
13	W8X28	W12X87	W12X45	100	0	0.5	36174	0.08
14	W10X45	W12X87	W12X45	90	0	0.5	36114	0.09
15 **	W8X40	W12X106	W8X40	80	20	0.5	36098	0.10
16	W8X28	W12X87	W8X40	90	0	0.5	35622	0.10
17	W12X50	W10X100	W12X45	80	0	0.5	35557	0.10
18	W10X45	W12X87	W8X40	80	10	0.5	35153	0.10
19	W12X50	W12X87	W12X45	80	0	0.5	34957	0.11
20	W12X50	W10X100	W12X45	70	0	0.5	33711	0.11
21	W10X45	W12X87	W12X45	70	0	0.5	32739	0.11
22	W12X96	W12X106	W8X58	40	0	0.5	32665	0.15
23	W12X96	W10X112	W8X40	40	0	0.5	32530	0.16
24	W8X40	W12X106	W12X96	40	20	0.5	32205	0.16
25	W12X50	W12X106	W12X96	40	0	0.5	30308	0.16
26	W10X45	W12X106	W12X96	40	0	0.5	29878	0.16
27	W12X50	W10X100	W8X40	40	0	0.5	28480	0.17
28	W8X28	W10X112	W8X40	40	0	0.5	27862	0.18
29 ***	W8X28	W10X112	W8X40	30	0	0.5	25514	0.19

*, The minimum EAL design

**, The median point of Pareto Front in the last generation

***, The minimum initial cost

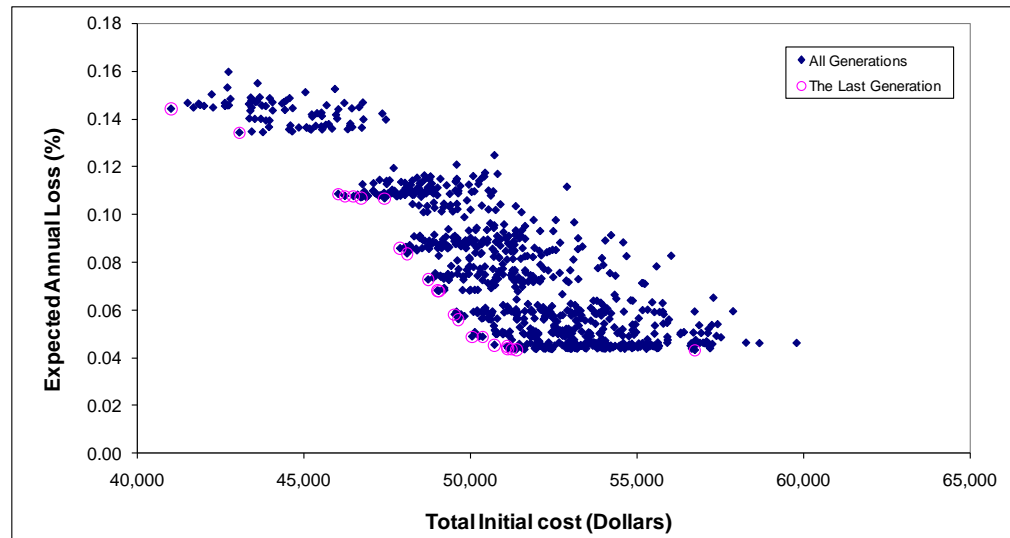


Figure 4.15 Pareto Front for Frame Design, Case 4.

The lowest initial construction cost design for Design Case 4 (Table 4.9) is much larger than that seen in Design Case 3 (Table 4.8). Design Case 4 resulted in the lowest EAL when compared to cases 2 and 3. The EAL for these two cases for the lowest cost designs in cases 3 and 4 are close to one another (0.14% and 0.19%). The column sizes are slightly smaller in Design Case 4 likely resulting from the relatively higher damper forces generated during the ground motions arising from the velocity exponent (1.5 for all dampers).

The damper coefficients and viscoelastic stiffness for the designs on the Pareto front in Design Case 4 are similar to those seen in Design Case 2. It is interesting to note that the lowest cost design in case 4 includes a low damping coefficient and low viscoelastic stiffness. A similar trend to that seen in design cases 2 and 3 is seen in this case. That is, as the damper coefficients coefficients and viscoelastic stiffness decreases, the expected annual loss decreases. This again demonstrates that the addition of dampers results in lower expected annual loss.

Table 4.9 Design Variables in the Last Generation, Case 4.

Designs	Columns			Dampers			Total Cost (\$)	EAL (%)
	Exterior	Interior		C	K _e	α		
	Variable 1	Variable 2	Variable 3	kips-sec/in	kips/in			
1 *	W8X58	W10X112	W10X88	100	0	1.5	56737	0.04
2	W8X28	W12X106	W10X45	100	10	1.5	51376	0.04
3	W8X28	W12X106	W8X40	100	20	1.5	51234	0.04
4	W8X28	W12X106	W8X40	100	10	1.5	51127	0.04
5	W8X28	W12X96	W10X45	100	20	1.5	51098	0.04
6	W8X28	W12X96	W10X45	100	10	1.5	50723	0.05
7	W8X28	W12X96	W8X40	80	0	1.5	50367	0.05
8	W8X28	W12X96	W8X40	80	10	1.5	50051	0.05
9	W8X28	W10X88	W10X45	60	10	1.5	49639	0.06
10	W8X28	W12X96	W8X40	60	10	1.5	49527	0.06
11 **	W8X28	W10X88	W10X45	40	10	1.5	49050	0.07
12	W8X28	W10X88	W8X40	40	10	1.5	49013	0.07
13	W8X28	W12X96	W10X45	40	10	1.5	48731	0.07
14	W8X28	W12X96	W8X40	30	0	1.5	48098	0.08
15	W8X28	W12X106	W10X45	30	20	1.5	47889	0.09
16	W8X28	W12X106	W8X58	20	10	1.5	47423	0.11
17	W8X28	W12X106	W8X40	20	20	1.5	46708	0.11
18	W8X28	W12X106	W10X45	20	20	1.5	46493	0.11
19	W8X28	W12X106	W12X96	20	10	1.5	46232	0.11
20	W8X28	W12X106	W12X96	20	20	1.5	46030	0.11
21	W8X28	W10X112	W12X96	10	20	1.5	43065	0.13
22 ***	W8X28	W12X106	W12X96	10	20	1.5	41012	0.14

*, The minimum EAL design

**, The median point of Pareto Front in the last generation

***, The minimum initial cost

A comparison of Pareto fronts at the final generation for design cases 1, 2, 3, and 4 is made in Figure 4.16. The results indicate that nonlinear dampers with exponent $\alpha = 0.5$ in the three story frame generate consistently lower initial construction costs and lower expected annual losses. There appears to be a trend that as the velocity exponent increases, the initial construction cost increases, while the EAL tends to decrease.

This trend is exhibited by the Pareto fronts in Figure 4.16 moving downward and rightward. This trend was alluded to earlier in Chapter 2 of the dissertation where was said that dampers are generally more economical and effective when the damper velocity exponent ranges from 0.3 to 1.0.

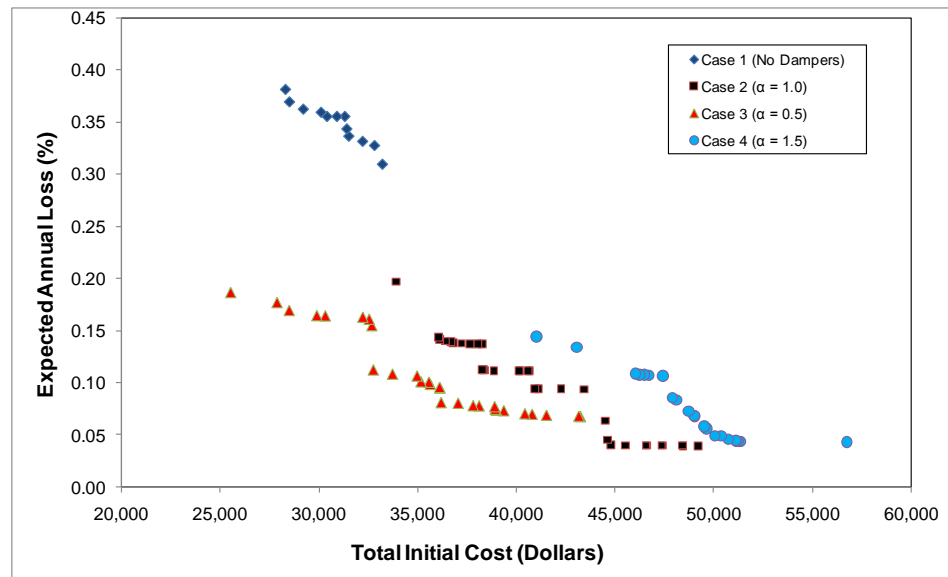


Figure 4.16 The Comparison of Pareto Fronts for Design Cases 1 through 4.

Figure 4.16 clearly illustrates the use of dampers in controlling losses due to seismic hazard and balancing these losses with initial construction cost. It also appears to indicate that the objectives of minimizing initial construction cost and minimizing expected annual loss can best be balanced with systems that include passive supplemental damping devices.

Two feasible designs with minimum initial construction cost are selected from design Cases 1 and 2 to represent the building frame without and with supplemental damping elements, respectively. Table 4.10 lists the design variables selected. The addition of linear dampers results in similar overall steel weight for the system.

Table 4.10 The Designs with the Minimum Initial Cost from Cases 1 & 2

Design Case	Columns			Dampers		
	Exterior	Interior		C	Ke	α
	Variable 1	Variable 2	Variable 3	kips-sec/in	kips/in	
Case 1	W14X233	W10X45	N/A	N/A	N/A	N/A
Case 3	W10X45	W10X112	W12X96	10	10	1.0

Table 4.11 illustrates the maximum interstory drift and floor level accelerations for the frame designs shown in Figure 4.10 when subjected to the fifteen ground motions defining the hazard level considered. The maximum inter-story drift at the first level is reduced from 16.09 inches to 6.15 inches when linear dampers are utilized. Peak floor level accelerations are also significantly reduced when supplemental dampers are utilized. Both of these tendencies are expected.

Table 4.11 Maximum Inter-Story Drift and Acceleration for Minimum Initial Cost Designs in Cases 1 & 2.

Design Cases	Story	Max. Inter-story Drift (in)			Max. Acceleration (in/sec ²)		
		2%in50	10%in50	50%in50	2%in50	10%in50	50%in50
1	1	16.09	1.11	0.50	1753.85	242.62	150.90
	2	7.17	0.88	0.42	1369.15	393.54	245.31
	3	1.30	0.53	0.27	1256.59	528.61	342.47
2	1	6.15	1.34	0.40	297.65	198.01	122.26
	2	3.15	1.06	0.30	442.73	321.54	167.96
	3	1.05	0.60	0.17	471.61	382.55	181.37

The loss distributions for the minimum initial construction cost designs in Cases 1 and 2 are shown in Table 4.12. As expected, the lower interstory drifts and smaller floor-level accelerations result in percentages of the total EAL resulting from nonstructural

drift-sensitive components (NSD) and nonstructural acceleration-sensitive components (NSA) being reduced for 2/50 and 50/50 ground motions.

Table 4.12 Loss Distribution for Minimum Initial Cost Designs in Cases 1 & 2

Designs	Seismic Losses	Distribution of Repair Cost (%)									Total EAL (%)
		2% in 50 yrs			10% in 50 yrs			50% in 50 yrs			
		SS	NSD	NSA	SS	NSD	NSA	SS	NSD	NSA	
1	EAL (%)	1.32E-02	2.26E-02	4.81E-02	4.29E-03	6.96E-03	6.52E-02	4.35E-03	7.57E-03	2.07E-01	3.79E-01
	Distribution	3.48	5.96	12.69	1.13	1.84	17.21	1.15	2.00	54.60	
2	EAL (%)	7.50E-03	1.17E-02	1.32E-02	6.06E-03	9.39E-03	4.35E-02	1.70E-03	2.97E-03	8.59E-02	1.82E-01
	Distribution	4.12	6.45	7.24	3.33	5.16	23.9	0.93	1.63	47.21	

It is interesting to note that the repair cost resulting from 10/50 ground motions actually increased for Design Case 2 when compare to Design Case 1. Interstory drifts for these ground motions were not significantly reduced (and actually increased in some levels) when dampers were added. Furthermore, accelerations for the 50/50 ground motions did not significantly change resulting resulting in NSD components picking up a larger percentage of the total repair cost.

The behavior shown in Tables 4.10 through 4.12 illustrate that the expected annual loss due to the seismic hazard considered is likely to be reduced significantly when dampers are considered. However, this reduced expected annual loss results in 10/50 and 50/50 ground motions contributing more to the repair costs. In other words, there appears to be a move toward a damage balance across all components and across all seismic events. NSA damage is the most important component damage to consider for the frame topology and seismic hazard examined.

4.5.3 Design Cases 5 and 6

Design cases 5 and 6 were intended to allow the algorithm to select different damper proportionality factors, viscoelastic stiffness magnitudes, and velocity exponents at each level within the framework. The dampers in Case 5 have the same velocity exponent ($\alpha = 1.0$) at each level. Design Case 6 was formulated to explore how allowing damper parameters to vary through the height of the frame would affect initial construction cost and expected annual loss. The motivation for comparing these two cases is to explore how the damping exponent affects the resulting designs generated.

The feasible designs generated for Design Case 5 plotted in objective space and the designs located along the Pareto front at the final generation are given in Figure 4.17.

Table 4.13 includes the design variable choices for the Pareto front.

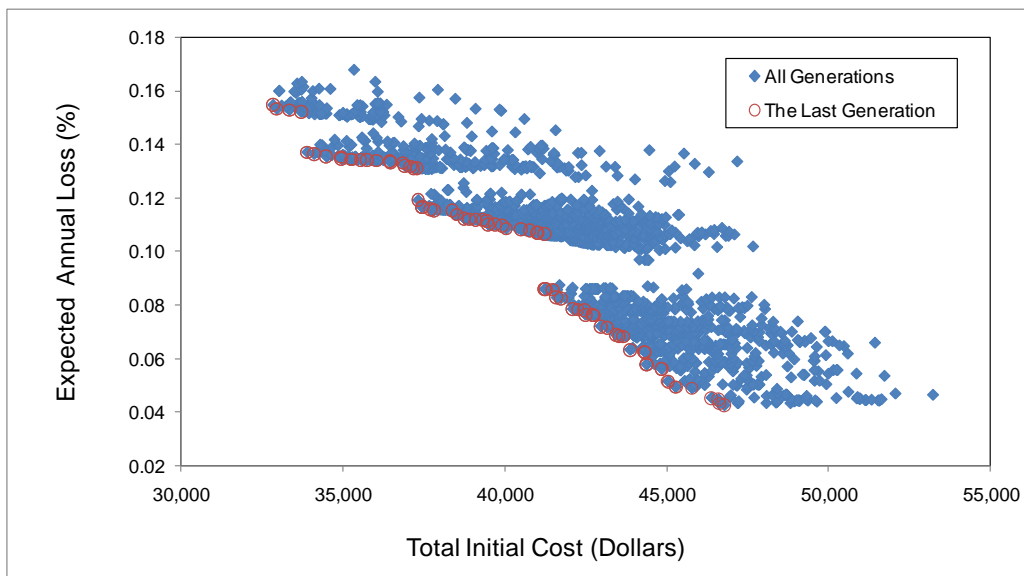


Figure 4.17 Pareto Front for Frame Design, Case 5.

It is interesting to note that the Pareto front designs for Design Case 5 include slightly lower initial construction costs and expected annual losses when compared to Design

Case 2 (common topology and damper velocity exponent). These results indicate that by allowing different dampers to be used at each level within the frame topology improved economy and reduced losses can be attained. It should also be noted that the Pareto front is well populated as a result of the increased number of design variables considered in the algorithm. The stepped nature to the Pareto front is of interest, but the reason(s) for the stepped shape could not be identified.

The designs in Table 4.13 indicate that the lower EAL designs include higher damper proportionality factors and lower viscoelastic stiffness magnitudes than the higher EAL designs. The magnitude of the damping coefficient also reduces as one rises in the framework. Thus, there appears to be a trend in Design Case 5 that lower stories should have larger magnitude proportionality factors and lower viscoelastic component if loss is to be minimized. If cost is to be minimized, this trend is reversed (opposite).

The designs developed during the evolution and the Pareto front generated at the final generation for Design Case 6 is given in Figure 4.18. The Pareto front shown in Figure 4.18 is very well dispersed throughout the objective space. There is no stepping as seen in the previous design case and there is a large number of designs from which to select. This behavior is a result of the increased number of design variables in case 6.

Design variables for this final Pareto front can be found in Table 4.14. The least construction cost design has an expected annual loss that is comparable with those values seen in Design Case 5. In general, all designs have larger damping coefficients at the first level with reductions occurring as one rises through the frame. Viscoelastic stiffness magnitudes selected were also on the low end of the set of possible choices (less than 10 kips/in). This behavior is consistent with that seen in Design Case 5.

Table 4.13 Design Variables in the Last Generation, Case 5

Columns		1st Story, Dampers			2nd Story, Dampers			3rd Story, Dampers			Total Cost	EAL
Exterior Variable 1	Interior Variable 2	C kips-sec/in	K _g kips/in	α	C kips-sec/in	K _g kips/in	α	C kips-sec/in	K _g kips/in	α	Total Cost (\$)	EAL (%)
W8X40	W12X96	100	10	1.0	80	0	1.0	80	10	1.0	46617	0.04
W8X40	W10X88	100	10	1.0	70	0	1.0	80	10	1.0	46591	0.04
W8X40	W12X96	100	10	1.0	70	0	1.0	80	10	1.0	46384	0.05
W8X40	W12X96	100	10	1.0	70	10	1.0	80	10	1.0	46377	0.05
W8X40	W10X88	100	10	1.0	80	0	1.0	30	10	1.0	45779	0.05
W8X40	W10X88	100	10	1.0	80	10	1.0	30	10	1.0	45778	0.05
W8X40	W12X96	100	10	1.0	80	0	1.0	30	10	1.0	45273	0.05
W8X40	W12X96	100	10	1.0	80	10	1.0	30	10	1.0	45263	0.05
W8X40	W12X96	100	10	1.0	70	0	1.0	30	10	1.0	45047	0.05
W8X40	W12X96	100	10	1.0	70	10	1.0	30	10	1.0	45037	0.05
W8X40	W12X96	80	10	1.0	80	0	1.0	30	10	1.0	44844	0.06
W8X40	W12X96	80	10	1.0	80	10	1.0	30	10	1.0	44833	0.06
W8X40	W12X96	100	10	1.0	50	0	1.0	30	10	1.0	44378	0.06
W8X40	W12X96	100	10	1.0	50	10	1.0	30	10	1.0	44370	0.06
W8X40	W12X96	70	10	1.0	70	0	1.0	30	10	1.0	44325	0.06
W8X40	W12X96	70	10	1.0	70	10	1.0	30	10	1.0	44313	0.06
W8X40	W12X96	100	10	1.0	40	10	1.0	30	10	1.0	43864	0.06
W8X40	W12X96	100	10	1.0	40	0	1.0	30	10	1.0	43863	0.06
W8X40	W12X96	70	10	1.0	50	0	1.0	30	10	1.0	43649	0.07
W8X40	W12X96	100	10	1.0	50	10	1.0	10	10	1.0	43527	0.07
W8X40	W12X96	80	10	1.0	40	10	1.0	30	10	1.0	43424	0.07
W8X40	W12X96	100	10	1.0	30	10	1.0	30	10	1.0	43166	0.07

Table 4.13 Design Variables in the Last Generation, Case 5 (continued)

Columns		1st Story, Dampers			2nd Story, Dampers			3rd Story, Dampers			Total Cost	EAL
Exterior	Interior	C	K _e	α	C	K _e	α	C	K _e	α	(\$)	(%)
		kips-sec/in	kips/in		kips-sec/in	kips/in		kips-sec/in	kips/in			
Variable 1	Variable 2	Variable 3										
W8X40	W12X96	W8X28	100	1.0	40	0	1.0	10	10	1.0	42963	0.07
W8X40	W12X96	W8X28	100	1.0	40	10	1.0	10	10	1.0	42956	0.07
W8X40	W12X96	W8X28	70	1.0	50	0	1.0	10	10	1.0	42755	0.08
W8X40	W12X96	W8X28	80	1.0	30	10	1.0	30	10	1.0	42714	0.08
W8X40	W12X96	W8X28	80	1.0	40	0	1.0	10	10	1.0	42480	0.08
W8X40	W12X106	W8X28	100	1.0	30	20	1.0	10	20	1.0	42450	0.08
W8X40	W12X106	W8X28	100	1.0	30	0	1.0	10	20	1.0	42257	0.08
W8X40	W12X96	W8X28	100	1.0	30	0	1.0	10	10	1.0	42091	0.08
W8X40	W12X106	W8X28	80	1.0	30	0	1.0	10	20	1.0	41728	0.08
W8X40	W12X96	W8X28	80	1.0	30	0	1.0	10	10	1.0	41594	0.08
W8X40	W12X106	W8X28	70	1.0	30	0	1.0	10	20	1.0	41470	0.09
W8X40	W12X96	W8X28	70	1.0	30	10	1.0	10	10	1.0	41266	0.09
W8X40	W12X96	W8X28	70	1.0	30	0	1.0	10	10	1.0	41225	0.09
W12X96	W12X96	W8X28	30	1.0	50	10	1.0	30	20	1.0	41217	0.11
W8X40	W12X106	W8X28	30	1.0	50	0	1.0	30	10	1.0	41019	0.11
W8X40	W12X106	W8X28	30	1.0	50	10	1.0	30	20	1.0	40989	0.11**
W12X96	W12X96	W8X28	30	1.0	70	30	1.0	10	10	1.0	40761	0.11
W8X40	W12X106	W8X28	100	1.0	10	10	1.0	30	20	1.0	40499	0.11
W8X40	W12X96	W8X28	100	1.0	10	10	1.0	30	10	1.0	40038	0.11
W8X40	W12X106	W8X28	100	1.0	10	0	1.0	30	20	1.0	39903	0.11
W12X96	W12X96	W8X28	30	1.0	50	10	1.0	10	20	1.0	39700	0.11
W8X40	W12X96	W8X28	100	1.0	10	0	1.0	30	10	1.0	39480	0.11
W8X40	W12X106	W8X28	30	1.0	50	0	1.0	10	20	1.0	39446	0.11
W12X96	W12X96	W8X28	30	1.0	40	0	1.0	10	30	1.0	39313	0.11

Table 4.13 Design Variables in the Last Generation, Case 5 (continued)

Columns		1st Story, Dampers			2nd Story, Dampers			3rd Story, Dampers			Total Cost	EAL
Exterior Variable 1	Interior Variable 2	C	K _g	α	C	K _g	α	C	K _g	α	(\$)	(%)
W12X96	W12X96	30	20	1.0	40	0	1.0	10	30	1.0	39092	0.11
W12X96	W12X96	30	10	1.0	40	0	1.0	10	30	1.0	38894	0.11
W12X96	W12X96	30	10	1.0	40	30	1.0	10	10	1.0	38736	0.11
W8X40	W12X106	30	10	1.0	40	10	1.0	10	20	1.0	38516	0.11
W12X96	W12X96	30	30	1.0	30	0	1.0	10	30	1.0	38372	0.12
W8X40	W12X96	100	10	1.0	10	0	1.0	10	10	1.0	37806	0.12
W12X96	W12X96	30	10	1.0	30	30	1.0	10	30	1.0	37706	0.12
W8X40	W12X106	30	10	1.0	30	0	1.0	10	20	1.0	37444	0.12
W8X40	W12X106	30	10	1.0	30	10	1.0	10	20	1.0	37439	0.12
W8X40	W12X96	70	10	1.0	10	0	1.0	10	10	1.0	37316	0.12
W12X96	W12X96	30	30	1.0	10	20	1.0	30	30	1.0	37286	0.13
W12X96	W12X96	30	20	1.0	10	20	1.0	30	30	1.0	37173	0.13
W12X96	W12X96	30	20	1.0	10	10	1.0	30	20	1.0	37072	0.13
W12X96	W12X96	30	10	1.0	10	10	1.0	30	30	1.0	36910	0.13
W8X40	W12X106	30	20	1.0	10	20	1.0	30	20	1.0	36845	0.13
W8X40	W12X106	30	20	1.0	10	10	1.0	30	20	1.0	36463	0.13
W8X40	W12X106	30	10	1.0	10	10	1.0	30	20	1.0	36450	0.13
W12X106	W12X106	30	10	1.0	10	30	1.0	10	30	1.0	36021	0.13
W12X96	W12X96	30	30	1.0	10	30	1.0	10	10	1.0	35737	0.13
W12X96	W12X96	30	10	1.0	10	30	1.0	10	30	1.0	35546	0.13
W12X96	W12X96	30	10	1.0	10	20	1.0	10	20	1.0	35264	0.13
W12X96	W12X96	30	10	1.0	10	20	1.0	10	30	1.0	35254	0.13
W12X96	W12X96	30	10	1.0	10	10	1.0	10	30	1.0	34954	0.13
W8X40	W12X106	30	10	1.0	10	0	1.0	10	20	1.0	34931	0.14
W8X40	W12X106	30	20	1.0	10	10	1.0	10	20	1.0	34473	0.14
W8X40	W12X106	30	10	1.0	10	0	1.0	10	10	1.0	34100	0.14

Table 4.13 Design Variables in the Last Generation, Case 5 (continued)

Columns		1st Story, Dampers			2nd Story, Dampers			3rd Story, Dampers			Total Cost	EAL
Exterior	Interior	C	K _e	α	C	K _e	α	C	K _e	α	(\$)	(%)
Variable 1	Variable 2	Variable 3										
W8X40	W12X96	W8X28	10	1.0	10	0	1.0	10	10	1.0	33886	0.14
W12X96	W12X106	W8X28	10	1.0	10	20	1.0	10	20	1.0	33698	0.15
W8X40	W12X106	W12X96	20	1.0	10	10	1.0	10	20	1.0	33340	0.15
W8X40	W12X106	W12X96	20	1.0	10	0	1.0	10	10	1.0	32952	0.15
W8X40	W12X106	W12X96	20	1.0	10	10	1.0	10	10	1.0	32834	0.15***

* , The minimum EAL design

** , The median point of Pareto Front in the last generation

*** , The minimum initial cost

It is interesting to note that the algorithm preferred to select relative velocity exponents that ranged from 0.5 to 1.0. Smaller magnitudes for this exponent were preferred in the lower cost designs, but this resulted in slight elevations in EAL. This suggests that having large damping coefficients results in lower relative velocity exponents to balance damper forces and the resulting axial loads in the adjacent columns.

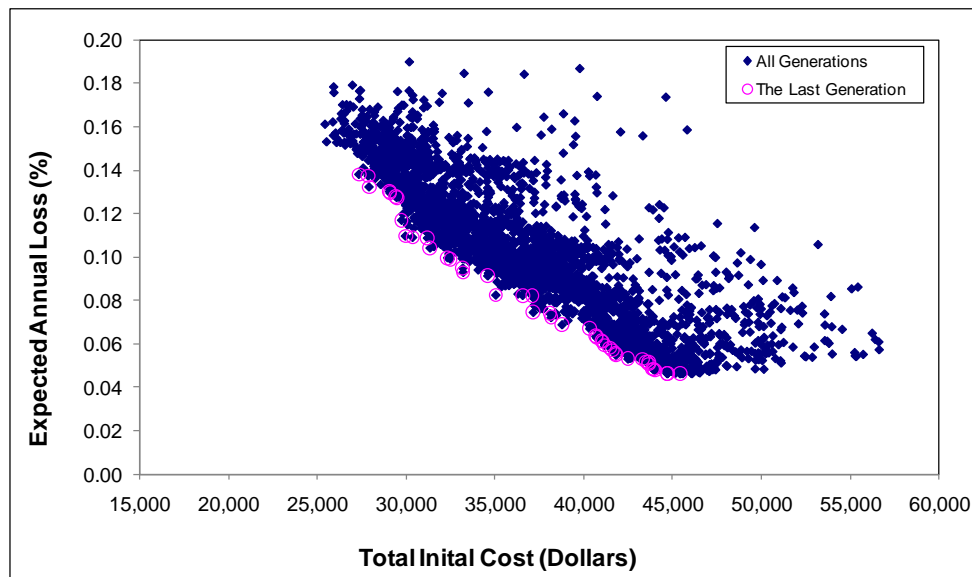


Figure 4.18 Pareto Front for Frame Design, Case 6

A comparison of the Pareto fronts at the final generation for Design Cases 5 and 6 is given in Figure 4.19. This figure again illustrates and confirms the benefit of more design variables. When more design variables are included, it is able to achieve better design solutions in lower initial construction cost and lower expected annual loss for the ground motions considered. The Pareto fronts for Design Case 6 are much better distributed through objective space.

Table 4.14 Design Variables in the Last Generation, Case 6

Columns		1st Story, Dampers			2nd Story, Dampers			3rd Story, Dampers			Total Cost	EAL
Exterior	Interior	C	K _g	α	C	K _g	α	C	K _g	α	(Dollars)	(%)
Variable 1	Variable 2	kips-sec/in	kips/in		kips-sec/in	kips/in		kips-sec/in	kips/in			
W8X28	W12X96	100	10	1.00	100	0	0.75	40	10	1.00	45419	0.05*
W8X28	W12X96	100	0	1.00	100	0	0.75	40	10	1.00	44705	0.05
W8X28	W12X96	100	10	1.00	100	0	0.75	40	10	1.00	44684	0.05
W8X28	W12X96	100	10	1.00	100	0	0.75	40	10	0.75	44000	0.05
W8X28	W12X96	100	10	1.00	100	0	0.75	30	10	1.00	43943	0.05
W8X28	W12X96	100	0	1.00	100	0	0.75	30	10	1.00	43884	0.05
W8X28	W12X96	90	0	1.00	100	0	0.75	40	10	0.75	43677	0.05
W8X28	W12X96	90	10	1.00	100	10	0.75	30	10	1.00	43664	0.05
W8X28	W12X106	100	0	1.00	100	10	0.50	40	10	1.00	43499	0.05
W8X28	W12X106	100	0	1.00	100	0	0.50	40	10	1.00	43324	0.05
W8X28	W12X106	100	0	1.00	100	0	0.50	40	20	0.75	42480	0.05
W8X28	W12X96	100	0	1.00	100	10	0.50	40	10	0.75	41806	0.05
W8X28	W12X96	100	10	1.00	100	10	0.50	40	10	0.75	41773	0.06
W8X28	W12X96	100	10	1.00	100	10	0.50	30	10	0.75	41578	0.06
W8X28	W12X96	100	10	1.00	100	0	0.50	30	10	0.75	41479	0.06
W8X28	W12X96	100	10	1.00	100	0	0.50	40	10	0.50	41161	0.06
W8X28	W12X96	100	0	1.00	100	10	0.50	40	10	0.50	41059	0.06
W8X28	W12X96	100	10	1.00	100	10	0.50	40	10	0.50	40997	0.06
W8X28	W12X96	100	0	1.00	100	0	0.50	20	10	0.75	40713	0.06
W8X28	W12X96	100	10	1.00	100	0	0.50	20	10	0.75	40674	0.06
W8X28	W12X96	90	0	1.00	100	0	0.50	30	10	0.50	40331	0.07
W8X28	W12X96	100	10	0.50	100	10	0.75	40	20	0.75	38772	0.07
W8X28	W12X96	100	10	0.50	100	0	0.75	40	10	0.50	38156	0.07

Table 4.14 Design Variables in the Last Generation, Case 6 (Continued)

Columns		1st Story, Dampers			2nd Story, Dampers			3rd Story, Dampers			Total Cost	EAL
Exterior Variable 1	Interior Variable 2	C kips-sec/in	K _e kips/in	α	C kips-sec/in	K _e kips/in	α	C kips-sec/in	K _e kips/in	α	(Dollars)	(%)
W8X28	W12X106	100	10	0.50	100	10	0.50	40	10	1.00	38102	0.07**
W8X28	W12X106	100	10	0.50	100	0	0.50	40	20	0.75	37151	0.07
W8X28	W12X106	100	0	0.50	100	0	0.50	40	20	0.75	37093	0.08
W8X28	W12X106	100	0	0.50	100	10	0.50	40	10	0.75	36552	0.08
W8X28	W12X106	100	0	0.50	100	0	0.50	40	10	0.50	35040	0.08
W8X28	W12X96	100	0	0.50	50	0	0.75	10	10	1.00	34587	0.09
W8X28	W12X96	100	0	0.50	100	0	0.50	10	10	0.75	33210	0.09
W8X28	W12X96	90	0	0.50	100	0	0.50	10	10	1.00	33185	0.09
W8X28	W12X96	100	10	0.50	50	0	0.50	20	10	0.75	32481	0.10
W8X28	W12X96	100	0	0.50	50	0	0.50	20	10	0.75	32327	0.10
W8X28	W12X106	90	10	0.50	50	10	0.50	10	10	0.75	31340	0.10
W8X28	W12X96	100	0	0.50	50	0	0.50	10	10	1.00	31193	0.11
W8X28	W12X96	90	0	0.50	50	0	0.50	10	10	0.75	30356	0.11
W8X28	W12X96	100	0	0.50	50	10	0.50	10	10	0.50	29951	0.11
W8X28	W12X96	90	0	0.50	50	0	0.50	10	10	0.75	29737	0.12
W8X28	W12X97	90	0	0.50	20	0	0.75	10	10	0.75	29457	0.13
W8X28	W12X98	70	10	0.50	50	10	0.50	10	10	0.75	29404	0.13
W8X28	W12X99	70	0	0.50	50	10	0.50	10	20	0.75	29095	0.13
W8X28	W12X100	90	0	0.50	20	0	0.75	10	10	0.50	29057	0.13
W8X28	W12X101	70	0	0.50	50	0	0.50	10	10	0.75	27903	0.13
W8X28	W12X102	70	10	0.50	20	0	0.75	10	10	0.75	27861	0.14
W8X28	W12X103	70	0	0.50	20	0	0.75	10	10	0.50	27332	0.14***

*, The minimum EAL design

**, The median point of Pareto Front in the last generation

***, The minimum initial cost

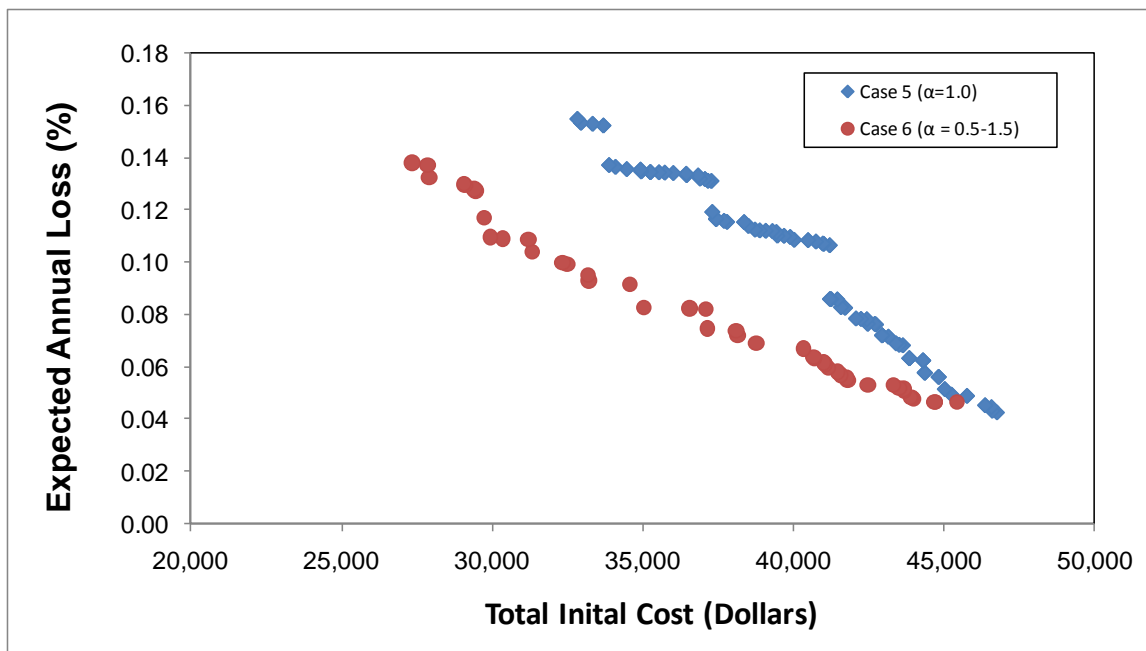


Figure 4.19 The Comparison of Pareto Fronts, Case 5 Vs. Case 6

4.6 Concluding Remarks

The algorithm outlined in Chapter 3 provides well-proportioned designs for a steel shear building model with and without supplemental dampers. When more design variables are included, it is able to achieve better design solutions with lower initial construction cost and lower expected annual loss for the ground motion suite considered. The use of dampers will result in lower expected annual losses due to ground motions while slightly increasing the initial construction costs. By comparing visco-elastic dampers vs. visco-inelastic ones, the nonlinear dampers with lower damping exponents generate consistently lower initial construction costs and lower expected annual losses. Furthermore, the objectives of minimizing initial construction cost and minimizing expected annual loss can best be balanced with systems that include passive supplemental dampers.

The distribution of losses changes with damping coefficient. Most of the total losses come from damage to non-structural acceleration sensitive (NSA) components when the ground motions are design basis motions (10/50) and when the ground motions correspond to frequently occurring earthquakes (50/50). The losses resulting from damage to non-structural acceleration-sensitive (NSA) components will be reduced with increased supplemental damper coefficient when subjected to the same hazard level. The proposed algorithm prefers to select relative velocity exponents that ranged from 0.5 to 1.0. Smaller magnitudes for this exponent were preferred in the lower cost designs, but this resulted in slight elevations in EAL. This suggests that having large damping coefficients results in lower relative velocity exponents to balance damper forces and the resulting axial loads in the adjacent columns.

In general, the visco-elastic stiffness chosen for all supplemental dampers chosen by the GA is very low in all cases. In other words, balancing initial construction cost and more importantly minimizing expected annual losses can be achieved using supplemental dampers with low viscoelastic stiffness.

Chapter 5

Summary, Conclusions and Future Work

The emphasis of the present thesis effort is to develop an accurate time history analysis tool which is suitable for conducting nonlinear time-history analysis of 2D multiple degree of freedom (MDOF) steel frame structures with linear/nonlinear viscous and viscoelastic dampers and to develop an optimization algorithm capable of automating the design of 2D frame structures modeled as shear buildings with linear/nonlinear viscous and viscoelastic dampers within the performance-based engineering methodology. The evolutionary algorithm developed was used to explore a vast number of combinations of column member sizes and dampers for shear building frames with prescribed topology that minimized initial construction cost and minimized expected annual losses. The research introduced the use of the distributed computing capability of MATLAB and the distributed computing toolbox on a personal computer cluster with 4 computer nodes to speed up the optimization algorithm for automated design and handle larger data sets.

The purpose of this chapter is to summarize the previous chapters, draw conclusions, and outline some ideas for future research work.

5.1 Summary

The objective and scope of the research were introduced in Chapter 1. Previous research efforts were reviewed for each of the primary components of this research effort: automated design with supplemental dampers, probabilistic performance-based design methods, and use of genetic algorithms (GAs) to solve optimization problems.

In Chapter 2, the foundational theory for simulating the response of damped structural system to horizontal ground accelerations was outlined and an algorithm used to compute the response of linear/nonlinear viscous and viscoelastically damped shear building models were described. The algorithm was validated by several benchmark case studies.

A performance- or risk-based seismic design optimization algorithm was formulated in Chapter 3. The objective functions and constraint criteria used for the multiple objective optimization problem were discussed in detail. The constraint criteria include strength, instability, damper stiffness, and constraints to beam – column. Penalty functions were then developed to convert the constrained optimization problem to an unconstrained problem suitable for solution with a GA .

Six case studies were presented in Chapter 4 to demonstrate the application of the evolutionary design algorithm. Designs for a 3-story, 4-bay shear-building frame with/without dampers and several design variable arrangements was investigated using Pareto-front curves. Three alternative designs, 1) the minimum total cost, 2) the minimum EAL, and 3) the median point in the last generation Pareto Fronts were selected for each case to study how supplemental dampers affect losses and initial construction costs. Scalability of the algorithm was demonstrated through increasing the number of design variables considered.

5.2 Conclusions

A number of conclusions can be drawn from this research effort. First of all, the algorithm developed to compute the response of viscous and viscoelastically damped

shear building models is able to perform accurate seismic analysis for 2D MDOF and SDOF systems with nonlinear material (spring) behavior and linear and nonlinear damper behavior. The program developed for shear buildings as part of this research effort and the solutions provided can serve as a benchmark-generating tool and as benchmark solutions for analyzing shear building systems with nonlinear linear viscous and viscoelastic damping systems.

The proposed automated design algorithm provides reasonable design results for shear-building frames with and without dampers. Moreover, the algorithm developed in the research effort generates consistent design results with Pareto curves that have good distribution throughout objective space. The algorithm is scalable and solutions quality improves as the number of design variables increases. In general, the number of design variables does not significantly improve the objective of minimizing expected annual loss, but it reduces the initial construction cost slightly.

Damping systems are very effective in reducing the impact of damage and losses resulting from seismic events. This suggests that the use of dampers, while adding initial construction expense, will result in lower expected annual losses due to ground motion. This supports the popularity of supplemental damping systems in seismic engineering.

Most of the expected annual losses for the design cases considered come from damage to non-structural acceleration sensitive components (NSA) when the seismic level is not severe (*e.g.* 50/50 ground motions) and when design basis ground motions are considered (*e.g.* 10/50 ground motions). The losses due to damage to non-structural acceleration sensitive components (NSA) will be reduced with increases in the damping coefficient, C , when subjected to the same hazard level.

When the seismic level is not severe, such as 50/50 ground motions, the contribution of losses from damage of NSA components is most significant portion of the total EAL. Loss resulting from damage to NSA components increases to almost 70% as the initial construction cost increases. This suggests that the added stiffness generated by viscoelastic dampers and column sizes actually serves to increase the tendency for acceleration-related damage to nonstructural components. This makes sense because added stiffness will tend to move accelerations of the floor levels closer to those of the ground.

In general, higher magnitudes of damping coefficient and lower magnitudes of viscoelastic stiffness tend to result in lower expected annual losses and higher initial construction costs.

A comparison of Pareto fronts at the final generation for design cases 1, 2, 3, and 4 indicate that nonlinear dampers with exponent $\alpha = 0.5$ in the three story frame generate consistently lower initial construction costs and lower expected annual losses. There appears to be a trend that as the velocity exponent increases, the initial construction cost increases, while the EAL tends to decrease. This trend is supported by the Pareto fronts generated and supports the hypothesis that dampers are generally more economical and effective when the damper velocity exponent ranges from 0.3 to 1.0.

The expected annual loss due to the seismic hazard considered is reduced significantly when supplemental dampers are utilized in the design. However, this reduced expected annual loss results in 10/50 and 50/50 ground motions contributing more to the repair costs resulting from damage. In other words, there appears to be a move toward a damage balance across all components and across all seismic events.

Nonstructural acceleration-sensitive component damage is the most important to consider for the frame topology, building type, and seismic hazard examined.

These results indicate that by allowing different dampers to be used at each level within the frame topology improved economy and reduced losses can be attained. It should also be noted that the Pareto front is very nicely dispersed and populated as a result of the increased number of design variables considered in the algorithm.

The magnitude of the damping coefficient in systems with reduced expected annual losses also reduces as one rises in the framework. Thus, there appears to be a trend that lower stories should have larger magnitude supplemental damper proportionality factors and lower viscoelastic stiffness if loss is to be minimized. If cost is to be minimized, this trend is reversed (opposite). As a result, supplemental damping systems offer a very nice vehicle for balancing initial construction cost and loss due to seismic hazard.

Smaller magnitudes for the velocity exponent were preferred in the lower cost designs, but this resulted in slight elevations in expected annual loss. This suggests that having large damping coefficients results in lower relative velocity exponents to balance damper forces and the resulting axial loads in the adjacent columns.

5.3 Recommendations for Future Work

This dissertation provides the development and initial implementation of an automated evolutionary design algorithm for shear building models with and without dampers.

However, a considerable amount of work remains to advance its performance and application. Furthermore the algorithm developed can be used to conduct further studies

exploring the use of supplemental damping systems in seismic design. The following discussion provides recommendations for future work.

The weight of a steel structure and a proportional multiplier of 1.2 are used as the basis for defining initial construction cost of a steel framing system. However, the initial construction cost includes material cost, fabrication cost, erection cost, foundation cost, etc. It is recommended that more accurate cost models be used.

Only direct economic loss due to the damage to structural and non-structural components is considered in the dissertation. The developed methodology should be extended to estimate casualty and downtime (indirect) losses by incorporating different repair cost ratio parameters.

Seeding the population with “good” initial design variables and limiting the shape database to reasonable sizes will help make the exploration and convergence of the algorithm more efficient. If a frame has already been analyzed in a previous study, the results could be reused to reduce the number of analyses and to shorten the duration of the evolution.

Other passive damping systems should be considered (*e.g.* buckling restrained braces) in the system. The proposed automated design algorithm can easily incorporate additional system types. The impact of damper presence on construction cost related to connections should also be addressed.

The algorithm developed can be used to conduct regionally-based studies where designs in Memphis, TN can be compared to those in Los Angeles. It is recommended that these regional studies be conducted as they will be able to shed some light on the benefits of supplemental damping systems on a regional basis.

It is recommended that the algorithm developed be enhanced to include non-shear-building models. Therefore, beam sizes can be included as design variables. This will require more advanced matrix-based analysis procedures, but open-source computer programs (*e.g.* OpenSees) can serve as the analytical engine for advancement in this regard.

It is recommended that an alternate programming language be used. For example, the C or C++ programming languages and programs would speed up the analysis considerably. Executing Matlab programs includes significant overhead resulting from it being a scripting language.

It is recommended that models for expected annual loss be refined to include better representations of ground motion hazard. For example, more ground motions can be considered in the suites. A better dispersion of ground motions to represent probabilities of recurrence can also be formulated. This would allow better representation of the seismic hazard to be included in the designs.

REFERENCES

Chapter 1

- [1.1] Constantinou, M. C., Soong, T. T., and Dargush, G. F., “Passive Energy Dissipation Systems for Structural Design and Retrofit”. Multidisciplinary Center for Earthquake Engineering Research, pp 1-8.
- [1.2] Uang, C. M., and Bertero V. V. (1988), “Use of Energy as Design Criterion in Earthquake – Resistant Design”, UCB/EERC-88/18, University of California, Berkeley.
- [1.3] Mahmoodi, P., and Keel, C. J. (1986). “Performance of Viscoelastic Structural Dampers for the Columbia Center Building.” *Building Motion in Wind*, N. Isyumov and T.Tschana. eds., ASCE, New York, N.Y., 83-106.
- [1.4] <http://taylordevices.com>
- [1.5] Merritt, S., Uang, C., M. and Benzoni, G. (2003). “SUBASSEMBLAGE TESTING OF STAR SEISMIC BUCKLING-RESTRAINED BRACES”. Final Report to Star Seismic, LLC. Report No. TR-2003/04.
- [1.6] Lin, R.C., Liang, Z., Soong, T. T., and Zhang, R. H., and Mahmoodi, P. (1991). “An Experimental Study on Seismic Behavior of Viscoelastic Damped Structures.” *Engrg. Struct.*, 13(1), 75-84.
- [1.7] Zhang, R.H., and Soong, T. T., (1992). “Seismic Design of Viscoelastic Dampers for Structural Applications.” *Journal of Structural Engineering*, Volume 118, Issue 5, ASCE, pp. 1375-1392.
- [1.8] FEMA (August 2006). FEMA 445 Next Generation Performance-Based Seismic Design Guidelines, Federal Emergency Management Agency, Washington, D.C.
- [1.9] Gluck, N., Reinborn, A. M., Gluck, J., and Levy, R. (1996). “Design of Supplemental Dampers for Control of Structures.” *Journal of Structural Engineering*, Volume 122, Issue 12, ASCE, pp. 1394-1399.
- [1.10] Shukla, A. K., and Datta, T. K. (1999). “Optimal Use of Viscoelastic Dampers in Building Frames for Seismic Force.” *Journal of Structural Engineering*, Volume 125, Issue 4, ASCE, pp. 401-409.
- [1.11] Agrawal, A. K., and Yang, J. N. (2000). “Optimal Placement of Passive Dampers on Seismic and Wind-excited Buildings Using Combinatorial Optimization.” *Journal of Intelligent Material Systems and Structures*, Volume 10, Issue 12, pp. 997-1014.

- [1.12] Lopez Garcia, D. (2001). "A Simple Method for the Design of Optimal Damper Configurations in MDOF Structures." *Earthquake Spectra*, Volume 17, No. 3, pp. 387-398.
- [1.13] Singh, M. P., and Moreschi, L. M. (2002). "Optimal Placement of Dampers for Passive Response Control." *Earthquake Engineering & Structural Dynamics*, Volume 31, pp. 955-976.
- [1.14] Wongprasert N. and Symans M. D. (2004). "Application of a Genetic Algorithm for Optimal Damper Distribution within the Nonlinear Seismic Benchmark Building". *Journal of Engineering Mechanics*, Volume 130, Issue 4, pp. 401-406.
- [1.15] Lagaros, N. D., Fragiadakis, M., Papadrakakis, M., and Tsompanakis, Y., (2006). "Structural Optimization: A Tool for Evaluating Seismic Design Procedures". *Engineering Structure*, Volume 28, pp. 1623-1633.
- [1.16] FEMA (June 2007). FEMA 461, Interim Testing Protocols for Determining the Seismic Performance Characteristics of Structural and Nonstructural Components, Federal Emergency Management Agency, Washington, D.C.
- [1.17] Cornell, C. A., and Krawinker, H. (2001) "A Framework for Performance-Based Design." 2001: A Structural Engineering Odyssey, Proceedings of the 2001 Structures Congress and Exposition American Society of Civil Engineers, Reston, VA, CD-ROM.
- [1.18] Hamburger, R., Rojahn, C., Meohle, J., Bachman, R., Comartin, C., and Whittaker, A. (2004) "The ATC-58 Project: Development of Next-Generation Performance-Based Earthquake Design Criteria for Buildings." 13th World Conference on Earthquake Engineering, Vancouver, BC, Canada, CD-ROM.
- [1.19] Krawinker, H. (2006) "Performance Assessment of an Old RC Frame Building - A PEER Testbed Study." 8th U.S. National Conference on Earthquake Engineering, San Francisco, CA, Earthquake Engineering Research Institute, CD-ROM.
- [1.20] Moehle, J., and Deierlein, G. (2004) "A Framework Methodology for Performance-Based Earthquake Engineering." 13th World Conference on Earthquake Engineering, Vancouver, BC, Canada, CD-ROM.
- [1.21] Zareian, F., and Krawinker, H. (2006) "Why and How to Predict the Probability of Collapse of Buildings." 8th U.S. National Conference on Earthquake Engineering, San Francisco, CA, Earthquake Engineering Research Institute, CD-ROM.

- [1.22] Zareian, F., and Krawinkler, H. (2006) "Simplified Performance-Based Earthquake Engineering." 8th U.S. National Conference on Earthquake Engineering, San Francisco, CA, Earthquake Engineering Research Institute, CD-ROM.
- [1.23] FEMA. (2000). FEMA 350 - Recommended Seismic Design Criteria for New Steel Moment-Frame Buildings, Federal Emergency Management Agency, Washington DC.
- [1.24] DHS. (2003). HAZUS-MH MR1: Advanced Engineering Building Module, Technical Users Manual, Department of Homeland Security - Emergency Preparedness Response Directorate, Washington, DC.
- [1.25] Miranda, E., and Aslani, H. (2003). "Probabilistic Response Assessment for Building Specific Loss Estimation." PEER 2003/03, Pacific Earthquake Engineering Research Center.
- [1.26] Chipperfield A., Fleming P., Pohlheim H., Fonseca C., "Genetic Algorithm Toolbox for Use with MATLAB, User's Guide". Department of Automatic Control and Systems Engineering, University of SHEFFIELD.
- [1.27] Foley, C.M. and Schinler, D., (2001) "Optimized Design of Partially Restrained Frames Using Distributed Plasticity", (Invited Paper - ASCE Committee on Methods of Analysis), Structures Congress - ASCE, Washington, DC (CD-ROM; 22 pp.).
- [1.28] Rojas, H. A., (2008) "Automating Design of Steel Moment-Frames Using a Probabilistic Performance-Based Approach and Evolutionary Computation". A Dissertation Presented for the Doctor of Philosophy Degree, The University of Memphis.
- [1.29] Kalyanmoy Deb (April 2002). "Multi-Objective Optimization Using Evolutionary Algorithms". Department of Mechanical Engineering, Indian Institute of Technology, Kanpur, India. Pp88-100.
- [1.30] Schinler, D. and Foley, C.M., (2001) "An Object-Oriented Evolutionary Algorithm for Automated Advanced Analysis Based Design", Proceedings of Bird-of-a-Feather Workshop on Optimal Structural Design Using Genetic and Evolutionary Computation, Genetic and Evolutionary Computation Conference (GECCO 2001), San Francisco, CA, July 7, pp. 73-78.
- [1.31] <http://www.illegal.uiuc.edu/web/>
- [1.32] <http://www.mathworks.com>

Chapter 2

- [2.1] <http://opensees.berkeley.edu>
- [2.2] Zhang R. H., and Soong T. T., (1998). “Seismic Response of Steel Frame Structures with Added Viscoelastic Dampers”. John Wiley & Sons, Ltd, pp. 389-396
- [2.3] Newmark, N. M., (1959). “A Method of Computation for Structural Dynamics”, ASCE Journal of the Engineering Mechanics Division, Vol. 85 No. EM3.
- [2.4] Chopra A. K., (1995). “Dynamics of Structures: Theory and Applications to Earthquake Engineering”. Prentice Hall, pp. 454-625, pp.99-103
- [2.5] Haskell, Gregg. “Fluid viscous Damping as an alternative to Base Isolation”. Taylor Devices Inc. <http://www.taylordevices.com>.
- [2.6] Matlab (2010). *ODE45 - Ordinary Differential Equation with Initial Conditions Solver*, Matlab Release 2010a, The Mathworks, Inc., Natick, MA.

Chapter 3

- [3.1] FEMA (April 2000). FEMA 349, “Action plan for performance based seismic design”. Federal Emergency Management Agency, Washington, D.C.
- [3.2] Foley C.M. , “Optimization of Structural and mechanical Systems”. World Scientific, pp. 59-108.
- [3.3] Gill, P. E., Murray, W. and Wright, M. H. (1981). Practical Optimization, Academic Press, NewYork, N. Y.
- [3.4] Luenberger, D. (1984). Linear and Nonlinear Programming. Addison-Wesley, PP. 330-350.
- [3.5] AISC (2005), Manual of Steel Construction Thirteenth Edition, American Institute of Steel Construction INC.
- [3.6] Pezeshk, S. (1997). “How to Optimize Frames using Plastic Design concept”, Guide to Structural Optimization, Arora, J.S., Ed., American Society of Civil Engineers, New York, NY, 197 – 209.
- [3.7] Pezeshk, S., Camp, C.V. and Chen, D. (2000). “Design of Nonlinear Framed Structures Using Genetic Optimization.” Journal of Structural Engineering, American Society of Civil Engineering, 126(3), 382-388.

- [3.8] Camp, C., Pezeshk, S. and Cao, G. (1996). "Design of Framed Structures Using a Genetic Algorithm." Proceedings of the First U.S. –Japan Joint Seminar on Structural Optimization held in conjunction with the ASCE Technical Committee on Optimal Structural Design Meeting at the Structures Congress XIV., Frangopol, D.M. and Cheng, F.Y., Ed., American Society of Civil Engineers, 19-30.
- [3.9] Camp, C., Pezeshk, S. and Cao, G. (1998). "Optimized Design of Two-Dimensional Structures Using A Genetic Algorithm." Journal of Structural Engineering, American Society of Civil Engineers, 124(5), 551-559.
- [3.10] HAZUS-MH MR1 Technical Manual, Multi-hazard Loss Estimation Methodology Earthquake Model, Department of Homeland Security Emergency Preparedness and Response Directorate, FEMA, Mitigation Division, Washington, D.C.
- [3.11] Fragiadakis, M., Lagaros, N., Papadrakakis M. (2006). "Performance-based multiobjective optimum design of steel structures considering life-cycle cost." Springer-Verlag.
- [3.12] ASCE/SEI 7-05 Minimum Design Loads for Building and Other Structures, Structural Engineering Institute of the American Society of Civil Engineering.
- [3.13] Foley, C.M and Schinler, D. (2003). "Automated Design of Steel Frames Using Advanced Analysis and Object-Oriented Evolutionary Computation, Journal of Structural Engineering, American Society of Civil Engineers, Vol. 129, No. 5, pp. 648-656

Chapter 4

- [4.1] "Improving Optimization Performance with Parallel Computing", <http://www.mathworks.com/mason/tag/proxy.html?dataid=11466>.
- [4.2] Foley, C. and Vinnakota, S. (1997) "Inelastic Analysis of Partially Restrained Unbraced Steel Frames", Engineering Structures, Vol. 19, No. 11, pp. 891-902.
- [4.3] Foley, C. and Vinnakota, S. (1994) "Parallel Processing in the Elastic Nonlinear Analysis of High-Rise Frameworks", Computers and Structures, Vol. 52, No. 6, pp. 1169-1179.
- [4.4] Foley, C.M (2001) "Advanced Analysis of Steel Frames Using Parallel Processing and Vectorization", Computer-Aided Civil and Infrastructure Engineering, Blackwell Publishers, Vol. 16, No. 5, pp. 305-325.
- [4.5] Leonid O., Andrew C., Jonathan C. John S., "Scientific Computations on Modern Parallel Vector Systems", CRD/NERSC, Lawrence Berkeley National Laboratory, Berkeley, CA 94720

- [4.6] Somerville P., Smith N. F., Punyamurthula S., and Sun J. (1997). Development of Ground Motion Time Histories for Phase 2 of the FEMA/SAC Steel Project. Report No. SAC/BD-97-04; SAC Joint Venture, Sacramento, CA.

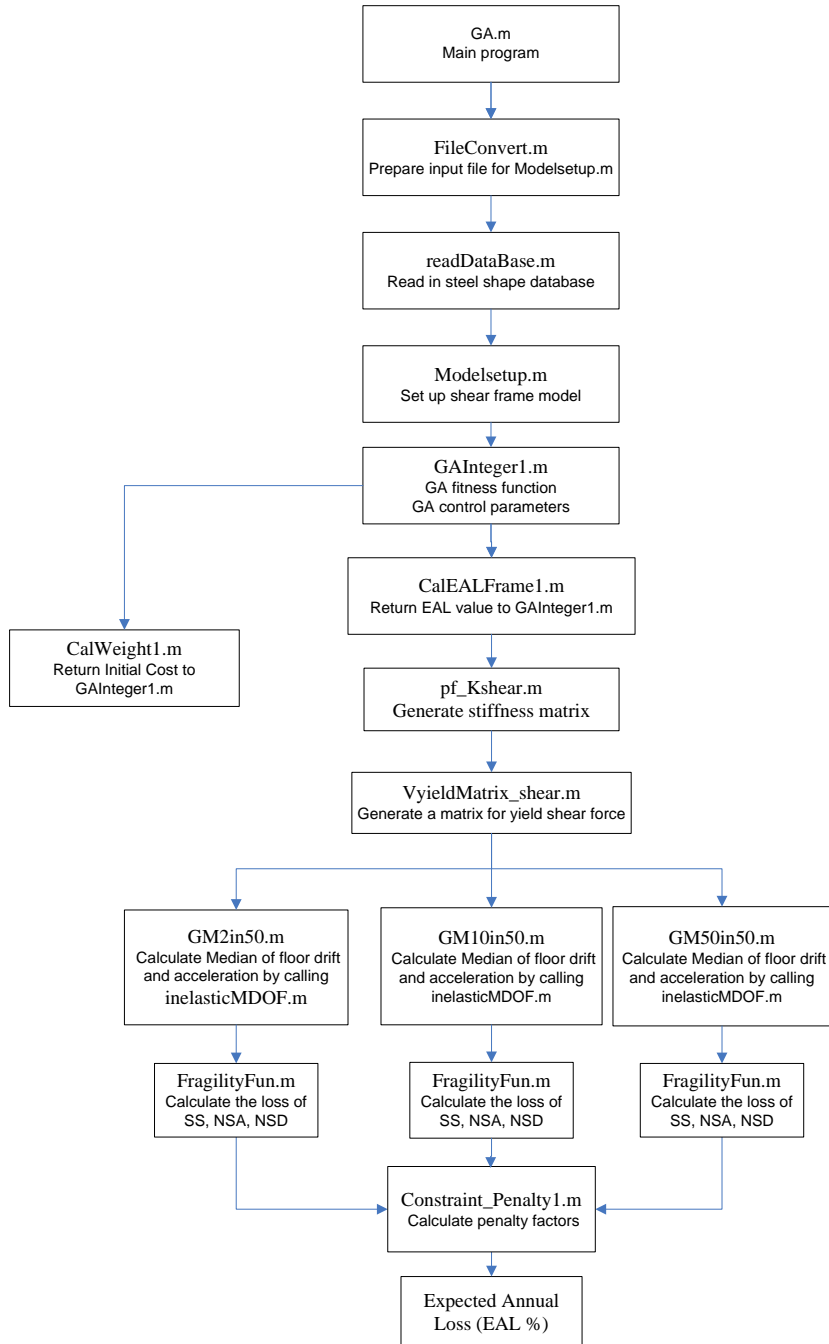
Appendices

M-File Source Code for the Design Algorithm

The six case studies discussed in Chapter 4 have different numbers of design variables. Appendix 2 through 21 lists the source code which was used in the calculation of Case 6. The variable, `numberOfVariables`, and the lower/upper bound matrixes, `LB/UB` in sub routine `GAInteger1.m` should be adjusted when the design variables are different from Case 6.

Appendix 1

Flow Chart of MATLAB Files



Appendix 2

Main Driving Program for Automated Design Algorithm

```

%%%%%%%%%%%%%%%%%%%%%%%%%%%%%%%%%%%%%%%%%%%%%%%%%%%%%%%%%%%%%%%%%%%%%%%%
%
% GA.m
%
%%%%%%%%%%%%%%%%%%%%%%%%%%%%%%%%%%%%%%%%%%%%%%%%%%%%%%%%%%%%%%%%%%%%%%%%

global Story;           % total story number in the model
global Bays;           % total Bay number in the model
global height;         % story height matrix
global Span;           % bay span matrix
global propertyEle;    % element property matrix
global Eletxt;         % element text description
global zeta;           % the percentage of damping in
                      % each mode desired
global freq1;          % first modal frequency for
                      % Rayleigh damping
global freq2;          % second modal frequency for
                      % Rayleigh damping
global nSol;           % the number of solution substeps within
                      % ground motion time intervals
global timeEnd;        % the ending time for the response
                      % computation
global Sigma_y;        % the yield strength of steel
global fid_penalty fid_column fid_s fid_fval fid_EAL;

[fid_penalty, message] = fopen('C:\GAInteger\Penalty_output.txt','w');

if ( fid_penalty == -1)
    disp('FILE - Penalty_output.txt - DOES NOT EXIST !!!!!');
end

[fid_column, message] = fopen('C:\GAInteger\Column_output.txt','w');

if ( fid_column == -1)
    disp('FILE - Column_output.txt - DOES NOT EXIST !!!!!');
end

[fid_s, message] = fopen('C:\GAInteger\Column_s.txt','w');

if ( fid_s == -1)
    disp('FILE - Column_s.txt - DOES NOT EXIST !!!!!');
end

[fid_fval, message] = fopen('C:\GAInteger\fval_output.txt','w');

if ( fid_fval == -1)
    disp('FILE - fval_output.txt - DOES NOT EXIST !!!!!');
end

[fid_EAL, message] = fopen('C:\GAInteger\EAL_output.txt','w');

```

```
if ( fid_EAL == -1)
    disp('FILE - EAL_output.txt - DOES NOT EXIST !!!!');
end

TimeStart] = datestr(now);           % timer starts

FileConvert;

[propertyEle, Eletxt] = readDataBase;

[Story, Bays, zeta, freq1, freq2, timeEnd, ...
    nSol, Sigma_y, m, height, Span] = Modelsetup;

[s,fval] = GAInteger1;

fclose(fid_penalty);                % file closes
fclose(fid_column);
fclose(fid_s);
fclose(fid_fval);
fclose(fid_EAL)

TimeEnd] = datestr(now);           %timer ends

% -----
```


Appendix 3

Sub-Function M-File to Establish Database of Cross-Section Shapes

(The database of wide-flange shapes considered in this dissertation is listed in Appendix 22. The user needs to develop an MS Excel® spreadsheet database of shapes if this is needed.

```

%%%%%%%%%%%%%%%%%%%%%%%%%%%%%%%%%%%%%%%%%%%%%%%%%%%%%%%%%%%%%%%%%%%%%%%%
%
% readDataBase.m
%
%%%%%%%%%%%%%%%%%%%%%%%%%%%%%%%%%%%%%%%%%%%%%%%%%%%%%%%%%%%%%%%%%%%%%%%%

function [propertyEle, Eletxt] = readDataBase

[propertyEle, Eletxt] = ...
    xlsread('c:\GAInteger\AISC_ShapesDatabase.xls', 'Column', 'B4:O53');

% -----

```

Appendix 4

Sub-Function M-File to set up 2D Steel Frame Model for Analysis

```

%%%%%%%%%%%%%%%%%%%%%%%%%%%%%%%%%%%%%%%%%%%%%%%%%%%%%%%%%%%%%%%%%%%%%%%%
%
% Modelsetup.m
%
%%%%%%%%%%%%%%%%%%%%%%%%%%%%%%%%%%%%%%%%%%%%%%%%%%%%%%%%%%%%%%%%%%%%%%%%

function [Story, Bays, zeta, freq1, freq2, timeEnd, nSol, ...
        Sigma_y, m, height, Span] = Modelsetup

global Eletxt;

% Open the data file for reading
fid = 0;
[fid,message]=fopen('C:\GAInteger\frame_inp.txt','r');
if ( fid == -1)
    disp('FILE - frame_inp.txt - DOES NOT EXIST !!!!');
end

% Read in the problem control parameters
Bays = fscanf(fid,'%d',1);
Story = fscanf(fid,'%d',1);
Nmaterial = fscanf(fid,'%d',1);
zeta = fscanf(fid,'%g',1);
freq1 = fscanf(fid,'%d',1);
freq2 = fscanf(fid,'%d',1);
timeEnd = fscanf(fid,'%d',1);
nSol = fscanf(fid,'%d',1);
Sigma_y = fscanf(fid,'%d',1);
Span = fscanf(fid,'%d',1);
for i = 1:Story
    kDamp(i) = fscanf(fid, '%g', 1);    % read in the damper stiffness
end
for j = 1:Story
    Coef(j) = fscanf(fid, '%g', 1);    % read in the damper
coefficients
end
for n = 1:Story
    alpha(n) = fscanf(fid, '%g', 1);    % read in the Damper exponents
end
for p = 1:Story
    m(p) = fscanf(fid, '%g', 1);    % read in mass matrix
end
for q = 1:Story
    height(q,1) = fscanf(fid, '%g', 1); % read in story height matrix
end
fclose(fid);    % file closed

```

Appendix 5

Sub-Function M-File to Control GA Algorithm

```

%%%%%%%%%%%%%%%%%%%%%%%%%%%%%%%%%%%%%%%%%%%%%%%%%%%%%%%%%%%%%%%%%%%%%%%%
%
% GAInteger1.m
%
%%%%%%%%%%%%%%%%%%%%%%%%%%%%%%%%%%%%%%%%%%%%%%%%%%%%%%%%%%%%%%%%%%%%%%%%

function [s,fval] = GAInteger1

FitnessFcn = @GA_fitness;
numberOfVariables = 12;           % number of design variables

% Lower bound of design variables
LB =[1 1 1 0 0 0 0 0 0 1 1 1 ]

% Upper bound of design variables
UB = [30 30 30 10 10 10 10 10 10 5 5 5];
Bound = [LB;UB];                 % If unbounded then Bound = []

options = gaoptimset('PopulationType','custom',...
    'CreationFcn',@int_pop,...
    'MutationFcn',@int_mutation,...
    'CrossoverFcn', @int_crossoverscattered,...
    'PopInitRange',Bound,...
    'Display','iter',...
    'Generations',200, ...
    'PopulationSize',100,...
    'ParetoFraction',0.9,...
    'PlotFcns',@gaplotpareto,...
    'TolFun',1e-4)
    'UseParallel','always');
[s,fval, EXITFLAG, OUTPUT, POPULATION] =
gamultiobj(FitnessFcn,numberOfVariables,[],[],[],[],...
    [1 1 1 0 0 0 0 0 0 1 1 1 ],...
    [30 30 30 10 10 10 10 10 10 5 5 5], options);
% -----

function mutationChildren = int_mutation(parents,options, ...
    GenomeLength, FitnessFcn,state,thisScore,thisPopulation)
shrink = .01;
scale = 1;
scale = scale - shrink * scale * state.Generation/options.Generations;
range = options.PopInitRange;
lower = range(1,:);
upper = range(2,:);
scale = scale * (upper - lower);
mutationPop = length(parents);

% The use of ROUND function will make sure that children are integers.
mutationChildren = repmat(lower,mutationPop,1) + ...
    round(repmat(scale,mutationPop,1) .*
    rand(mutationPop,GenomeLength));
% End of mutation function

```

```

%-----

function Population = int_pop(GenomeLength,FitnessFcn,options)

totalpopulation = sum(options.PopulationSize);
range = options.PopInitRange;
lower= range(1,:);
span = range(2,:) - lower;

% The use of ROUND function to make sure that individuals are integers.
Population = repmat(lower,totalpopulation,1) + ...
    round(repmat(span,totalpopulation,1) .*
    rand(totalpopulation,GenomeLength));

% End of creation function
%-----

% GA fitness function
function [fval] = GA_fitness(s)
global fid_fval;

fval(2) =
    CalEALFrame1(s(1),s(2),s(3),s(4),s(5),s(6),s(7),s(8),s(9),...
        s(10),s(11), s(12));

fval(1) = CalWeight1(s(1),s(2),s(3),s(4),s(5),s(6),s(7),s(8),s(9),...
        s(10),s(11), s(12));

cost = fval(1);
EAL = fval(2);

fprintf(fid_fval, '[ %1.5e %1.5e ]\n', [cost,EAL]);

% End of fitness function
%-----

```

Appendix 6

Sub-Function M-File to Calculate Expected Annual Loss

```

%%%%%%%%%%%%%%%%%%%%%%%%%%%%%%%%%%%%%%%%%%%%%%%%%%%%%%%%%%%%%%%%%%%%%%%%
%                                                                 %
% CalEALFrame1.m                                                                 %
%                                                                 %
%%%%%%%%%%%%%%%%%%%%%%%%%%%%%%%%%%%%%%%%%%%%%%%%%%%%%%%%%%%%%%%%%%%%%%%%

function [fval1] = CalEALFrame1(s1,s2,s3,s4,s5, s6, s7, s8, s9, s10, ...
                               s11, s12,)

global zeta;
global freq1;
global freq2;
global timeEnd;
global nSol;
global m;
global FDamper_max;
global FDamper_min;
global PHI_all;
global PHI_kRatio;
global fid_EAL;
Col = [s1 s2 s2 s3 s1; s1 s2 s2 s3 s1; s1 s2 s2 s3 s1];
Var = [s1 s2 s3; s1 s2 s3; s1 s2 s3];
VarDamper = [s4 s5 s6; s7 s8 s9; s10 s11 s12];
[kCol]=pf_Kshear(Col);
[Vyld] = VyieldMatrix_shear(Col);
Coef = [s4*10 s7*10 s10*10];
kDamp = [s5*10 s8*10 s11*10];
alpha = [0.5+(s6-1)*0.25 0.5+(s9-1)*0.25 0.5+(s12-1)*0.25];

[AveffloorAcc2in50, AveffloorDrift2in50, FDmax2in50, FDmin2in50] =
CalGM2in50(zeta, freq1, freq2, m, kCol, kDamp, Coef, alpha, Vyld, timeEnd, nSol);
[fval2in50] = FragilityFun(AveffloorAcc2in50, AveffloorDrift2in50);
fvalTEMP = fval2in50 * 0.000404;
fprintf(fid_EAL, ' %1.5e \t', fvalTEMP);
fprintf(fid_EAL, ' %s \n', '2in50');
fval2in50 = fval2in50 * 0.000404;

[AveffloorAcc10in50, AveffloorDrift10in50, FDmax10in50, FDmin10in50] =
CalGM10in50(zeta, freq1, freq2, m, kCol, kDamp, Coef, alpha, Vyld, timeEnd, nSol);
[fval10in50] = FragilityFun(AveffloorAcc10in50, AveffloorDrift10in50);
fvalTEMP =fval10in50 * 0.002107;
fprintf(fid_EAL, ' %1.5e \t', fvalTEMP);
fprintf(fid_EAL, ' %s \n', '10in50');
fval10in50 =  fval10in50 * 0.002107;

[AveffloorAcc50in50, AveffloorDrift50in50, FDmax50in50, FDmin50in50] =
CalGM50in50(zeta, freq1, freq2, m, kCol, kDamp, Coef, alpha, Vyld, timeEnd, nSol);
[fval50in50] = FragilityFun(AveffloorAcc50in50, AveffloorDrift50in50);
fvalTEMP = fval50in50 * 0.013863;
fprintf(fid_EAL, ' %1.5e \t', fvalTEMP);
fprintf(fid_EAL, ' %s \n', '50in50');
fval50in50 =  fval50in50 * 0.013863;

```

```

Angle = atan(156/360); %the angle between damper and beam.
FDamper_max = zeros(1,Story);
FDamper_min = zeros(1,Story);
for i = 1 : Story
    FDamper_max(1,i) = max([FDmax2in50(1,i) FDmax10in50(1,i)
    FDmax50in50(1,i)]);
    FDamper_min(1,i) = min([FDmin2in50(1,i) FDmin10in50(1,i)
    FDmin50in50(1,i)]);
end
FDamper_max = FDamper_max/cos(Angle);
FDamper_min = FDamper_min/cos(Angle);

[PHI_all ,PHI_kRatio] =
Constraint_Penalty1(Var,VarDamper,AvefloorDrift10in50,kCol,...
    FDamper_max, FDamper_min);
fval1 = (fval2in50 + fval10in50 + fval50in50) * PHI_all * PHI_kRatio;

%-----

```

Appendix 7

Sub-Function M-File to Calculate the Initial Construction Cost

```

%%%%%%%%%%%%%%%%%%%%%%%%%%%%%%%%%%%%%%%%%%%%%%%%%%%%%%%%%%%%%%%%%%%%%%%%
%
% CalWeight1.m
%
%%%%%%%%%%%%%%%%%%%%%%%%%%%%%%%%%%%%%%%%%%%%%%%%%%%%%%%%%%%%%%%%%%%%%%%%

function [fval2] = CalWeight1(s1,s2,s3,s4,s5, s6, s7, s8, s9, ...
                             s10, s11,s12)

global propertyEle;
global height;
global PHI_all;
global PHI_kRatio;
global Story;
global FDamper_max;
global FDamper_min;
global fid_column;
global Eletxt;
global fid_s;
global fid_fval;

% To generate weight matrix for current generation
columns = [s1 s2 s2 s3 s1; s1 s2 s2 s3 s1; s1 s2 s2 s3 s1];
col=[s1 s2 s3 s4 s5 s6 s7 s8 s9 s10 s11 s12 ];
for ii = 1:3
    output1 = char(Eletxt(col(ii)));

    % output selected columns for current generation
    fprintf(fid_column, '    %s\t',output1);
end

fprintf(fid_column, ' %s \n', '---');
fprintf(fid_s, '    %u\t',col); % output all design variables
fprintf(fid_s, ' %s \n', '---');

[row, col] = size(columns);
weight = zeros(row, col);
totalweight = 0;

for i = 1:row
    for j = 1:col
        weight(i,j)=propertyEle(columns(i,j),2);
    end
end

for i = 1 : row
    for j = 1:col
        totalweight = totalweight + weight(i,j) * height(i)/(12*1000);
        %unit: kips
    end
end
end

```

```

% To calculate the cost of columns, assume that the cost is $1.2/lb.
TotalCost = totalweight * 1.2 * 1000;
Col_Cost = TotalCost * PHI_all;

% to calculate the damper cost
Dampermin = abs(FDamper_min);
TotalDamperCost = 0.0;
for i = 1 : Story
    if FDamper_max(i) >= Dampermin(i)
        FD = FDamper_max(i);
    else
        FD = Dampermin(i);
    end;
    % 1kip = 0.4536 tons
    TotalDamperCost = TotalDamperCost + (11000-3200)/(200-25)*FD*0.4536
end
Damper_Cost = TotalDamperCost * PHI_kRatio;
fprintf(fid_fval, '[ %1.5e %1.5e ]\t', [Col_Cost,Damper_Cost]);
fval2 = TotalCost * PHI_all + TotalDamperCost * PHI_kRatio;

% -----

```


Appendix 8

Sub-Function M-File to Calculate Constraint and Penalty Factors

```

%%%%%%%%%%%%%%%%%%%%%%%%%%%%%%%%%%%%%%%%%%%%%%%%%%%%%%%%%%%%%%%%%%%%%%%%
%
% Constraint_Penalty1.m
%
%%%%%%%%%%%%%%%%%%%%%%%%%%%%%%%%%%%%%%%%%%%%%%%%%%%%%%%%%%%%%%%%%%%%%%%%

function [PHI_all,PHI_kRatio]=Constraint_Penalty1(Var,VarDamper,...
        AveffloorDrift10in50,kCol, FDamper_max, FDamper_min )

global Story; %Total number stories in the model
global Bays; %Total number bays in the model
global m; %mass matrix
global height; %height matrix
global propertyEle; %Element property matrix from database.
global fid_penalty;

%Compute the flexural buckling capacity for all columns
G_B = 4.71 * sqrt(29000/50);
Kx = 1.0; %In-plane behavior: fixed-fixed
Ky = 1.0; %out-of-plane behavior: pin - pin
E = 29000; %elastic modulus
Fy = 50; %material yield stress
g = 386.4; %gravity acceleration
[m1,n1]=size(Var);
Pn = zeros(Story, n1); % nominal flexural buckling strength

for i = 1 : Story
    for j = 1 : n1
        lamda_y = Ky * height(i,1)/propertyEle(Var(i,j),11);
        %out-plane
        lamda_x = Kx * height(i,1)/propertyEle(Var(i,j),6);
        %in-plane
        lamda = max(lamda_x, lamda_y);
        Fe = (pi^2)* E/(lamda)^2;
        if lamda <= G_B
            Fcr = (0.658^(Fy/Fe))* Fy;
            Pn(i,j) = Fcr * propertyEle(Var(i,j),3);
        else
            Fcr = 0.877 * Fe;
            Pn(i,j) = Fcr * propertyEle(Var(i,j),3);
        end
    end
end

for i = 1 : Story
    SumWeight = 0.0;
    for j = i : Story
        SumWeight = SumWeight + m(j);
    end
    W(i) = SumWeight * g;
    Pal(i) = W(i)/(Bays); % max axial load applied to inter-columns,

```

```

end

% the axial forces introduced by dampers.
Angle = atan(156/360);           %the angle between damper and beam.
FD(1,1) = 0;
FD(1,2) = 0;
FD(1,3) = FDamper_max(1) *sin(Angle);
FD(1,4) = 0;
FD(1,5) = 0;

for i = 2 : Story
% only the second and third columns are affected by the damper forces.
    FD(i,1) = 0;
    FD(i-1,2) = abs(FDamper_min(i)) *sin(Angle);
    FD(i,3) = FDamper_max(i) *sin(Angle);
    FD(i,4) = 0;
    FD(i,5) = 0;
end

FD_axial(Story,Bays+1) = zeros;
for i = 1 : Story
    for j = 1 : Bays+1
        for k = i : Story
            FD_axial(i,j)=FD_axial(i,j)+FD(k,j);
        end
    end
end

% calculate penalty factors
PHI_strength = 1.0;

for i = 1 : Story
    phi1 = Pa1(i)/(2*Pn(i,1)); % 2 external columns, carries 1/2 of
    Pal
    if phi1 <= 1.0
        q1 = 1.0;
    else
        q1 = phi1;
    end
    p1 = 1.0 + 5 * (q1 -1)^2;
    phi4 = Pa1(i)/(Pn(i,3)); % internal columns without dampers.
    if phi4 <= 1.0
        q4 = 1.0;
    else
        q4 = phi4;
    end
    p4 = 1.0 + 5 * (q4 -1)^2;
    phi2 = (Pa1(i)+ FD_axial(i,2))/Pn(i,2); %left column with damper
    if phi2 <= 1.0
        q2 = 1.0;
    else
        q2 = phi2;
    end
    p2 = 1.0 + 5 * (q2 -1)^2;
    phi3 = (Pa1(i)+ FD_axial(i,3))/Pn(i,2); %right column with damper

```

```

if phi3 <= 1.0
    q3 = 1.0;
else
    q3 = phi3;
end

p3 = 1.0 + 5 * (q3 -1)^2;
PHI_strength = PHI_strength * p1^2 * p4^(Bays-3)* p2 * p3;
end

% Beam-column constraints, Columns are fully Lateral_supported
PHI_BC = 1.0;
for i = 1 : Story
    phi1 = Pa1(i)/(2*Pn(i,1)); % 2 external columns
    m_p = Fy*propertyEle(Var(i,1),5);
    m_t = min(6*E*propertyEle(Var(i,1),4)*AveffloorDrift10in50(i)/ ...
        (height(i))^2, m_p);

    if phi1 >= 0.2
        phi_B = phi1 + (8/9)*(m_t/m_p);
    else
        phi_B = phi1/2 + (m_t/m_p);
    end

    if phi_B <= 1.0
        q1 = 1.0;
    else
        q1 = phi_B;
    end

    p1 = 1.0 + 5 * (q1 -1)^2;

    phi2 = Pa1(i)/(Pn(i,3)); % internal columns
    m_p = Fy*propertyEle(Var(i,3),5); %internal column without damper
    m_t = min(6*E*propertyEle(Var(i,3),4)*AveffloorDrift10in50(i)/ ...
        (height(i))^2, m_p); % the fourth column from the left.

    if phi2 >= 0.2
        phi_B = phi2 + (8/9)*(m_t/m_p);
    else
        phi_B = phi2/2 + (m_t/m_p);
    end

    if phi_B <= 1.0
        q2 = 1.0;
    else
        q2 = phi_B;
    end

    p2 = 1.0 + 5 * (q2 -1)^2;

    phi3 = (Pa1(i)+ FD_axial(i,2))/(Pn(i,2)); % internal columns
    m_p = Fy*propertyEle(Var(i,2),5); %internal column with damper
    m_t = min(6*E*propertyEle(Var(i,2),4)*AveffloorDrift10in50(i)/ ...
        (height(i))^2, m_p); % the second column from left.

```

```

if phi3 >= 0.2
    phi_B = phi3 + (8/9)*(m_t/m_p);
else
    phi_B = phi3/2 + (m_t/m_p);
end

if phi_B <= 1.0
    q3 = 1.0;
else
    q3 = phi_B;
end

p3 = 1.0 + 5 * (q3 -1)^2;

phi4 = (Pa1(i)+ FD_axial(i,3))/(Pn(i,2)); % internal columns
m_p = Fy*propertyEle(Var(i,2),5); %internal column with damper
m_t = min(6*E*propertyEle(Var(i,2),4)*AvefloorDrift10in50(i)/ ...
    (height(i))^2, m_p); % the third column from left.

if phi4 >= 0.2
    phi_B = phi4 + (8/9)*(m_t/m_p);
else
    phi_B = phi4/2 + (m_t/m_p);
end
if phi_B <= 1.0
    q4 = 1.0;
else
    q4 = phi_B;
end

p4 = 1.0 + 5 * (q4 -1)^2;

PHI_BC = PHI_BC * p1^2 * p2^(Bays-3) * p3 * p4;
end

% shape and weight constraints

PHI_shp = 1.0;
for i =2 :Story
    for j = 1 : 3
        phi = propertyEle(Var(i,j),2)/propertyEle(Var((i-1),j),2);
        if phi <= 1.0
            q = 1.0;
        else
            q = phi;
        end
        p(j) = 1.0 + 5 * (q -1)^2;
    end
    PHI_shp = PHI_shp * p(1)^2 *p(2)^2*p(3);
end
end

```

```

PHI_wt = 1.0;
for i = 2 : Story
    for j = 1 : 3 % 4 vars for each story
        phi = propertyEle(Var(i,j),1)/propertyEle(Var((i-1),j),1);
        if phi <= 1.0
            q = 1.0;
        else
            q = phi;
        end
        p(j) = 1.0 + 5 * (q - 1)^2;
    end
    PHI_wt = PHI_wt * p(1)^2 * p(2)^2 * p(3);
end

% Couolumn web slenderness limit

PHI_web = 1.0;
for i = 1 : Story
    if Pa1(i)/(2* Fy* propertyEle(Var(i,1),3)) <= 0.125
        webslender1 = (640/sqrt(Fy))* ...
            (1-((2.75*Pa1(i))/(2*Fy*propertyEle(Var(i,1),3))));
    else
        webslender1 = max(((191/sqrt(Fy))*(2.33- ...
            (Pa1(i)/(2*Fy*propertyEle(Var(i,1),3))))), 253/sqrt(Fy));
    end

    phi = propertyEle(Var(i,1),14)/webslender1;
    if phi <= 1.0
        q = 1.0;
    else
        q = phi;
    end
    p1 = 1.0 + 5 * (q - 1)^2;

    if Pa1(i)/(Fy* propertyEle(Var(i,3),3)) <= 0.125
        webslender4 = (640/sqrt(Fy))* ...
            (1-((2.75*Pa1(i))/(Fy*propertyEle(Var(i,3),3))));
    else
        webslender4 = max(((191/sqrt(Fy))*(2.33- ...
            (Pa1(i)/(Fy*propertyEle(Var(i,3),3))))), 253/sqrt(Fy));
    end
    phi = propertyEle(Var(i,3),14)/webslender4;

    if phi <= 1.0
        q = 1.0;
    else
        q = phi;
    end
    p4 = 1.0 + 5 * (q - 1)^2;

```

```

if (Pa1(i)+FD_axial(i,2))/(Fy* propertyEle(Var(i,2),3)) <= 0.125
    %the left column with dampers
    webslender2 = (640/sqrt(Fy))* ...
        (1-((2.75*Pa1(i))/(Fy*propertyEle(Var(i,2),3))));
else
    webslender2 = max(((191/sqrt(Fy))*(2.33-
        (Pa1(i)/(Fy*propertyEle(Var(i,2),3))))), 253/sqrt(Fy));
end

phi = propertyEle(Var(i,2),14)/webslender2;
if phi <= 1.0
    q = 1.0;
else
    q = phi;
end
p2 = 1.0 + 5 * (q -1)^2;

if (Pa1(i)+FD_axial(i,3))/(Fy* propertyEle(Var(i,2),3)) <= 0.125
    %the right column with dampers
    webslender3 = (640/sqrt(Fy))* ...
        (1-((2.75*Pa1(i))/(Fy*propertyEle(Var(i,2),3))));
else
    webslender3 = max(((191/sqrt(Fy))*(2.33-
        (Pa1(i)/(Fy*propertyEle(Var(i,2),3))))), 253/sqrt(Fy));
end
phi = propertyEle(Var(i,2),14)/webslender3;

if phi <= 1.0
    q = 1.0;
else
    q = phi;
end
p3 = 1.0 + 5 * (q -1)^2;
PHI_web = PHI_web * p1^2 * p2*p3*p4^(Bays-3);
end

% Couolumn flange slenderness limit
PHI_f = 1.0;

for i = 1 : Story
    for j = 1 : 3
        phi = propertyEle(Var(i,j),13)/(0.30*sqrt(E/Fy));
        if phi <= 1.0
            q = 1.0;
        else
            q = phi;
        end
        p(j) = 1.0 + 5 * (q -1)^2;
    end

    PHI_f = PHI_f * p(1)^2 * p(2)^2* p(3);
end

```

```

% damper's stiffness constraints and penalty.
PHI_kRatio = 1.0;

for i =1 :Story
    phi = VarDamper(i,2)*10/(kCol(i)*0.1);
    if phi <= 1.0
        q = 1.0;
    else
        q = phi;
    end
    p = 1.0 + 5 * (q -1)^2;
    [PHI_kRatio] = PHI_kRatio * p;
end
fprintf(fid_penalty, '[%1.5e %1.5e %1.5e %1.5e %1.5e %1.5e %1.5e]\n', ...
        [PHI_strength, PHI_shp, PHI_wt , PHI_web, PHI_f, PHI_BC, ...
        PHI_kRatio]);
[PHI_all] = PHI_strength * PHI_shp * PHI_wt * PHI_web * PHI_f *
PHI_BC;

%-----

```

Appendix 9

Sub-Function M-File to Calculate Constraint and Penalty Factors

```

%%%%%%%%%%%%%%%%%%%%%%%%%%%%%%%%%%%%%%%%%%%%%%%%%%%%%%%%%%%%%%%%%%%%%%%%
%
% inelasticMDOF.m
%
%%%%%%%%%%%%%%%%%%%%%%%%%%%%%%%%%%%%%%%%%%%%%%%%%%%%%%%%%%%%%%%%%%%%%%%%

function
[u_g_dd, recTime, solTime, x, x_d, x_dd, intFrc, F_d_elas_time, F_d_visc_time,
Omega, M, K, Coef, elapsedTime] = inelasticMDOF
(fileName, zeta, freq1, freq2, m, kCol, kDamp, Coef, alpha, Vyld, timeEnd, nSol)

% MatLab function uses Newmark's 'average acceleration' method to
% compute the response to ground motion for an MDF shear building.
%
% Input Arguments:
% fileName = filename containing the ground acceleration record
%           data to follow (must be contained in single quotes,
%           (i.e. '1940ImperialValley.txt')).
%           The first line of the ground acceleration file must
%           contain the following line before acceleration data:
%           del_time gFact
%           where:
%           del_time= the time increment for the ground
%                   acceleration data
%           gFact   = acceleration multiplier to make accelerations
%                   in the file consistent with in/s^2 units
% zeta           = the percentage of damping in each mode desired
% freq1         = first modal frequency for Rayleigh damping computations
% freq2         = second modal frequency for Rayleigh damping computations
% m             = the building mass list at each floor level (vector)
% k             = the building stiffness at each story (vector)
% Vyld          = the story yield force (vector)
% timeEnd       = the ending time for the response computation
% nSol          = the number of solution sub steps within ground motion time
%               intervals
% alpha         = the velocity exponent for the supplemental dampers at each
%               story (vector)
% Coef          = the coefficient for the supplemental damper at each story
%
% Returned Arguments:
% time = vector of time for response plotting
% x     = story displacement vector (relative to ground)
% V     = vector of story shears
% u_dd = ground acceleration vector
%
% Read in the time-history acc. data and store in an appropriate
% array. Time history input is assumed to be in 'g-units'.

```



```

numRec = 1 ;
fid = fopen(fileName,'r') ;    % File identifier for read-in
delTime = fscanf(fid,'%g',1) ; % Read in the time increment for GM
gFact = fscanf(fid,'%g',1) ;   % Acceleration due to gravity multiplier
u_g_dd(numRec) = 0.0 ;

while feof(fid) == 0
    numRec = numRec + 1 ;
    accel(numRec) = fscanf(fid,'%g',1) ;
    u_g_dd(numRec) = accel(numRec)*gFact ; % Convert to 'in/s^2' units
end

status = fclose(fid) ;

% Generate time and ground motion arrays of needed length

timeRec = delTime * numRec ;
timeStop = max(timeEnd,timeRec) ;

if timeEnd >= timeRec
    recInc = timeEnd / delTime ;
    for i = numRec+1:recInc
        u_g_dd(i) = 0.0 ;
    end
    numRec = recInc ;
end

recTime(1) = 0.0 ;
for i = 2:numRec
    recTime(i) = recTime(i-1) + delTime ;
end

% Generate an array of time vs. ground acceleration values at solution
% increment desired

delSol = delTime / nSol ;
u_dd(1) = 0.0 ;
time = 0.0 ;
solIndx = 1 ;

for i = 2:numRec
    for j = 1:nSol
        solIndx = solIndx + 1 ;
        time = time + delSol ;
        u_dd(solIndx) = u_g_dd(i-1) + ( time - recTime(i-1) ) / ...
            (recTime(i) - recTime(i-1)) * ( u_g_dd(i) - u_g_dd(i-1) );
    end
end

numSol = solIndx ;
solTime(1) = 0.0 ;

for i = 2:numSol
    solTime(i) = solTime(i-1) + delSol ;
end

```

```

% Compute the number of rows and columns for the matrices in the system

numRows = length(m) ;
numCols = length(m) ;

% Initialize the inelastic analysis parameters

for j = 1:numRows
    yldKey(j) = 0.0 ;
    xMax(j) = Vyld(j)/kCol(j) ;
    xMin(j) = -1.0*Vyld(j)/kCol(j) ;
    stryFrc(j,1) = 0.0 ;
    inf(j,1) = 1.0 ;
    fInt(j,1) = 0.0 ;
end

% Compute the stiffness matrix for the shear building
kElas = kCol ;
[K] = assembleK(kCol+kDamp) ;

% Compute the mass matrix for the shear building
M(1:numRows,1:numCols) = 0.0 ; % Initialize the mass matrix
for i = 1:numRows
    M(i,i) = m(i);
end

% Compute natural frequencies via Eigen value analysis
[Phi,omega] = eig(K,M); % Compute Mode Shape and Natural
Frequencies

for i = 1:numRows
    Omega(i) = sqrt(omega(i,i)); % Take square root of frequencies
end

Omega = sort(Omega); % Sort frequencies low to high

%Compute the classical damping matrix assuming Rayleigh damping

omega_i = Omega(freq1);
omega_j = Omega(freq2);
a_0 = zeta * ( 2.0*omega_i*omega_j ) / ( omega_i + omega_j ) ;
a_1 = zeta * ( 2.0 ) / ( omega_i + omega_j ) ;
C_Ray = a_0*M + a_1*K ;

% Initialize
for i = 1:numRows
    u_aa(i,1) = 0.0; % Zero the displacement response vector
    u_aa_d(i,1) = 0.0; % Zero the velocity response vector
    u_aa_dd(i,1) = 0.0; % Zero the acceleration response vector
    del_u_aa_d(i,1) = 0.0; % Zero the incremental velocity response
end

```

```

for i = 1:numRows
    for j = 1:numSol
        x(i,j) = 0.0; % Zero the deformation vector
        x_d(i,j) = 0.0; % Zero the velocity vector
        x_dd(i,j) = 0.0; % Zero the first column of the acceleration
        intFrc(i,j) = 0.0; % Zero the internal spring force vector
    end
    F_d(i) = 0.0 ;
    F_d_slope(i)=alpha(i) * Coef(i) * (abs(0.000001))^(alpha(i) - 1) ;
end

% Initialize quantities prior to time stepping. Newmark's Average
% Acceleration method coded

beta = 0.25;
gamma = 1.0/2.0;
p = -1.00*M*inf*u_dd(1); % Compute load vector for first time value

% Begin the time stepping
for i = 1:numSol-1
    [C] = assembleC(F_d_slope) ;
    C = C + C_Ray ;

    % Compute Newmark coefficient vector; 'a'
    A = 1.0/(beta*delSol)*M + gamma/beta*C;

    % Compute Newmark coefficient vector; 'b'
    B = 1.0/(2.0*beta)*M + delSol*(gamma/(2.0*beta)-1.0)*C ;
    del_p = -1.00*M*inf*( u_dd(i+1) - u_dd(i) ) ;
    p = p + del_p ;
    del_p_hat = del_p + a*u_aa_d + b*u_aa_dd ;

    [kCol,yldKey,xMax,xMin] =
        kCurrent(kCol,kElas,yldKey,Vyld,xMax,xMin,u_aa_d,u_aa) ;
    [K] = assembleK(kCol+kDamp) ;
    K_hat = K + gamma/(beta*delSol)*C + 1.0/(beta*delSol*delSol)*M ;

    del_u = inv(K_hat)*del_p_hat ;
    del_u_d = gamma/(beta*delSol)*del_u - gamma/beta*u_aa_d ...
        + delSol*(1.0-gamma/(2.0*beta))*u_aa_dd ;
    del_u_dd = 1.0/(beta*delSol*delSol)*del_u - 1.0/(beta*delSol)* ...
        u_aa_d - 1.0/(2.0*beta)*u_aa_dd ;
    u_aa = u_aa + del_u ;
    u_aa_d = u_aa_d + del_u_d ;
    u_aa_dd = u_aa_dd + del_u_dd ;

    [fInt,stryFrc] =

internalForce(kCol,kElas,yldKey,Vyld,xMax,xMin,stryFrc,del_u);
[F_d_slope] = DamperSlope( Coef, alpha, u_aa_d ) ;
[F_d_elas,F_d_visc] = DamperForce(Coef, alpha, u_aa_d, kDamp,u_aa );

```

```
for j = 1:numRows
    x(j,i+1) = u_aa(j,1) ;
    x_d(j,i+1) = u_aa_d(j,1) ;
    x_dd(j,i+1) = u_aa_dd(j,1) ;
    intFrc(j,i+1) = stryFrc(j,1) ;
    F_d_elas_time(j,i+1) = F_d_elas(j) ;
    F_d_visc_time(j,i+1) = F_d_visc(j) ;
end
end
%-----
```

Appendix 10

Sub-Function M-File to Calculate Evaluate the damages and Repair Cost

```

%%%%%%%%%%%%%%%%%%%%%%%%%%%%%%%%%%%%%%%%%%%%%%%%%%%%%%%%%%%%%%%%%%%%%%%%
%
% FragilityFun.m
%
%%%%%%%%%%%%%%%%%%%%%%%%%%%%%%%%%%%%%%%%%%%%%%%%%%%%%%%%%%%%%%%%%%%%%%%%

function [fval] = FragilityFun(AveffloorAcc, AveffloorDrift)
global Story;
global height;
global fid_EAL;

SS = [0.4, 1.9, 9.6, 19.2];
NSD = [0.7, 3.3, 16.4, 32.9];
NSA = [0.9, 4.8, 14.4, 47.9];
EDP = AveffloorDrift./height;
Bate = 0.5;
EDP_ds = [0.004, 0.008, 0.02, 0.0533];

x1 = (1/Bate) * log(EDP/EDP_ds(1));
P1= 0.5 * erfc(-x1/sqrt(2));

x2 = (1/Bate) * log(EDP/EDP_ds(2));
P2= 0.5 * erfc(-x2/sqrt(2));

x3 = (1/Bate) * log(EDP/EDP_ds(3));
P3= 0.5 * erfc(-x3/sqrt(2));

x4 = (1/Bate) * log(EDP/EDP_ds(4));
P4= 0.5 * erfc(-x4/sqrt(2));

E_SS = (P1-P2)*SS(1)+(P2-P3)*SS(2)+(P3-P4)*SS(3)+P4*SS(4);

% non structural drift sensitive components

EDP_ds = [0.004, 0.008, 0.025, 0.050];
x5 = (1/Bate) * log(EDP/EDP_ds(1));
P5= 0.5 * erfc(-x5/sqrt(2));

x6 = (1/Bate) * log(EDP/EDP_ds(2));
P6= 0.5 * erfc(-x6/sqrt(2));

x7 = (1/Bate) * log(EDP/EDP_ds(3));
P7= 0.5 * erfc(-x7/sqrt(2));

x8 = (1/Bate) * log(EDP/EDP_ds(4));
P8= 0.5 * erfc(-x8/sqrt(2));

E_NSD = (P5-P6)*NSD(1)+(P6-P7)*NSD(2)+(P7-P8)*NSD(3)+P8*NSD(4);

```

```

% non structural acceleration sensitive components

EDP = AveffloorAcc/386.4;
Bate = 0.6;
EDP_ds = [0.30, 0.6, 1.2, 2.4];

x9 = (1/Bate) * log(EDP/EDP_ds(1));
P9= 0.5 * erfc(-x9/sqrt(2));

x10 = (1/Bate) * log(EDP/EDP_ds(2));
P10= 0.5 * erfc(-x10/sqrt(2));

x11= (1/Bate) * log(EDP/EDP_ds(3));
P11= 0.5 * erfc(-x11/sqrt(2));

x12 = (1/Bate) * log(EDP/EDP_ds(4));
P12= 0.5 * erfc(-x12/sqrt(2));

E_NSA = (P9-P10)*NSA(1)+(P10-P11)*NSA(2)+(P11-P12)*NSA(3)+P12*NSA(4);

storyEAL = (E_SS+E_NSD+E_NSA);
E1 = 0;
E2 = 0;
E3 = 0;

for ii = 1:Story
    E1 = E1 + E_SS(ii);
    E2 = E2 + E_NSD(ii);
    E3 = E3 + E_NSA(ii);
end

fprintf(fid_EAL, '[ %1.5e %1.5e %1.5e ]\t', [E1,E2,E3]);
fval = 0;

for i = 1: Story
    fval = fval + storyEAL(i);
end
%-----

```

Appendix 11

Sub-Function to Assembly the Structure Stiffness Matrix

```

%%%%%%%%%%%%%%%%%%%%%%%%%%%%%%%%%%%%%%%%%%%%%%%%%%%%%%%%%%%%%%%%%%%%%%%%
%
% pf_Kshear.m
%
%%%%%%%%%%%%%%%%%%%%%%%%%%%%%%%%%%%%%%%%%%%%%%%%%%%%%%%%%%%%%%%%%%%%%%%%

function [kCol]=pf_Kshear(Col)

global height;
global Story;
global Bays;
global propertyEle;

youngs = 29000;
for i = 1:Story
    k = 0;
    for j = 1:(Bays +1)
        k = k + 12*youngs * propertyEle(Col(i,j),4)/height(i)^3;
    end
    kCol(i) = k;
end
% -----

```

Appendix 12

Sub-Function M-File to Generate the Matrix of Yield Strength

```

%%%%%%%%%%%%%%%%%%%%%%%%%%%%%%%%%%%%%%%%%%%%%%%%%%%%%%%%%%%%%%%%%%%%%%%%
%
% VyieldMatrix_shear.m
%
%%%%%%%%%%%%%%%%%%%%%%%%%%%%%%%%%%%%%%%%%%%%%%%%%%%%%%%%%%%%%%%%%%%%%%%%

function [Vyld] = VyieldMatrix_shear(Col)
global height;
global Story;
global Bays;
global propertyEle;

for i = 1:Story
    V = 0;
    for j = 1:(Bays +1)
        V = V + 2*(50*propertyEle(Col(i,j),5)/height(i));
    end
    Vyld(i) = V;
end

% -----

```


Appendix 13

Sub-Function M-File to Generate the Matrix of Current Frame Stiffness

```

%%%%%%%%%%%%%%%%%%%%%%%%%%%%%%%%%%%%%%%%%%%%%%%%%%%%%%%%%%%%%%%%%%%%%%%%
%
% kCurrent.m
%
%%%%%%%%%%%%%%%%%%%%%%%%%%%%%%%%%%%%%%%%%%%%%%%%%%%%%%%%%%%%%%%%%%%%%%%%

function[k,yldKey,xMax,xMin] =
    kCurrent(k,kElas,yldKey,Vyld,xMax,xMin,u_d,u)

numRows = length(k); % Set size of stiffness matrix
for j = 1:numRows % Compute story yielding condition and stiffness
    currVel = u_d(j,1); % Set the current story velocity
    if j == 1
        currDsp = u(j,1); % Set the current story displacement
    else
        currDsp = u(j,1) - u(j-1,1) ;
    end

    if yldKey(j) == 0 % System is currently on an elastic branch

        % Yielding in positive direction has occurred
        if currVel >= 0
            if currDsp > xMax(j)
                yldKey(j) = 1 ; % Set yield key
                k(j)= 0.0; % Set story stiffness to "zero"
            else
                yldKey(j) = 0 ; % System remains elastic
                k(j)= kElas(j); % Return story stiffness
            end
        else
            if currDsp < xMin(j) % Yielding in negative direction
                yldKey(j) = -1 ; % System has yielded in neg. direction
                k(j) = 0.0; % Set story stiffness to "zero"
            else
                yldKey(j) = 0 ; % System remains elastic
                k(j)= kElas(j); % Return story stiffness
            end
        end

        % Currently on a yielded branch in positive direction
        elseif yldKey(j) == 1

            if currVel >= 0
                yldKey(j) = 1 ; % System continues to yield in (+)
            direction
                k(j) = 0.0; % Set story stiffness to "zero"
            else
                yldKey(j) = 0 ; % System unloads to elastic response
                k(j) = kElas(j); % Set story stiffness to initial elastic
                xMax(j)= currDsp ; % Set max. displacement to current
            end
        end
    end
end

```

```
        % Set min. displacement
        xMin(j)=currDsp - 2.0*Vyld(j)/kElas(j);
    end

else          % Currently on a yielded branch in (-) direction

    if currVel <= 0
        % System continues to yield in (-) direction
        yldKey(j) = -1 ;
        k(j)= 0.0 ;          % Set story stiffness to "zero"
    else
        yldKey(j) = 0 ;      % System unloads to elastic response
        k(j) = kElas(j);    % Set story stiffness to initial elastic
        xMin(j) = currDsp;% Set min. displacement to current
        % Set max. displacement
        xMax(j)= currDsp+2.0*Vyld(j)/kElas(j);
    end
end
end
end

%-----
```

Appendix 14

Sub-Function M-File to Calculate Internal Forces in Columns

```

%%%%%%%%%%%%%%%%%%%%%%%%%%%%%%%%%%%%%%%%%%%%%%%%%%%%%%%%%%%%%%%%%%%%%%%%
%
% internalForce.m
%
%%%%%%%%%%%%%%%%%%%%%%%%%%%%%%%%%%%%%%%%%%%%%%%%%%%%%%%%%%%%%%%%%%%%%%%%

function [fInt,stryFrc] =

    internalForce(k,kElas,yldKey,Vyld,xMax,xMin,stryFrc,del_u);

numRows = length(k);    % Set size of stiffness matrix

for j = 1:numRows      % Compute story yielding condition and stiffness

    if j == 1
        incDsp = del_u(j,1) ;
    else
        incDsp = del_u(j,1) - del_u(j-1,1) ;
    end

    if yldKey(j) == 0    % System is currently on an elastic branch
        stryFrc(j,1) = stryFrc(j,1) + k(j)*incDsp ;
        if stryFrc(j,1) <= -1.0*Vyld(j)
            stryFrc(j,1) = -1.0*Vyld(j) ;
        end
        if stryFrc(j,1) >= Vyld(j)
            stryFrc(j,1) = Vyld(j) ;
        end
    end
    % Currently on a yielded branch in(+) direction
    elseif yldKey(j) == 1
        stryFrc(j,1) = Vyld(j) ;
    else
        % Currently on a yielded branch in(-) direction
        stryFrc(j,1) = -1.0*Vyld(j) ;
    end
end

for j = 1:numRows
    if j == numRows
        fInt(j,1) = stryFrc(j) ;
    else
        fInt(j,1) = stryFrc(j) - stryFrc(j+1) ;
    end
end

% -----

```

Appendix 15

Sub-Function M-File to Calculate the Current Damper Force

```

%%%%%%%%%%%%%%%%%%%%%%%%%%%%%%%%%%%%%%%%%%%%%%%%%%%%%%%%%%%%%%%%%%%%%%%%
%
% DamperForce.m
%
%%%%%%%%%%%%%%%%%%%%%%%%%%%%%%%%%%%%%%%%%%%%%%%%%%%%%%%%%%%%%%%%%%%%%%%%

function [F_d_elas, F_d_visc] = DamperForce(c, alpha, x_d, kDamp, x )

for i = 1:length(c)

    if i == 1
        relVel = x_d(i) ;
        relDsp = x(i) ;
    else
        relVel = x_d(i) - x_d(i-1) ;
        relDsp = x(i) - x(i-1) ;
    end

    F_d_visc(i) = sign(relVel)*c(i)*(abs(relVel))^(alpha(i)) ;
    F_d_elas(i) = relDsp*kDamp(i) ;
end
%-----

```

Appendix 16

Sub-Function M-File to Compute the Current Slope in the Damper Force vs. Velocity

```

%%%%%%%%%%%%%%%%%%%%%%%%%%%%%%%%%%%%%%%%%%%%%%%%%%%%%%%%%%%%%%%%%%%%%%%%
%
% DamperSlope.m
%
%%%%%%%%%%%%%%%%%%%%%%%%%%%%%%%%%%%%%%%%%%%%%%%%%%%%%%%%%%%%%%%%%%%%%%%%

function [ F_d_slope ] = DamperSlope( c, alpha, x_d )

for i = 1:length(c)

    if i == 1
        relVel = x_d(i) ;
        if relVel == 0.0
            F_d_slope(i) = alpha(i)*c(i)*(abs(0.000001))^(alpha(i)-1) ;
        else
            F_d_slope(i) = alpha(i) * c(i)*(abs(relVel))^(alpha(i)-1) ;
        end
    else
        relVel = x_d(i) - x_d(i-1) ;
        if relVel == 0.0
            F_d_slope(i) = alpha(i)*c(i)*(abs(0.000001))^(alpha(i)-1) ;
        else
            F_d_slope(i) = alpha(i)*c(i)*(abs(relVel))^(alpha(i)-1) ;
        end
    end
end

end

%-----

```

Appendix 17

Sub-Function M-File to Assemble the Stiffness Matrix

```

%%%%%%%%%%%%%%%%%%%%%%%%%%%%%%%%%%%%%%%%%%%%%%%%%%%%%%%%%%%%%%%%%%%%%%%%
%
% assembleK.m
%
%%%%%%%%%%%%%%%%%%%%%%%%%%%%%%%%%%%%%%%%%%%%%%%%%%%%%%%%%%%%%%%%%%%%%%%%

function [K] = assembleK(k)

numRows = length(k);           % Establish number of rows and
columns = length(k);
numCols = length(k);

K(1:numRows,1:numCols) = 0.0 ; % Initialize the stiffness matrix

for i = 1:numRows              % Compute the upper triangle
    for j = i:numCols
        if i == j
            if i == numRows
                K(i,j) = k(numRows);
            else
                K(i,j) = k(i) + k(i+1);
            end
        elseif j > i + 1
            K(i,j) = 0.0 ;
        else
            K(i,j) = -1.0*k(i+1);
        end
    end
end

for i = 1:numRows              % Pick up the lower diagonal
    for j = i:numCols
        K(j,i) = K(i,j);
    end
end
%-----

```

Appendix 18

Sub-Function M-File to Assembly the Damping Coefficient C Matrix

```

%%%%%%%%%%%%%%%%%%%%%%%%%%%%%%%%%%%%%%%%%%%%%%%%%%%%%%%%%%%%%%%%%%%%%%%%
%
% assembleC.m
%
%%%%%%%%%%%%%%%%%%%%%%%%%%%%%%%%%%%%%%%%%%%%%%%%%%%%%%%%%%%%%%%%%%%%%%%%

function [C] = assembleC(c)

numRows = length(c);           % Establish number of rows and
columns
numCols = length(c);
C(1:numRows,1:numCols) = 0.0 ; % Initialize the stiffness matrix

for i = 1:numRows              % Compute the upper triangle
    for j = i:numCols
        if i == j
            if i == numRows
                C(i,j) = c(numRows);
            else
                C(i,j) = c(i) + c(i+1);
            end
        elseif j > i + 1
            C(i,j) = 0.0 ;
        else
            C(i,j) = -1.0*c(i+1);
        end
    end
end

for i = 1:numRows              % Pick up the lower diagonal
    for j = i:numCols
        C(j,i) = C(i,j);
    end
end

%-----

```

Appendix 19

Sub-Function M-File to Calculate the Damage Loss due to Seismic 2in50

```

%%%%%%%%%%%%%%%%%%%%%%%%%%%%%%%%%%%%%%%%%%%%%%%%%%%%%%%%%%%%%%%%%%%%%%%%
%
% CalGM2in50.m
%
%%%%%%%%%%%%%%%%%%%%%%%%%%%%%%%%%%%%%%%%%%%%%%%%%%%%%%%%%%%%%%%%%%%%%%%%

Function[AveffloorAcc2in50,AveffloorDrift2in50,FDamper_max,FDamper_min]=
CalGM2in50(zeta,freq1,freq2,m,kCol,kDamp,Coef,alpha,Vyld,timeEnd,nSol)

global Story;
floorAcc2in50 = zeros(5,Story);
floorDrift2in50 = zeros(5,Story);
AveffloorAcc2in50 = zeros(Story,1);
AveffloorDrift2in50 = zeros(Story,1);

fileName = 'C:\GAInteger\GM_LA\la2in50\la21.txt';
[u_g_dd,recTime,solTime,x,x_d,x_dd,intFrc,F_d_elas_time,F_d_visc_time,
Omega,M,K,Coef,elapsedTime] =
inelasticMDOF(fileName,zeta,freq1,freq2,m,kCol,kDamp,Coef, ...
              alpha,Vyld,timeEnd,nSol);
floorAcc2in50(1,1) = max(abs(x_dd(1,:)));
floorDrift2in50(1,1) = max(abs(x(1,:)));
for StoryN = 2:Story
    floorAcc2in50(1,StoryN) = max(abs(x_dd(StoryN,:)));
    floorDrift2in50(1,StoryN) = max(abs(x(StoryN,:)- x(StoryN -1,:)));
end

FDamper = F_d_visc_time + F_d_elas_time;

for i = 1 : Story
    FDamper2in50_max(1,i) = max(FDamper(i , :));
    FDamper2in50_min(1,i) = min(FDamper(i , :));
end

fileName = 'C:\GAInteger\GM_LA\la2in50\la22.txt';
[u_g_dd,recTime,solTime,x,x_d,x_dd,intFrc,F_d_elas_time,F_d_visc_time,
Omega,M,K,Coef,elapsedTime] =
inelasticMDOF(fileName,zeta,freq1,freq2,m,kCol,kDamp,Coef, ...
              alpha,Vyld,timeEnd,nSol);
floorAcc2in50(2,1) = max(abs(x_dd(1,:)));
floorDrift2in50(2,1) = max(abs(x(1,:)));
for StoryN = 2:Story
    floorAcc2in50(2,StoryN) = max(abs(x_dd(StoryN,:)));
    floorDrift2in50(2,StoryN) = max(abs(x(StoryN,:)- x(StoryN -1,:)));
end

FDamper = F_d_visc_time + F_d_elas_time;

for i = 1 : Story
    FDamper2in50_max(2,i) = max(FDamper(i , :));
    FDamper2in50_min(2,i) = min(FDamper(i , :));
end

```



```

end

fileName = 'C:\GAInteger\GM_LA\la2in50\la26.txt';
[u_g_dd, recTime, solTime, x, x_d, x_dd, intFrc, F_d_elas_time, F_d_visc_time,
Omega, M, K, Coef, elapsedTime] =
inelasticMDOF(fileName, zeta, freq1, freq2, m, kCol, kDamp, Coef, ...
              alpha, Vyld, timeEnd, nSol);
floorAcc2in50(3,1) = max(abs(x_dd(1, :)));
floorDrift2in50(3,1) = max(abs(x(1, :)));
for StoryN = 2:Story
    floorAcc2in50(3, StoryN) = max(abs(x_dd(StoryN, :)));
    floorDrift2in50(3, StoryN) = max(abs(x(StoryN, :) - x(StoryN - 1, :)));
end

FDamper = F_d_visc_time + F_d_elas_time;

for i = 1 : Story
    FDamper2in50_max(3,i) = max(FDamper(i, :));
    FDamper2in50_min(3,i) = min(FDamper(i, :));
end

fileName = 'C:\GAInteger\GM_LA\la2in50\la28.txt';
[u_g_dd, recTime, solTime, x, x_d, x_dd, intFrc, F_d_elas_time, F_d_visc_time,
Omega, M, K, Coef, elapsedTime] =
inelasticMDOF(fileName, zeta, freq1, freq2, m, kCol, kDamp, Coef, ...
              alpha, Vyld, timeEnd, nSol);
floorAcc2in50(4,1) = max(abs(x_dd(1, :)));
floorDrift2in50(4,1) = max(abs(x(1, :)));
for StoryN = 2:Story
    floorAcc2in50(4, StoryN) = max(abs(x_dd(StoryN, :)));
    floorDrift2in50(4, StoryN) = max(abs(x(StoryN, :) - x(StoryN - 1, :)));
end

FDamper = F_d_visc_time + F_d_elas_time;

for i = 1 : Story
    FDamper2in50_max(4,i) = max(FDamper(i, :));
    FDamper2in50_min(4,i) = min(FDamper(i, :));
end

fileName = 'C:\GAInteger\GM_LA\la2in50\la30.txt';
[u_g_dd, recTime, solTime, x, x_d, x_dd, intFrc, F_d_elas_time, F_d_visc_time,
Omega, M, K, Coef, elapsedTime] =
inelasticMDOF(fileName, zeta, freq1, freq2, m, kCol, kDamp, Coef, ...
              alpha, Vyld, timeEnd, nSol);
floorAcc2in50(5,1) = max(abs(x_dd(1, :)));
floorDrift2in50(5,1) = max(abs(x(1, :)));
for StoryN = 2:Story
    floorAcc2in50(5, StoryN) = max(abs(x_dd(StoryN, :)));
    floorDrift2in50(5, StoryN) = max(abs(x(StoryN, :) - x(StoryN - 1, :)));
end

FDamper = F_d_visc_time + F_d_elas_time;

for i = 1 : Story
    FDamper2in50_max(5,i) = max(FDamper(i, :));
    FDamper2in50_min(5,i) = min(FDamper(i, :));
end

```

```
end

for i = 1 : Story
    AveffloorAcc2in50(i) = median([floorAcc2in50(1,i) floorAcc2in50(2,i)...
        floorAcc2in50(3,i) floorAcc2in50(4,i) floorAcc2in50(5,i)] );

    AveffloorDrift2in50 (i) = median ([floorDrift2in50(1,i)...
        floorDrift2in50(2,i) floorDrift2in50(3,i)...
        floorDrift2in50(4,i) floorDrift2in50(5,i)]);
    FDamper_max(i) = max([FDamper2in50_max(1,i) ...
        FDamper2in50_max(2,i) FDamper2in50_max(3,i) ...
        FDamper2in50_max(4,i) FDamper2in50_max(5,i)]);
    FDamper_min(i) = min([FDamper2in50_min(1,i)...
        Damper2in50_min(2,i) FDamper2in50_min(3,i) ...
        FDamper2in50_min(4,i) FDamper2in50_min(5,i)]);

end
%-----
```

Appendix 20

Sub-Function M-File to Calculate the Damage Loss due to Seismic 10in50

```

%%%%%%%%%%%%%%%%%%%%%%%%%%%%%%%%%%%%%%%%%%%%%%%%%%%%%%%%%%%%%%%%%%%%%%%%
%
% CalGM10in50.m
%
%%%%%%%%%%%%%%%%%%%%%%%%%%%%%%%%%%%%%%%%%%%%%%%%%%%%%%%%%%%%%%%%%%%%%%%%
function
[AvefloorAcc10in50,AvefloorDrift10in50,FDamper_max,FDamper_min] = ...
CalGM10in50(zeta,freq1,freq2,m,kCol,kDamp,Coef,alpha,Vyld,timeEnd,nSol)

global Story;
floorAcc10in50 = zeros(5,Story);
floorDrift10in50 = zeros(5,Story);
FDamper10in50_max = zeros(5, Story);
FDamper10in50_min = zeros(5, Story);
AvefloorAcc10in50 = zeros(Story,1);
AvefloorDrift10in50 = zeros(Story,1);
FDamper_max = zeros(Story,1);
FDamper_min = zeros(Story,1);
fileName = 'C:\GAInteger\GM_LA\la10in50\la01.txt';
[u_g_dd,recTime,solTime,x,x_d,x_dd,intFrc,F_d_elas_time,F_d_visc_time,
Omega,M,K,Coef,elapsedTime]=
    inelasticMDOF(fileName,zeta,freq1,freq2,m,kCol,kDamp,Coef, ...
        alpha,Vyld,timeEnd,nSol);
floorAcc10in50(1,1) = max(abs(x_dd(1,:)));
floorDrift10in50(1,1) = max(abs(x(1,:)));
for StoryN = 2:Story
    floorAcc10in50(1,StoryN) = max(abs(x_dd(StoryN,:)));
    floorDrift10in50(1,StoryN) = max(abs(x(StoryN,:)- x(StoryN -1,:)));
end
FDamper = F_d_visc_time + F_d_elas_time;

for i = 1 : Story
    FDamper10in50_max(1,i) = max(FDamper(i , :));
    FDamper10in50_min(1,i) = min(FDamper(i , :));
end

fileName = 'C:\GAInteger\GM_LA\la10in50\la02.txt';
[u_g_dd,recTime,solTime,x,x_d,x_dd,intFrc,F_d_elas_time,F_d_visc_time,
Omega,M,K,Coef,elapsedTime]=
    inelasticMDOF (fileName,zeta,freq1,freq2,m,kCol,kDamp,Coef,...
        alpha,Vyld,timeEnd,nSol);
floorAcc10in50(2,1) = max(abs(x_dd(1,:)));
floorDrift10in50(2,1) = max(abs(x(1,:)));
for StoryN = 2:Story
    floorAcc10in50(2,StoryN) = max(abs(x_dd(StoryN,:)));
    floorDrift10in50(2,StoryN) = max(abs(x(StoryN,:)- x(StoryN -1,:)));
end
FDamper = F_d_visc_time + F_d_elas_time;

for i = 1 : Story
    FDamper10in50_max(2,i) = max(FDamper(i , :));
    FDamper10in50_min(2,i) = min(FDamper(i , :));
end

```

```

fileName = 'C:\GAInteger\GM_LA\la10in50\la04.txt';
[u_g_dd, recTime, solTime, x, x_d, x_dd, intFrc, F_d_elas_time, F_d_visc_time,
Omega, M, K, Coef, elapsedTime] =
inelasticMDOF(fileName, zeta, freq1, freq2, m, kCol, kDamp, Coef, ...
               alpha, Vyld, timeEnd, nSol);

floorAcc10in50(3,1) = max(abs(x_dd(1, :)));
floorDrift10in50(3,1) = max(abs(x(1, :)));
for StoryN = 2:Story
    floorAcc10in50(3, StoryN) = max(abs(x_dd(StoryN, :)));
    floorDrift10in50(3, StoryN) = max(abs(x(StoryN, :) - x(StoryN - 1, :)));
end
FDamper = F_d_visc_time + F_d_elas_time;

for i = 1 : Story
    FDamper10in50_max(3,i) = max(FDamper(i, :));
    FDamper10in50_min(3,i) = min(FDamper(i, :));
end

fileName = 'C:\GAInteger\GM_LA\la10in50\la08.txt';
[u_g_dd, recTime, solTime, x, x_d, x_dd, intFrc, F_d_elas_time, F_d_visc_time,
Omega, M, K, Coef, elapsedTime] =
inelasticMDOF(fileName, zeta, freq1, freq2, m, kCol, kDamp, Coef, ...
               alpha, Vyld, timeEnd, nSol);

floorAcc10in50(4,1) = max(abs(x_dd(1, :)));
floorDrift10in50(4,1) = max(abs(x(1, :)));
for StoryN = 2:Story
    floorAcc10in50(4, StoryN) = max(abs(x_dd(StoryN, :)));
    floorDrift10in50(4, StoryN) = max(abs(x(StoryN, :) - x(StoryN - 1, :)));
end
FDamper = F_d_visc_time + F_d_elas_time;

for i = 1 : Story
    FDamper10in50_max(4,i) = max(FDamper(i, :));
    FDamper10in50_min(4,i) = min(FDamper(i, :));
end

fileName = 'C:\GAInteger\GM_LA\la10in50\la09.txt';
[u_g_dd, recTime, solTime, x, x_d, x_dd, intFrc, F_d_elas_time, F_d_visc_time,
Omega, M, K, Coef, elapsedTime] =
inelasticMDOF(fileName, zeta, freq1, freq2, m, kCol, kDamp, Coef, ...
               alpha, Vyld, timeEnd, nSol);

floorAcc10in50(5,1) = max(abs(x_dd(1, :)));
floorDrift10in50(5,1) = max(abs(x(1, :)));

for StoryN = 2:Story
    floorAcc10in50(5, StoryN) = max(abs(x_dd(StoryN, :)));
    floorDrift10in50(5, StoryN) = max(abs(x(StoryN, :) - x(StoryN - 1, :)));
end

FDamper = F_d_visc_time + F_d_elas_time;

for i = 1 : Story
    FDamper10in50_max(5,i) = max(FDamper(i, :));
    FDamper10in50_min(5,i) = min(FDamper(i, :));
end

```

```
for i = 1 : Story
    AveffloorAcc10in50(i)=
        median([floorAcc10in50(1,i) floorAcc10in50(2,i)...
            floorAcc10in50(3,i) floorAcc10in50(4,i) floorAcc10in50(5,i)] );
    AveffloorDrift10in50 (i) = median([floorDrift10in50(1,i)...
        floorDrift10in50(2,i) floorDrift10in50(3,i)...
        floorDrift10in50(4,i) floorDrift10in50(5,i)]);
    FDamper_max(i) = max([FDamper10in50_max(1,i) ...
        FDamper10in50_max(2,i) FDamper10in50_max(3,i) ...
        FDamper10in50_max(4,i) FDamper10in50_max(5,i)]);
    FDamper_min(i) = min([FDamper10in50_min(1,i)...
        Damper10in50_min(2,i) FDamper10in50_min(3,i) ...
        FDamper10in50_min(4,i) FDamper10in50_min(5,i)]);
end

%-----
```

Appendix 21

Sub-Function M-File to Calculate the Damage Loss due to Seismic 50in50

```

%%%%%%%%%%%%%%%%%%%%%%%%%%%%%%%%%%%%%%%%%%%%%%%%%%%%%%%%%%%%%%%%%%%%%%%%
%
% CalGM50in50.m
%
%%%%%%%%%%%%%%%%%%%%%%%%%%%%%%%%%%%%%%%%%%%%%%%%%%%%%%%%%%%%%%%%%%%%%%%%
function[AveffloorAcc50in50, AveffloorDrift50in50, ...
FDamper_max,FDamper_min] =
CalGM50in50(zeta, freq1, freq2, m, kCol, kDamp, Coef, alpha, Vyld, timeEnd, nSol)

global Story;
floorAcc50in50 = zeros(5, Story);
floorDrift50in50 = zeros(5, Story);
AveffloorAcc50in50 = zeros(Story, 1);
AveffloorDrift50in50 = zeros(Story, 1);

fileName = 'C:\GAInteger\GM_LA\la50in50\la42.txt';
[u_g_dd, recTime, solTime, x, x_d, x_dd, intFrc, F_d_elas_time, F_d_visc_time,
Omega, M, K, Coef, elapsedTime]=
    inelasticMDOF(fileName, zeta, freq1, freq2, m, kCol, kDamp, Coef, ...
        alpha, Vyld, timeEnd, nSol);
floorAcc50in50(1, 1) = max(abs(x_dd(1, :)));
floorDrift50in50(1, 1) = max(abs(x(1, :)));
for StoryN = 2:Story
    floorAcc50in50(1, StoryN) = max(abs(x_dd(StoryN, :)));
    floorDrift50in50(1, StoryN) = max(abs(x(StoryN, :)- x(StoryN -1, :)));
end

FDamper = F_d_visc_time + F_d_elas_time;

for i = 1 : Story
    FDamper50in50_max(1, i) = max(FDamper(i , :));
    FDamper50in50_min(1, i) = min(FDamper(i , :));
end

fileName = 'C:\GAInteger\GM_LA\la50in50\la43.txt';
[u_g_dd, recTime, solTime, x, x_d, x_dd, intFrc, F_d_elas_time, F_d_visc_time,
Omega, M, K, Coef, elapsedTime]=
    inelasticMDOF(fileName, zeta, freq1, freq2, m, kCol, kDamp, Coef, ...
        alpha, Vyld, timeEnd, nSol);
floorAcc50in50(2, 1) = max(abs(x_dd(1, :)));
floorDrift50in50(2, 1) = max(abs(x(1, :)));

for StoryN = 2:Story
    floorAcc50in50(2, StoryN) = max(abs(x_dd(StoryN, :)));
    floorDrift50in50(2, StoryN) = max(abs(x(StoryN, :)- x(StoryN -1, :)));
end

FDamper = F_d_visc_time + F_d_elas_time;

for i = 1 : Story
    FDamper50in50_max(2, i) = max(FDamper(i , :));
    FDamper50in50_min(2, i) = min(FDamper(i , :));
end

```

```

fileName = 'C:\GAIInteger\GM_LA\la50in50\la45.txt';
[u_g_dd,recTime,solTime,x,x_d,x_dd,intFrc,F_d_elas_time,F_d_visc_time,
Omega,M,K,Coef,elapsedTime]=
    inelasticMDOF (fileName,zeta,freq1,freq2,m,kCol,kDamp,Coef,...
        alpha,Vyld,timeEnd,nSol);
floorAcc50in50(3,1) = max(abs(x_dd(1,:)));
floorDrift50in50(3,1) = max(abs(x(1,:)));

for StoryN = 2:Story
    floorAcc50in50(3,StoryN) = max(abs(x_dd(StoryN,:)));
    floorDrift50in50(3,StoryN) = max(abs(x(StoryN,:)- x(StoryN -1,:)));
end

FDamper = F_d_visc_time + F_d_elas_time;

for i = 1 : Story
    FDamper50in50_max(3,i) = max(FDamper(i , :));
    FDamper50in50_min(3,i) = min(FDamper(i , :));
end

fileName = 'C:\GAIInteger\GM_LA\la50in50\la46.txt';
[u_g_dd,recTime,solTime,x,x_d,x_dd,intFrc,F_d_elas_time,F_d_visc_time,
Omega,M,K,Coef,elapsedTime]=
    inelasticMDOF (fileName,zeta,freq1,freq2,m,kCol,kDamp,Coef,...
        alpha,Vyld,timeEnd,nSol);
floorAcc50in50(4,1) = max(abs(x_dd(1,:)));
floorDrift50in50(4,1) = max(abs(x(1,:)));

for StoryN = 2:Story
    floorAcc50in50(4,StoryN) = max(abs(x_dd(StoryN,:)));
    floorDrift50in50(4,StoryN) = max(abs(x(StoryN,:)- x(StoryN -1,:)));
end

FDamper = F_d_visc_time + F_d_elas_time;

for i = 1 : Story
    FDamper50in50_max(4,i) = max(FDamper(i , :));
    FDamper50in50_min(4,i) = min(FDamper(i , :));
end

fileName = 'C:\GAIInteger\GM_LA\la50in50\la49.txt';
[u_g_dd,recTime,solTime,x,x_d,x_dd,intFrc,F_d_elas_time,F_d_visc_time,
Omega,M,K,Coef,elapsedTime]=
    inelasticMDOF (fileName,zeta,freq1,freq2,m,kCol,kDamp,Coef, ...
        alpha,Vyld,timeEnd,nSol);
floorAcc50in50(5,1) = max(abs(x_dd(1,:)));
floorDrift50in50(5,1) = max(abs(x(1,:)));

for StoryN = 2:Story
    floorAcc50in50(5,StoryN) = max(abs(x_dd(StoryN,:)));
    floorDrift50in50(5,StoryN) = max(abs(x(StoryN,:)- x(StoryN -1,:)));
end

FDamper = F_d_visc_time + F_d_elas_time;

```

```

for i = 1 : Story
    FDamper50in50_max(5,i) = max(FDamper(i , :));
    FDamper50in50_min(5,i) = min(FDamper(i , :));
end

for i = 1 : Story
    AveffloorAcc50in50(i)= median([floorAcc50in50(1,i)
    floorAcc50in50(2,i)...
    floorAcc50in50(3,i) floorAcc50in50(4,i) floorAcc50in50(5,i)]);
    AveffloorDrift50in50 (i) = median ([floorDrift50in50(1,i) ...
    floorDrift50in50(2,i) floorDrift50in50(3,i) ...
    floorDrift50in50(4,i) floorDrift50in50(5,i)]);
    FDamper_max(i) = max([FDamper50in50_max(1,i) ...
    FDamper50in50_max(2,i)FDamper50in50_max(3,i) ...
    FDamper50in50_max(4,i) FDamper50in50_max(5,i)]);
    FDamper_min(i) = min([FDamper50in50_min(1,i)...
    Damper50in50_min(2,i)FDamper50in50_min(3,i) ...
    FDamper50in50_min(4,i)FDamper50in50_min(5,i)]);

end
%-----

```


Appendix 22 Wide-Flange Shape Database

AISC Shape	Nominal Depth D	Nominal Wt. W	Area A	Axis X-X				Axis Y-Y				Torsion Properties		Compact Section Criteria	
				I _x in ⁴	Z _x in ³	S _x in ³	R _x in	I _y in ⁴	Z _y in ³	S _y in ³	R _y in	J in ⁴	b _f /2t _f	h/t _w	
W14X342	14	342	101	4900	672	558	6.98	1810	338	221	4.24	178	3.31	7.41	
W14X311	14	311	91.4	4330	603	506	6.88	1610	304	199	4.20	136	3.59	8.09	
W14X283	14	283	83.3	3840	542	459	6.79	1440	274	179	4.17	104	3.89	8.84	
W14X257	14	257	75.6	3400	487	415	6.71	1290	246	161	4.13	79.1	4.23	9.71	
W14X233	14	233	68.5	3010	436	375	6.63	1150	221	145	4.10	59.5	4.62	10.7	
W14X211	14	211	62.0	2660	390	338	6.55	1030	198	130	4.07	44.6	5.06	11.6	
W14X193	14	193	56.8	2400	355	310	6.50	931	180	119	4.05	34.8	5.45	12.8	
W14X176	14	176	51.8	2140	320	281	6.43	838	163	107	4.02	26.5	5.97	13.7	
W14X159	14	159	46.7	1900	287	254	6.38	748	146	96.2	4.00	19.7	6.54	15.3	
W14X145	14	145	42.7	1710	260	232	6.33	677	133	87.3	3.98	15.2	7.11	16.8	
W14X132	14	132	38.8	1530	234	209	6.28	548	113	74.5	3.76	12.3	7.15	17.7	
W14X120	14	120	35.3	1380	212	190	6.24	495	102	67.5	3.74	9.37	7.80	19.3	
W14X109	14	109	32.0	1240	192	173	6.22	447	92.7	61.2	3.73	7.12	8.49	21.7	
W14X99	14	99.0	29.1	1110	173	157	6.17	402	83.6	55.2	3.71	5.37	9.34	23.5	
W14X90	14	90.0	26.5	999	157	143	6.14	362	75.6	49.9	3.70	4.06	10.2	25.9	
W14X82	14	82.0	24.0	881	139	123	6.05	148	44.8	29.3	2.48	5.07	5.92	22.4	
W14X74	14	74.0	21.8	795	126	112	6.04	134	40.5	26.6	2.48	3.87	6.41	25.4	
W14X68	14	68.0	20.0	722	115	103	6.01	121	36.9	24.2	2.46	3.01	6.97	27.5	
W14X61	14	61.0	17.9	640	102	92.1	5.98	107	32.8	21.5	2.45	2.19	7.75	30.4	
W14X53	14	53.0	15.6	541	87.1	77.8	5.89	57.7	22.0	14.3	1.92	1.94	6.11	30.9	

Appendix 22 Wide-Flange Shape Database (continued)

AISC Shape	Nominal Depth D	Nominal Wt. W	Area A	Axis X-X			Axis X-X			Axis X-X			Torsion Properties		Compact Section Criteria	
				I _x in ⁴	Z _x in ³	S _x in ³	R _x in	I _y in ⁴	Z _y in ³	S _y in ³	R _y in	J in ⁴	b _f /2t _f	h/t _w		
W14X48	14	48.0	14.1	484	78.4	70.2	5.85	51.4	19.6	12.8	1.91	1.45	6.75	33.6		
W14X43	14	43.0	12.6	428	69.6	62.6	5.82	45.2	17.3	11.3	1.89	1.05	7.54	37.4		
W12X336	12	336	98.8	4060	603	483	6.41	1190	274	177	3.47	243	2.26	5.47		
W12X305	12	305	89.6	3550	537	435	6.29	1050	244	159	3.42	185	2.45	5.98		
W12X279	12	279	81.9	3110	481	393	6.16	937	220	143	3.38	143	2.66	6.35		
W12X252	12	252	74.0	2720	428	353	6.06	828	196	127	3.34	108	2.89	6.96		
W12X230	12	230	67.7	2420	386	321	5.97	742	177	115	3.31	83.8	3.11	7.56		
W12X210	12	210	61.8	2140	348	292	5.89	664	159	104	3.28	64.7	3.37	8.23		
W12X190	12	190	55.8	1890	311	263	5.82	589	143	93.0	3.25	48.8	3.65	9.16		
W12X170	12	170	50.0	1650	275	235	5.74	517	126	82.3	3.22	35.6	4.03	10.1		
W12X152	12	152	44.7	1430	243	209	5.66	454	111	72.8	3.19	25.8	4.46	11.2		
W12X136	12	136	39.9	1240	214	186	5.58	398	98.0	64.2	3.16	18.5	4.96	12.3		
W12X120	12	120	35.3	1070	186	163	5.51	345	85.4	56.0	3.13	12.9	5.57	13.7		
W12X106	12	106	31.2	933	164	145	5.47	301	75.1	49.3	3.11	9.13	6.17	15.9		
W12X96	12	96.0	28.2	833	147	131	5.44	270	67.5	44.4	3.09	6.85	6.76	17.7		
W12X87	12	87.0	25.6	740	132	118	5.38	241	60.4	39.7	3.07	5.10	7.48	18.9		
W12X79	12	79.0	23.2	662	119	107	5.34	216	54.3	35.8	3.05	3.84	8.22	20.7		
W12X72	12	72.0	21.1	597	108	97.4	5.31	195	49.2	32.4	3.04	2.93	8.99	22.6		
W12X65	12	65.0	19.1	533	96.8	87.9	5.28	174	44.1	29.1	3.02	2.18	9.92	24.9		
W12X58	12	58.0	17.0	475	86.4	78.0	5.28	107	32.5	21.4	2.51	2.10	7.82	27.0		
W12X53	12	53.0	15.6	425	77.9	70.6	5.23	95.8	29.1	19.2	2.48	1.58	8.69	28.1		

Appendix 22 Wide-Flange Shape Database (continued)

AISC Shape	Nominal Depth D	Nominal Wt. Wt.	Area A	Axis X-X				Axis X-X				Torsion Properties			Compact Section Criteria	
				I _x in ⁴	Z _x in ³	S _x in ³	R _x in	I _y in ⁴	Z _y in ³	S _y in ³	R _y in	J in ⁴	b _f /2t _f	h/t _w		
W12X50	12	50.0	14.6	391	71.9	64.2	5.18	56.3	21.3	13.9	1.96	1.71	6.31	26.8		
W10X54	10	54.0	15.8	303	66.6	60.0	4.37	103	31.3	20.6	2.56	1.82	8.15	21.2		
W10X49	10	49.0	14.4	272	60.4	54.6	4.35	93.4	28.3	18.7	2.54	1.39	8.93	23.1		
W10X45	10	45.0	13.3	248	54.9	49.1	4.32	53.4	20.3	13.3	2.01	1.51	6.47	22.5		
W10X39	10	39.0	11.5	209	46.8	42.1	4.27	45.0	17.2	11.3	1.98	0.976	7.53	25.0		
W10X33	10	33.0	9.71	171	38.8	35.0	4.19	36.6	14.0	9.20	1.94	0.583	9.15	27.1		
W12X45	10	45.0	13.1	348	64.2	57.7	5.15	50.0	19.0	12.4	1.95	1.26	7.00	29.6		
W12X40	10	40.0	11.7	307	57.0	51.5	5.13	44.1	16.8	11.0	1.94	0.906	7.77	33.6		
W10X112	10	112	32.9	716	147	126	4.66	236	69.2	45.3	2.68	15.1	4.17	10.4		
W10X100	10	100	29.4	623	130	112	4.60	207	61.0	40.0	2.65	10.9	4.62	11.6		
W10X88	10	88.0	25.9	534	113	98.5	4.54	179	53.1	34.8	2.63	7.53	5.18	13.0		
W10X77	10	77.0	22.6	455	97.6	85.9	4.49	154	45.9	30.1	2.60	5.11	5.86	14.8		
W10X68	10	68.0	20.0	394	85.3	75.7	4.44	134	40.1	26.4	2.59	3.56	6.58	16.7		
W10X60	10	60.0	17.6	341	74.6	66.7	4.39	116	35.0	23.0	2.57	2.48	7.41	18.7		